



All Theses and Dissertations

---

2009-04-17

# Synthesis of 2,4,5-Triaminocyclohexane Carboxylic Acid as a Novel 2-Deoxystreptamine Mimetic

Sarah Elizabeth Roberts

*Brigham Young University - Provo*

Follow this and additional works at: <https://scholarsarchive.byu.edu/etd>

 Part of the [Biochemistry Commons](#), and the [Chemistry Commons](#)

---

## BYU ScholarsArchive Citation

Roberts, Sarah Elizabeth, "Synthesis of 2,4,5-Triaminocyclohexane Carboxylic Acid as a Novel 2-Deoxystreptamine Mimetic" (2009). *All Theses and Dissertations*. 2091.

<https://scholarsarchive.byu.edu/etd/2091>

This Thesis is brought to you for free and open access by BYU ScholarsArchive. It has been accepted for inclusion in All Theses and Dissertations by an authorized administrator of BYU ScholarsArchive. For more information, please contact [scholarsarchive@byu.edu](mailto:scholarsarchive@byu.edu), [ellen\\_amatangelo@byu.edu](mailto:ellen_amatangelo@byu.edu).

SYNTHESIS OF 2, 4, 5-TRIAMINOCYCLOHEXANECARBOXYLIC ACID AS A  
NOVEL 2-DOS MIMETIC

By

Sarah Elizabeth Roberts

A thesis submitted to the faculty of

Brigham Young University

In partial fulfillment of the requirements for the degree of

Masters of Science

Department of Chemistry and Biochemistry

Brigham Young University

August 2009

BRIGHAM YOUNG UNIVERSITY

GRADUATE COMMITTEE APPROVAL

of a thesis submitted by

Sarah Elizabeth Roberts

This thesis has been read by each member of the following graduate committee  
and by majority vote has been found to be satisfactory.

\_\_\_\_\_

Date

\_\_\_\_\_

Young Wan Ham, Ph.D., Chair

\_\_\_\_\_

Date

\_\_\_\_\_

Heidi R. Vollmer-Snarr, Ph.D.

\_\_\_\_\_

Date

\_\_\_\_\_

Steven R. Herron, Ph.D.

BRIGHAM YOUNG UNIVERSITY

As chair of the candidate's graduate committee, I have read the thesis of Sarah Elizabeth Roberts in its final form and have found that (1) its format, citations, and bibliographical style are consistent and acceptable and fulfill university and department style requirements; (2) its illustrative materials including figures, tables, and charts are in place; and (3) the final manuscript is satisfactory to the graduate committee and is ready for submission to the university library.

---

Date

---

Young Wan Ham  
Chair, Graduate Committee

Accepted for the Department

---

David D. Dearden  
Graduate Coordinator

Accepted for the College

---

Thomas W. Sederberg, Associate Dean  
College of Physical and Mathematical Sciences

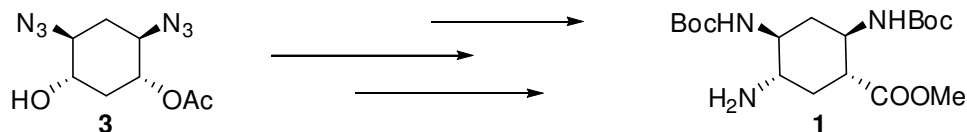
# ABSTRACT

## SYNTHESIS OF 2, 4, 5-TRIAMINOCYCLOHEXANECARBOXYLIC ACID AS A NOVEL 2-DOS MIMETIC

Sarah Elizabeth Roberts

Department of Chemistry and Biochemistry

Master of Science



RNAs have become increasingly recognized as possible drug targets due to their involvement in important biochemical functions, as well as their unique but well-defined structures. Recently published crystal structures depict the binding of a series of aminoglycosides- or more specifically- 2-deoxystretamine (2-DOS), the most preserved central scaffold of aminoglycosides, to a conserved 5'-GU-3' region on their target RNAs.

A novel unnatural  $\gamma$ -amino acid, **1**, has been synthesized using 2-deoxystreptamine as a template through structure-based rational design. The unnatural amino acid has been designed to replace a glycosidic linkage with an amide bond, which may limit the promiscuous binding characteristics of aminoglycosides through increased rigidity of the ligands and additional hydrogen bonding. The binding selectivity and affinity will be studied in the future through a fluorescence assay.

## ACKNOWLEDGEMENTS

First and foremost, I would like to thank Dr. Young Wan Ham for being such an inspirational chemist and patient advisor. Without him I would not have had the opportunity to work on such an amazing and challenging project as well as learn a whole new side of organic chemistry. On this same note, I would like to thank Dr. Maruthi Chittapragada whose vast knowledge in synthesis greatly improved the quality of the research in our lab and whose wonderful personality and perspective on life made working with him a true honor. I also wish to thank my laboratory associates for their assistance, encouragement, and friendship.

Next, I would like to thank Dr. Steve R. Herron and Dr. Scott R. Burt for their assistance in X-ray crystallography and NMR techniques. Their help has been greatly appreciated. I would also like to thank all of my friends who kept me going when I was struggling and for always being there.

I would also like to give a big thank you to my family, especially my husband, Andrew N. Roberts, for always being there to provide encouragement whenever research was giving me a hard time, and for preventing me from dropping out of the program altogether. I love you so much and appreciate everything you have done for me.

I dedicate this degree to my grandmother Evangeline L. Jablonski and my mother Debra G. Shephard for instilling in me their deep love of science. It is because of them that I chose to pursue chemistry.

# TABLE OF CONTENTS

Table of Contents .....	i
List of Figures .....	iii
List of Schemes .....	iv
List of Tables .....	v
List of Abbreviations .....	vi
Chapter 1. Introduction .....	1
1.1 RNA as a Drug Target .....	1
1.2 Aminoglycosides .....	2
1.3 Molecular Mechanism of Action for Aminoglycosides .....	5
1.4 2-DOS Mimetics.....	9
1.5 References .....	16
Chapter 2. Design and Synthesis of a novel 2-DOS Mimic .....	20
2.1 The design of 2, 4, 5-triaminocyclohexanecarboxylic acid as a novel 2-DOS mimetic.....	20
2.2 The Synthesis of 2,4,5-Triaminocyclohexanecarboxylic acid as a 2-DOS mimic.....	24
2.2.1 Introduction of Aldehyde Functionality .....	23
2.2.2 Introduction of Acid Functionality .....	29
2.2.3 Introduction of the Amine Functionality .....	34
2.3 Conclusion and Future Works.....	35
2.4 References .....	39

Chapter 3. Experimental and Spectroscopic Data .....	40
3.1 General Methods .....	40
3.2 Experimental Data .....	41
3.3 Selected NMR Spectra .....	57



# LIST OF FIGURES

## Chapter 1. Introduction

Figure 1.1 Aminoglycoside Structures .....	3
Figure 1.2 X-ray Crystal Structures of the A-Site .....	6
Figure 1.3 X-ray Crystal Structures of Paromomycin Bound A-site .....	9
Figure 1.4 Bacterial A-Site Recognition by 2-DOS .....	11
Figure 1.5 2-DOS Based RNA Binding Small Molecules .....	12
Figure 1.6 2-DOS Amide Analogs.....	12
Figure 1.7 2-DOS in Conjugation with Heterocyclic Compounds.....	13

## Chapter 2. Research

Figure 2.1 Modification of 2-DOS.....	21
Figure 2.2 Hydrogen Bonding Interactions.....	23
Figure 2.3 Novel Building Block <b>1</b> .....	23
Figure 2.4 NOE studies on transformation from <b>27</b> to <b>2</b> .....	34
Figure 2.5 Fluorescence Assay .....	36

## LIST OF SCHEMES

### Chapter 2. Research

Scheme 2.1 Overall Retrosynthesis of Molecule <b>1</b> .....	24
Scheme 2.2 Initial Retrosynthetic Analysis to make <b>1</b> .....	24
Scheme 2.3 Synthetic Attempts from <b>3</b> to <b>8</b> .....	25
Scheme 2.4 Synthesis from <b>8</b> to produce an aldehyde, <b>5</b> .....	25
Scheme 2.5 Synthesis of <b>8</b> to produce equatorial nitrile compound <b>12</b> ...	26
Scheme 2.6 Synthesis from compound <b>6</b> to introduce aldehyde .....	27
Scheme 2.7 Retrosynthetic analysis to introduce acid functionality .....	29
Scheme 2.8 Synthesis from <b>3</b> to introduce either aldehyde or acid functionality .....	30
Scheme 2.9 Reaction of <b>20</b> to form <b>25</b> and <b>26</b> .....	30
Scheme 2.10 Synthesis of <b>25</b> to <b>27</b> .....	32
Scheme 2.11 Epimerization of <b>27</b> to <b>2</b> .....	32
Scheme 2.12 Formation of compound <b>1</b> from <b>2</b> .....	35
Scheme 2.13 Proposed synthesis of initial molecular structure for RNA binding study .....	37

## LIST OF TABLES

### Chapter 1. Introduction

Table 1.1 2-DOS RNA Stem Loop Binder Dimers .....	14
---	----

### Chapter 2. Research

Table 2.1 Conditions for Aldehyde Transformation.....	28
---	----

Table 2.2 Esterification Reaction Studies .....	31
---	----

Table 2.3 Epimerization reaction studies .....	32
--	----

Table 2.4 Coupling Constants.....	33
-----------------------------------	----

## LIST OF ABBREVIATIONS

$^{13}\text{C}$ NMR	Carbon nuclear magnetic resonance
$^1\text{H}$ NMR	Proton nuclear magnetic resonance
A	Adenine
2AP	2-Aminopurine
Ar	Argon gas
BnBr	Benzyl bromide
Boc	<i>tert</i> -Butyloxycarbonyl
Boc <sub>2</sub> O	di- <i>tert</i> -Butyl dicarbonate
br d	Broad doublet
br dt	Broad doublet of triplets
br q	Broad quartet
br s	Broad singlet
BuLi	<i>n</i> -Butyl lithium
C	Cytosine
Calcd	Calculated
CDCl <sub>3</sub>	Deuterated chloroform
CF <sub>3</sub>	Trifluoromethane
CH <sub>2</sub> Cl <sub>2</sub>	Dichloromethane
CHCl <sub>3</sub>	Chloroform
CH <sub>3</sub> CN	Acetonitrile
conc.	Concentrated

CSA	Camphorsulfonic acid
d	Doublet
dd	Doublet of doublets
ddd	Doublet of doublet of doublets
dt	Doublet of triplets
DEAD	Diethyl azodicarboxylate
DIBAL-H	Diisobutylaluminum hydride
DIPA	Diisopropyl amine
$\delta$	Chemical shift in parts per million
	Downfield from tetramethylsilane
DMF	<i>N,N</i> -Dimethylformamide
DMSO	Dimethylsulfoxide
DMSO- $d_6$	Deuterated dimethylsulfoxide
DNA	Deoxyribonucleic acid
2-DOS	2-Deoxystreptamine
DPPA	Diphenyl phosphorazidate
dsRNA	Double stranded RNA
dy.	Day
EDCI	1-Ethyl-3-(3'-dimethylaminopropyl) carbodiimide
eq. or equiv.	Equivalent
ESI	Electrospray ionization
et al.	And everyone else

EtOAc	Ethyl Acetate
G	Guanine
hr	Hour
H	Hydrogen
H <sub>2</sub>	Hydrogen gas
HCl	Hydrochloric acid
H <sub>2</sub> O <sub>2</sub>	Hydrogen Peroxide
H <sub>2</sub> SO <sub>4</sub>	Sulfuric acid
H-DNA	Hinged DNA
HIV-1 RRE	Human immunodeficiency virus type-1 Rev response element
HIV-1 TAR	HIV-1 transactivation response
HRMS	High resolution mass spectrometry
Hz	Hertz
IC <sub>50</sub>	Concentration of inhibitor required to produce 50 per cent inhibition
<i>J</i>	Coupling Constant
K <sub>2</sub> CO <sub>3</sub>	Potassium carbonate
KHMDS	Potassium hexamethyldisilazide
K <sub>d</sub>	Dissociation constant
LAH	Lithium aluminum hydride
LD <sub>50</sub>	Median lethal dose
LDA	Lithium diisopropylamide

LiHMDS	Lithium hexamethyldisilazide
LiOH	Lithium hydroxide
M	Moles per liter
m	Multiplet
MeOH	Methanol
mg	Milligram
MgSO <sub>4</sub>	Magnesium Sulfate
MHz	Megahertz
min	Minute (s)
ml	Milliliter
μM	Micromoles per liter
mM	Millimoles per liter
mmol	Millimoles
MOM	Methoxymethyl
MOMCl	Methoxymethyl Chloride
MP	Melting Point
mRNA	Messenger RNA
MS	Mass spectrometry
MsCl	Methnesulfonyl Chloride
N	Nitrogen
N	Normality
N/A	Not applicable
Na	Sodium

NaH	Sodium Hydride
NaHCO <sub>3</sub>	Sodium Bicarbonate
Na <sub>2</sub> CO <sub>3</sub>	Sodium Carbonate
NaCN	Sodium Cyanide
NaN <sub>3</sub>	Sodium Azide
NaOH	Sodium hydroxide
NaOMe	Sodium methoxide
Na <sub>2</sub> S <sub>2</sub> O <sub>5</sub>	Sodium Tartrate
NEt <sub>3</sub>	Triethyl Amine
NH <sub>2</sub>	Amine
NH <sub>4</sub> <sup>+</sup>	Ammonium
NH <sub>4</sub> OH	Ammonium hydroxide
NMR	Nuclear magnetic resonance
NOE	Nuclear Overhauser Effect
O	Oxygen
OH	Hydroxyl
Oxid.	Oxidation
P	Phosphorous
Pd/C	Palladium on Carbon
PMB	<i>p</i> -Methoxybenzyl
PMBTCA	<i>p</i> -Methoxybenzyl trichloroacetoimidate
PNBA	<i>p</i> -Nitrobenzoic acid
PPh <sub>3</sub>	Triphenyl Phosphine



ppm	Parts per million
pyr.	Pyridine
q	Quartet
R <sub>f</sub>	Retention factor
RNA	Ribonucleic acid
RNAi	RNA interference
RNase P	Ribonuclease protein
rRNA	Ribosomal RNA
rt	Room temperature
s	Singlet
s	Second (s)
t	Triplet
TBAB	Tetrabutylammonium bromide
TBDMSCI	<i>tert</i> -Butyl(chloro)dimethylsilane
Temp	Temperature
TFA	Trifluoroacetic acid
Tf <sub>2</sub> O	Trifluoromethanesulfonic anhydride
THF	Tetrahydrofuran
TLC	Thin layer Chromatography
tmRNA	Transfer-messenger-RNA
TMSCI	Trimethylsilyl chloride
TPP	Triphenyl Phosphine
tRNA	Transfer RNA

$[\alpha]$

Specific optical rotation

$^{\circ}\text{C}$

Degree Celsius

# CHAPTER 1. INTRODUCTION

## 1.1 RNA as a Drug Target

In the past, proteins have been the most commonly utilized target for pharmaceutical application. However, ribonucleic acid (RNA) has recently been proven to be a valuable tool for drug targeting. Although the presence of nucleic acids has been known since 1868 in eukaryotes<sup>1</sup> and eventually prokaryotes, the discovery of RNA's function is more recent with its suspected role of protein synthesis occurring in 1939,<sup>2</sup> to the realization of its catalytic potential as well as its role in viral pathogens,<sup>3</sup> and more recently, the unveiling of RNA interference (RNAi),<sup>4,5</sup> microRNAs<sup>6</sup>, and gene regulatory RNAs.<sup>7</sup>

Due to its vast involvement in biological systems and its complexity, RNA serves as a promising model to study the binding mechanisms of pharmaceuticals which could lead to improved drug design.<sup>8</sup> Consequently, antisense and RNAi strategies have become largely accepted as prevailing tools to control RNA gene expression, thereby allowing the regulation of the development of organisms and their cellular functions.<sup>9-11</sup> However, the concept of targeting RNA is still novel and this is due to the following: RNA has the ability to fold into intricate three-dimensional structures which antisense nucleotides cannot target; antisense nucleotides recognize RNA in an unspecific manner; and there is not an efficient method of transporting antisense nucleotides through the cell membrane.<sup>12</sup> Thus, there is not yet a general paradigm to pursue the concept of using RNA as a drug target. These challenges make the development

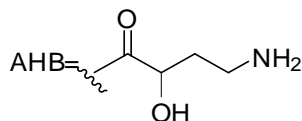
of other RNA targeting methods, such as small molecules which are already known to bind to RNA, crucial.

## 1.2 Aminoglycosides

Many naturally occurring small molecules have the ability to bind to RNA and hinder its function. Most of these RNA-binding compounds have evolved to incorporate antibiotic activity. Among these antibacterial agents is a group of small molecules called aminoglycosides. Aminoglycosides and some semisynthetic derivatives include several drugs that share the same basic chemical structure, an aminocyclitol ring linked to aminosugars.<sup>13,14</sup> The aminocyclitol ring is comprised of streptomycin or 2-deoxystreptomycin (2-deoxy-*myo*-inoso-1,3-diamine or all-trans-1,3-diamino-4,5,6-trihydroxycyclohexane or 2-DOS), and serves as the central scaffold of aminoglycosides. These units are all-trans cyclohexitols that are 1,3-disubstituted with two amino groups. They are numbered based on streptomycin's biogenic precursor *myo*-inositol even though 2-deoxy-streptomycin or 2-deoxy-*myo*-inoso-1,3-diamine is actually derived biosynthetically from D-glucose-6-phosphate.<sup>15</sup>

Apart from the conserved 1,3-diamino functionality, the central scaffold contains two, three, and sometimes four hydroxyls. When the cyclohexitol ring has three hydroxyl groups it is termed 2-deoxystreptomycin and streptomycin when there are four. Likewise, when there are only two hydroxyl substituents, the cyclohexitol ring is termed 2,5-dideoxystreptomycin. Aminoglycosides can be divided further into three subclasses: 4-, 4,5-, or 4,6-linked 2-DOS structures (Figure 1.1).

Substitution	Ring I	Ring II	Ring III, IV, V	R <sub>1</sub>	R <sub>2</sub>	R <sub>3</sub>	R <sub>4</sub>	Aminoglycoside	
4-monosubstituted				NH <sub>2</sub>	OH	H		Neamine Paromamine	
				ring 3				R <sub>1</sub> connectivity	Apramycin
4,5-disubstituted				ring 3	NH <sub>2</sub>	OH	H		Ribostamycin Butirosin B
				ring 3	NH <sub>2</sub>	OH	H		Neomycin B Paromomycin
				ring 3					Lividomycin A
4,6-disubstitution				ring 3	NH <sub>2</sub>	OH	OH	H	Kanamycin A Kanamycin B Kanamycin C Tobramycin Amikacin
				ring 3					Gentamicin C <sub>1</sub> Gentamicin C <sub>2</sub> Gentamicin C <sub>1A</sub> G-418(Genteticin)



**Figure 1.1** Structures of aminoglycosides with 4-, 4,5-, and 4-6-substituted connectivity around 2-DOS.

There are three structures that fall under the 4-monosubstituted category: neamine, paromamine, and apramycin. Paromamine and neamine differ only in  $R_1$  and are typically not used alone as pharmaceuticals, leaving apramycin as the only 4-monosubstituted compound that is used as a drug.

The next category includes ribostamycin, butirosin B, neomycin B, paromomycin, and lividomycin A, all of which are classified under the 4,5-disubstituted aminoglycosides (Figure 1.1). Each of these compounds not only differs in small  $R_1$ ,  $R_2$ , and  $R_3$  groups, but also in the ring structures that are attached to the ring II unit. Each of these drugs can be further classified due to their common substitution. Ribostamycin and butirosin B are typically grouped together because they both have the same additional ring III unit attached to ring II. Their only difference is specific functionality on the main structure, ring I and ring II (Figure 1.1).

The next group includes neomycin B and paromomycin. These two compounds have the same ring III and ring IV, but differ only in the functionality on ring I and II. Lividomycin A, is in its own category due to its unique five-ring substituent (Figure 1.1).

4,6-disubstituted aminoglycosides include: kanamycin A, kanamycin B, kanamycin C, tobramycin, and amikacin in one category; and gentamicin C1, gentamicin C2, gentamicin C1A, and geneticin in another. The major differences between the two subclasses is a variation on the 6' position of the ring I unit, as well as the different structures of ring III (Figure 1.1).

These aminoglycosides interact with the rRNA of Gram-negative bacteria and interfere with the translational process of bacterial RNAs and mRNAs, as well as viral mRNAs such as HIV-1 RRE and TAR.<sup>16-24</sup> Aminoglycosides bind to RNA with a high affinity, but low specificity, due to an ability to bend to fit into different secondary structures of RNA, and also vast amounts of electrostatic (due to the large numbers of amino group attachments) and hydrogen bonding interaction capability. Consequently, aminoglycosides tend to bind to many regions, or secondary structures, of RNA. Some studies demonstrate that the binding of aminoglycosides to certain secondary structures depends on the size of the asymmetric interior loops of the RNA itself.<sup>19,25</sup> These observations make designing RNA binding small molecules that are sequence or site specific challenging.

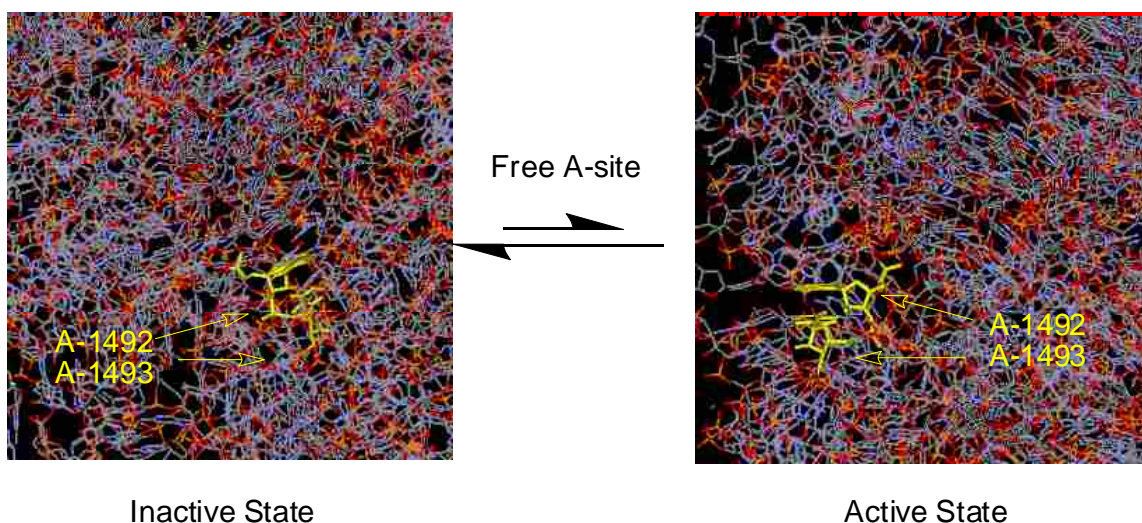
### **1.3 Molecular Mechanism of Action for Aminoglycosides**

Due to flexible and highly promiscuous structural properties, aminoglycosides have been recognized to have binding capabilities with several different RNA targets such as the prokaryotic ribosomal A-site, HIV TAR, HIV RRE, Group 1 intron, RNase P, tmRNA, and even in some cases the eukaryotic A site with relatively low micromolar binding affinities.<sup>16-24</sup> Recent crystal structure and NMR data have provided support for the previous theorized aminoglycoside binding mechanisms to bacterial rRNA.<sup>26-28</sup>

In general, aminoglycoside bactericidal activity is typically attributed to the irreversible binding to the ribosome, or more specifically, the 30S ribosomal subunit of the 16S rRNA-decoding site.<sup>29, 30</sup> This binding inhibits the translocation

of the peptidyl-tRNA from the A-site to the P-site and also causes misreading of mRNA, leaving the bacterium unable to synthesize proteins vital to its growth, or to the synthesis of nonfunctional misfolded proteins, and thus results in the overall death of the bacteria.<sup>25</sup>

Crystal and NMR structures of the bacterial A-site have revealed that during the decoding process, a small helix is formed between the codon of the mRNA and the anti-codon of the associated aminoacyl-tRNA, a critical step for aminoacyl-tRNA selection.<sup>31-34</sup> Upon this formation, the A-site conformation is changed from an inactive position, where the two conserved adenines A1492 and A1493 are folded within the shallow groove of the A-site, to an activated state, where A1492 and A1493 are flipped out from the A-site and interact with the corresponding codon–anticodon mini-helix (Figure 1.2).<sup>35</sup> This conformational change is known as a molecular switch and reversibly determines the continuation of translation (Figure 1.2).



**Figure 1.2** Resolved X-ray crystal structures of the A-site. A1492 and A1493 in the bacterial decoding site are in conformational equilibrium between the inactive and active states with equilibrium lying mostly towards the inactive state. (PDB 1IBL and PDB 1J5E)<sup>36</sup>



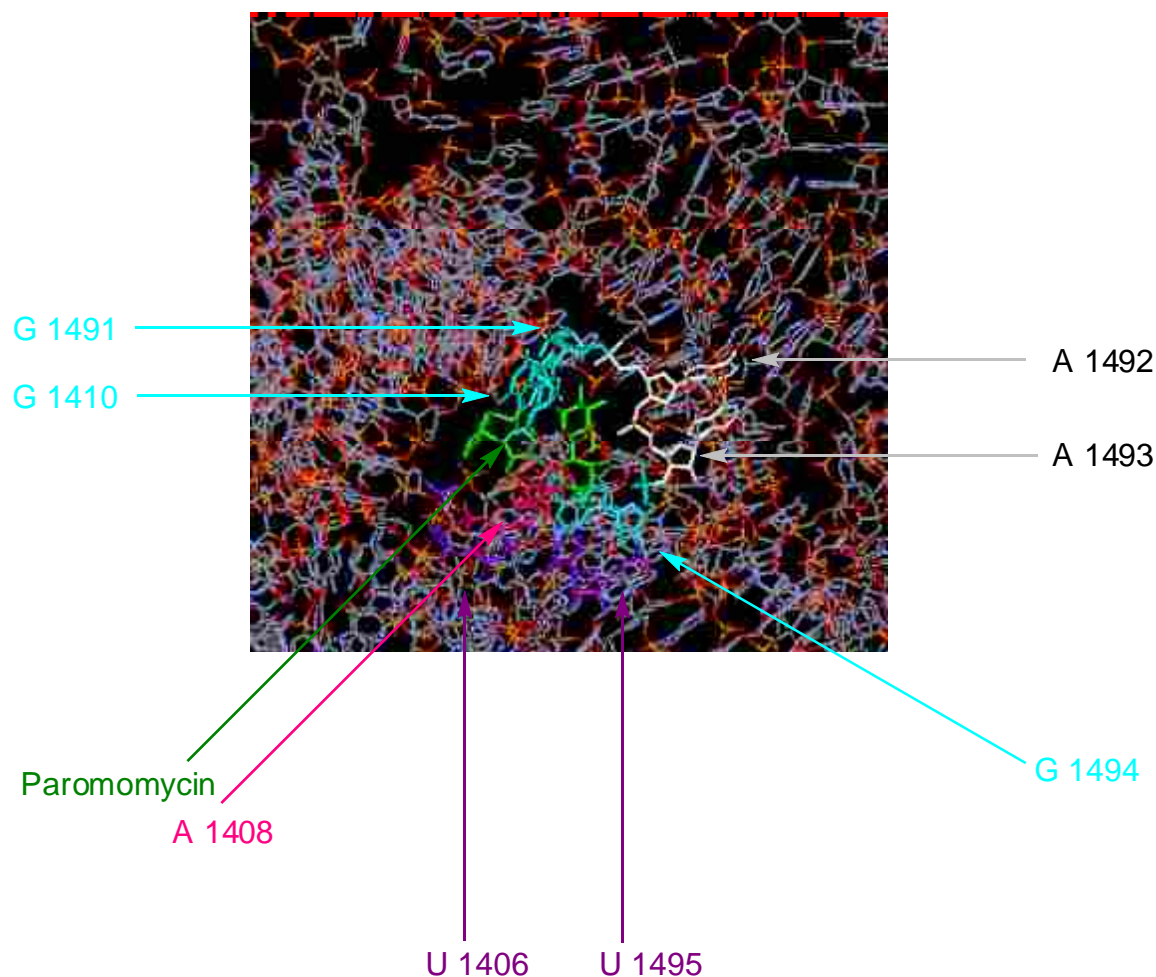
When aminoglycosides bind to the bacterial A-site, the conformation equilibrium of the conserved adenines, A1492 and A1493, becomes locked into the open conformation without the presence of the cognate tRNA–mRNA complex. This increases the affinity of the A-site for a non-cognate mRNA–tRNA complex, and prevents the ribosomes ability to efficiently discern between non-cognate and cognate a complex, which ultimately leads to the production of mistranslated proteins.<sup>37</sup>

This mechanism is currently accepted as the primary mode of action for the majority of the 4,5- and 4,6-disubstituted 2-DOS aminoglycosides. However, apramycin functions through a slightly different mechanism, which is understandable due to its unique aminoglycoside structure. In general, apramycin reduces bacterial protein synthesis through inhibition of the elongation step by blocking ribosome translocation.<sup>34</sup> Specifically, it binds to the deep/major groove of the A site and stabilizes the decoding active state with A1492 and A1493 bulged out.<sup>24</sup>

Studies performed with apramycin have shown that the actual molecular mechanism is more complex than the “molecular switch” theory. Further investigation of the narrow drug pocket within the bacterial ribosome, or the A-site, show that it is able to accommodate a framework of hydrogen bond donors and acceptors as well as electrostatic interactions that are the foundation for the witnessed strong ribosome to aminoglycoside interactions; the wobble base pair U1495-U1406; bases A1408, A1492, and A1493; as well as the base pair

C1409-G1491 are the components responsible in the A-site for the strong hydrogen bonding ability.<sup>38</sup>

When an aminoglycoside such as paromomycin binds to the A-site, the puckered sugar ring I is inserted into the A-site helix by stacking against the guanine residue and by forming two hydrogen bonds to the Watson-Crick sites of the universally conserved A1408 (Figure 1.3).<sup>39</sup> This interaction, in particular, is a major component in maintaining the residues A1492 and A1493 in the bulged-out conformation that causes the misreading of RNA complexes.<sup>39</sup> The highly conserved 2-DOS (ring II) piece forms similar hydrogen bonds in the three complexes made possible by the highly adaptable and universally conserved U1406-U1495 base pair as well as several electrostatic interactions with the phosphate backbone.<sup>36</sup> Additional rings of the aminoglycoside have the ability to contact different nucleotides within the A-site depending on the substitution and structures attached to ring II.

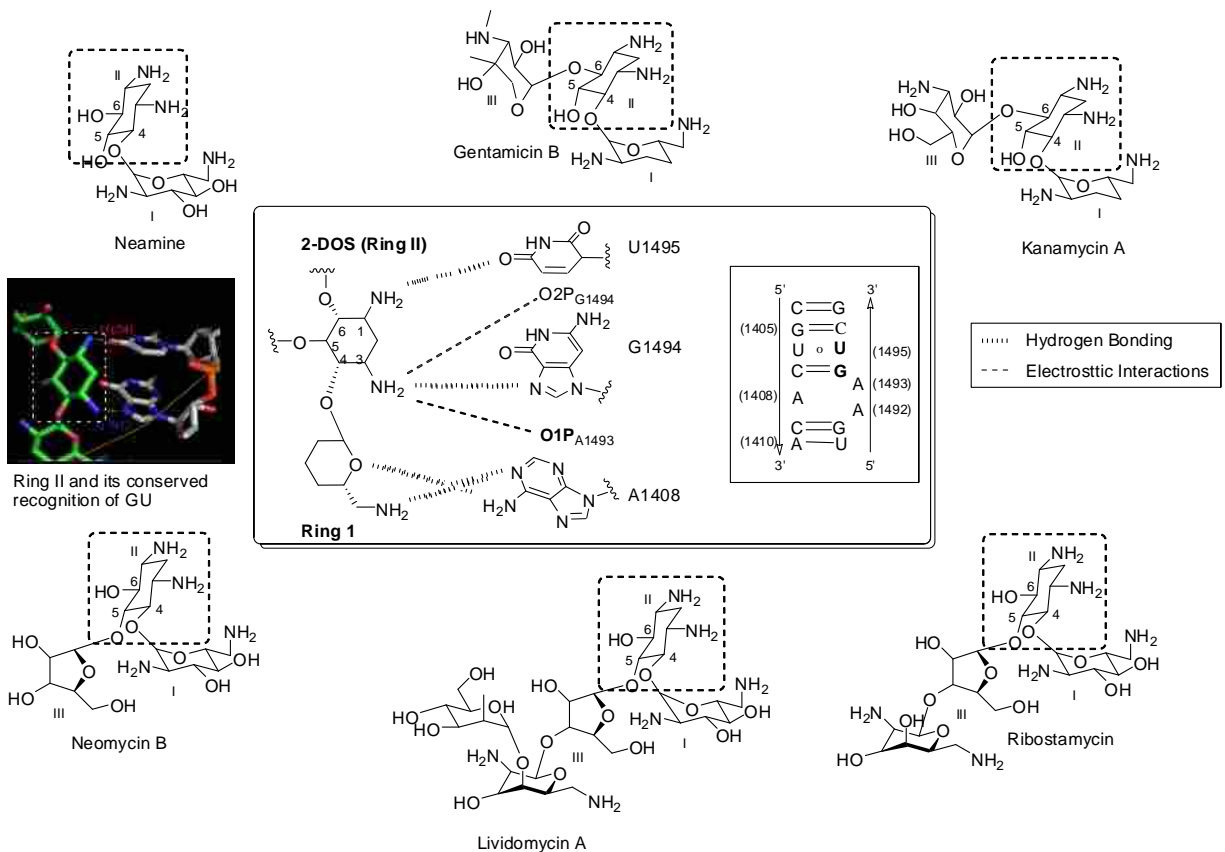


**Figure 1.3** Resolved X-ray crystal structures of the paromomycin bound A-site. Paromomycin (green) is stacked against the guanine residues (blue) 1491 and 1410 and hydrogen bonded to A1408 (pink) causing residues A1492 and 1493 (white) to remain locked into the bulged out confirmation. The 2-DOS structure of paromomycin also forms hydrogen bonds with U1406 and 1495 (purple) residues. (PDB 1IBL)

## 1.4 2-DOS Mimetics

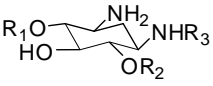
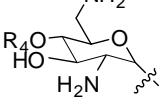
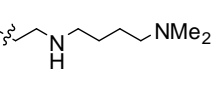
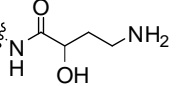
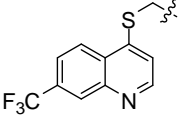
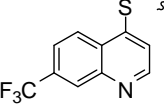
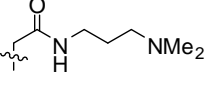
Several methods have been employed to not only better understand the RNA to small molecule binding mechanism but to also find pharmaceuticals with improved binding affinity as well as specificity. This section describes some of the most recent research on 2-DOS based aminoglycoside mimetics as well as provides the background that lead to the design of our research.

2-DOS has recently been discovered to be the major component responsible for the aminoglycosides high binding affinity to RNA. Although with a moderate binding affinity by itself ( $\sim 1$  mM or  $88 \mu\text{M } k_d$ ),<sup>26</sup> studies on 2-DOS have shown that it is the single most important piece for any sort of sequence specific binding characteristic as it has the ability to specifically recognize the two 5'-GU-3' base steps (G1494-U1495 and G1405-U1406)<sup>38, 40</sup>. The highly conserved 2-DOS (ring II) piece forms hydrogen bonds in the three complexes made possible by the highly adaptable and universally conserved U1406-U1495 base pair as well as several electrostatic interactions with the phosphate backbone.<sup>36</sup> Additional rings of the aminoglycoside have the ability to contact different nucleotides within the A-site depending on the substitution and structures attached to ring II. Further studies have shown that 2-DOS coupled to ring I (neamine) is responsible for the highly conserved bacterial A-site recognition that is indicative of aminoglycosides (Figure 1.4).<sup>38</sup>



**Figure 1.4** Highly conserved bacterial A-site recognition by rings I and II (2-DOS) in six different aminoglycosides. Hydrogen-bonding (.....) and electrostatic interactions (----) that are conserved throughout the aminoglycosides are indicated with dashed lines. Ring I shows highly conserved binding pattern with A1408. The 2-DOS (ring II) unanimously recognizes the 5'-GU-3' base step in A-site regardless of aminosugar substitution among different aminoglycosides.<sup>38</sup>

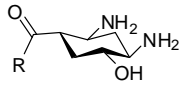
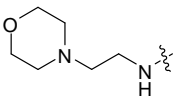
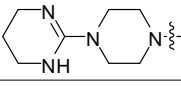
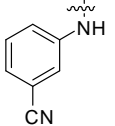
Two recently reported examples of novel aminoglycoside antibiotics removed one or both aminosugars from the original aminoglycoside structures, but left the core 2-DOS as the main component of the compounds. These demonstrated a strong affinity to the target RNA A-site and also inhibited bacterial translation (Figure 1.5).<sup>41</sup>

	R <sub>1</sub>	R <sub>2</sub>	R <sub>3</sub>	R <sub>4</sub>
				
K <sub>d</sub> = 88 μM			H	N/A

**Figure 1.5** 2-DOS based RNA binding small molecules.

Due to those results, generating libraries of synthetic compounds that mimic the conformation and function of aminoglycosides but lack aminosugar residues has become a possibility.

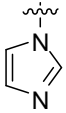
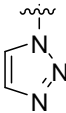
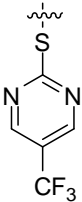
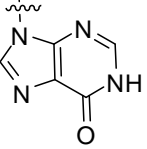
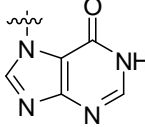
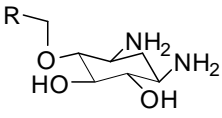
Another group prepared a number of small molecules that consisted of a monomeric 2-DOS analog in conjugation with heterocycles through an amide linkage (Figure 1.6).<sup>42</sup>

2-DOS mimic	R=	IC <sub>50</sub> (μM)
	H	> 1000
		> 1000
		> 1000
		450

**Figure 1.6** 2-DOS Amide analogs.

Although some of the synthetic compounds showed an increased binding affinity to the target RNA A-site, most of the compounds did not exhibit an enhanced binding activity. This is in contrast to the above example where one unit of the 2-DOS amide showed a dramatic increase in binding affinity with the addition of an alkyl tertiary amine, even though the amide functionality was present in a different position. It is hypothesized that the heterocycles involved in the second study may not have the ability to make the necessary electrostatic or hydrogen bonding interactions which could be due to inappropriate positioning of the amino groups within the synthesized rigid structures. Whereas, the first experiment employed a more flexible alkyl-amino arm that then participated in electrostatic interactions with the phosphate backbone and thus enhanced the binding affinity. These two contrasting experiments exemplify the significance of the subunits connected around the 2-DOS when involved in interactions with the target RNA.


Another pertinent experiment was done by Ding et al.<sup>43</sup> This group also prepared a series of heterocyclic 2-DOS-neamine mimics (Figure 1.7).

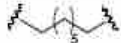

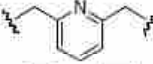
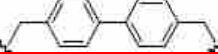
$K_d$ ( $\mu\text{M}$ )	275	355	1079	100	100
R					
					

**Figure 1.7** Ding et al. 2-DOS in conjugation with heterocyclic compounds.

Most of the compounds they developed demonstrated a modest increase in binding affinity with a conjugation of a variety of heterocycles, while the binding affinity of the compound containing an electron withdrawing group (CF<sub>3</sub>) did not show any increase. This implies that the subunit that is conjugated to the DOS analog has important implications in the role of small molecule to RNA binding and also suggests that the choice of the subunit has an influence in modifying the binding affinity for novel 2-DOS based RNA binding molecules.

Hergenrother et al.<sup>44</sup> provided very interesting results involving two 2-DOS analogs in the design of RNA-binding molecules that also gave evidence of the strong binding affinity between the RNA target site and 2-DOS (Table 1.1).



R	K <sub>d</sub> values (μM)			
	A	B	C	D
	299	157	280	288
	34	11	11	8
	325	138	97	200
	163	56	69	67
2-DOS monomer	>1000	>1000	>1000	>1000

Target RNA hairpins:

```

U G       U G
G U       G U
CG U      A A
GC        CG
CG        CG
GC        GC
5'CG3'    5'CG3'
A         B

```

```

U A G     U C A G
G U       G U
A A       A A
GC        GC
5'CG3'    5'CG3'
C         D

```

**Table 1.1** Hergenrother et al.<sup>44</sup> 2-DOS RNA stem loop binder dimers.

The 2-DOS dimer binds to a variety of RNA hairpin loops that contain two 5'-GU-3' recognition steps in the low micromolar range. Aminoglycosides, and other RNA binding small molecules, do not usually recognize those hairpin loops. It is



hypothesized that this increased binding affinity is simply due to the existence of an extra 2-DOS moiety, because the uncomplicated alkyl chain connectors cannot affect the binding affinity due to the nature of having an inadequate binding motif. The possibility of designing molecules solely on 2-DOS is clearly exemplified through this study.

Thus far, it is evident that RNA-binding molecules that contain at least two 2-DOS analogs can bind to target RNAs with an increased binding affinity, whereas molecules containing only one DOS analog bind with moderate to poor affinity. However, no studies mentioned have addressed the issue of sequence specificity. Therefore, it is pertinent that sequence specificity be investigated through compounds that use the monomeric building block. Experimenting in this way may result in a novel class of small RNA binding ligands that not only have a strong binding affinity, but also recognize their targets in a sequence specific manner.

## 1.5 References

- (1) Dahm, R. *Dev. Biol.* **2005**, *278*, 274-288.
- (2) Caspersson, T.; Schultz, J. *Nature* **1939**, *143*, 602-603.
- (3) Szathmáry, E. *Trends Genet.* **1999**, *15*, 223-229.
- (4) Napoli, C.; Lemieux, C.; Jorgensen, R. *Plant Cell* **1990**, *2*, 279-289.
- (5) Dafny-Yelin, M.; Chung, S.; Frankman, E.; Tzfira, T. *Plant Physiol.* **2007**, *145*, 1272-1281.
- (6) Ruvkun, G. *Science* **2001**, *294*, 797-799.
- (7) Fichou, Y.; Férec, C. *Trends Biotechnol.* **2006**, *24*, 563-570.
- (8) Zaman, G. J. R.; Michiels, P. J. A.; van Boeckel, C. A. A. *Drug Discov. Today* **2003**, *8*, 297-306.
- (9) Inouye, M. *Gene* **1988**, *72*, 25-34.
- (10) Simons, R. W. *Gene* **1988**, *72*, 25-34.
- (11) Mello, C. J. *Nature* **2004**, *431*, 338-342.
- (12) Gilmore, I.; Hollins, A.; Akthar, S. *Curr. Drug. Deliv.* **2006**, *3*, 147-155.
- (13) Zembower, T. R.; Noskin, G. A.; Postelnick, M. J.; Nguyen, C.; Peterson, L. R. *Int. J. Antimicrob. Agents* **1998**, *10*, 95.
- (14) Mingeot-Leclercq, M. P.; Glupczynski, Y.; Tulkens, P. M. *Antimicrob. Agents Chemother.* **1999**, *43*, 727-737.
- (15) Fletcher, H. G.; Anderson, L.; Lardy, H. A. *J. Org. Chem.* **1951**, *16*, 1238-1243.
- (16) Ennifar, E.; Paillart, J. C.; Marquet, R.; Ehresmann, B.; Ehresmann, C.; Dumas, P.; Walter, P. *J. Biol Chem.* **2003**, *273*, 2723.

- (17) Cabrera, C.; Gutierrez, A.; Barretina, J.; Blanco, J.; Litovchick, A.; Lapidot, A.; Clotet, B.; Este, J. A. *Antiviral Res.* **2002**, *53*, 1.
- (18) Faber, C.; Sticht, H.; Schweimer, K.; Rosch, P. *J. Biol Chem.* **2000**, *275*, 20660.
- (19) Mei, H. Y.; Galan, A. A.; Halim, N. S.; Mack, D. P.; Moreland, D. W.; Sanders, K. B.; Truong, H. N.; Czarnik, A. W. *Bioorg. Med. Chem. Lett.* **1995**, *5*, 2755.
- (20) Tok, J. B. -.; Dunn, L. J.; Des Jean, R. C. *Bioorg. Med. Chem. Lett.* **2001**, *11*, 1127-1132.
- (21) Eubank, T. D.; Biswas, R.; Jovanovic, M.; Litovchick, A.; Lapidot, A.; Gopalan, V. *FEBS lett.* **2002**, *511*, 107.
- (22) von Ahsen, U.; Noller, H. F. *Science* **1993**, *260*, 1500.
- (23) Corvaisier, S.; Bordeau, V.; Felden, B. *J. Biol Chem.* **2003**, *278*, 14788.
- (24) Kondo, J.; Francois, B.; Urzhumtsev, A.; Westhof, E. *Angew. Chem. Int. Ed.* **2006**, *45*, 3310.
- (25) Hobbie, S. N.; Pfister, P.; Brull, C.; Westhof, E.; Bottger, E. C. *Antimicrob. Agents Chemother.* **2005**, *49*, 5112-5118.
- (26) Yoshizawa, S.; Fourmy, D.; Eason, R. G.; Puglisi, J. D. *Biochemistry* **2002**, *41*, 6263-6270.
- (27) Vicens, Q.; Westhof, E. *ChemBiochem* **2003**, *4*, 1018-1023.
- (28) Vicens, Q.; Westhof, E. *Chemistry and Biology* **2002**, *9*, 747-755.
- (29) Moazed, D.; Noller, H. F. *Nature* **1987**, *327*, 389.

- (30) Fourmy, D.; Recht, M. I.; Blanchard, S. C.; Puglisi, J. D. *Science* **1996**, *274*, 1367.
- (31) Carter, A. P.; Clemons, W. M.; Brodersen, D. E.; Morgan-Warren, R. J.; Wimberly, B. T.; Ramakrishnan, V. *Nature* **2000**, *407*, 340-348.
- (32) Schluenzen, F.; Tocilj, A.; Zarivach, R.; Harms, J.; Gluehmann, M.; Janell, D.; Bashan, A.; Bartels, H.; Agmon, I.; Franceschi, F.; Yonath, A. *Cell* **2000**, *102*, 615-623.
- (33) Fourmy, D.; Yoshizawa, S.; Puglisi, J. D. *J. Mol. Biol.* **1998**, *277*, 333.
- (34) Vicens, Q.; Westhof, E. *Biopolymer* **2003**, *70*, 42.
- (35) Ogle, J. M.; Murphy, F. V.; Tarry, M. J.; Ramakrishnan, V. *Cell* **2002**, *111*, 721-732.
- (36) Pfister, P.; Hobbie, S.; Vicens, Q.; Bottger, E. C.; Westhof, E. *ChemBiochem* **2003**, *4*, 1078.
- (37) Ogle, J. M.; Ramakrishnan, V. *Annu. Rev. Biochem.* **2005**, *74*, 129-177.
- (38) Francois, B.; Russell, R. J. M.; Murray, J. B.; Aboula-ela, F.; Masquida, B.; Vicens, Q.; Westhof, E. *Nucleic Acids Res.* **2005**, *33*, 5677-5690.
- (39) Ogle, J. M.; Brodersen, D. E.; Clemons, W. M. J.; Tarry, M. J.; Carter, A. P.; Ramakrishnan, V. *Science* **2001**, *292*, 897-902.
- (40) Recht, M. I.; Fourmy, D.; Blanchard, S. C.; Dahlquist, K. D.; Puglisi, J. D. *J. Mol. Bio.* **1996**, *262*, 421-436.
- (41) Wang, X. J.; Migawa, M. T.; Sannes-Lowery, K. A.; Swayze, E. E. *Bioorg. Med. Chem. Lett.* **2005**, *15*, 4919-4922.

- (42) Vourloumis, D.; Takahashi, M.; Winters, G. C.; Simonsen, K. B.; Ayida, B. K.; Barluenga, S.; Qamar, S.; Shandrick, S.; Zhao, Q.; Hermann, T. *Bioorg. Med. Chem. Lett.* **2002**, *12*, 3367-3372.
- (43) Ding, Y. L.; Hofstadler, S. A.; Swayze, E. E.; Griffey, R. H. *Org. Lett.* **2001**, *3*, 1621-1623.
- (44) Liu, X. J.; Thomas, J. R.; Hergenrother, P. J. *J. Am. Chem. Soc.* **2004**, *126*, 9196-9197.

## CHAPTER 2. RESEARCH

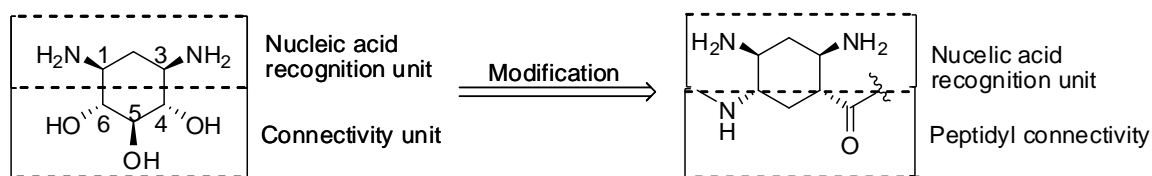
### **2.1 The design of 2, 4, 5-triaminocyclohexanecarboxylic acid as a novel 2-DOS mimetic**

Aminoglycosides are known to bind to RNA, however their binding is more dependent on the size of the asymmetric internal loop rather than the actual sequence of RNA.<sup>1,2</sup> This is due to the high degree of electrostatic interactions with the amine groups of aminoglycosides as well as their flexible glycosidic linkages. As a result there is no method for the development of small molecules that will recognize RNA in a sequence specific manner. Recent research has shown that the most conserved unit of aminoglycosides, 2-DOS, has the ability to recognize the 5'-3' GU region in a somewhat specific manner regardless of the sugar moieties that are attached.<sup>3</sup> Also, when 2-DOS is administered to RNA without aminosugar subunits, the small molecule still recognizes this region, however with a lowered binding affinity.<sup>4</sup> Thus, 2-DOS is a potential scaffold that can be used for the development of sequence specific RNA-binding small molecules.

The field of designing RNA binding small molecules based on structural information is still novel. Despite promising information regarding the sequence specific recognition ability of 2-DOS, there are no studies that have been performed to address the sequence specificity or selectivity in the design of 2-DOS based compounds. Thus, it is our goal to design and synthesize a novel

small molecule based on the structure of 2-DOS that not only has a high binding affinity but also has the ability to target a specific sequence of RNA.

Structure-based drug design has been a major proponent in understanding the interactions between a variety of RNA targets and small organic molecules. Our approach uses the highly conserved sequence-specific recognition pattern of 2-DOS to our advantage by creating a novel monomer that will have a more rigid connectivity as well as an increased hydrogen bonding capability through amide linkages (Figure 2.1).



**Figure 2.1** Modification of 2-DOS.

As depicted in Figure 1.4, the 1- and 3-NH<sub>2</sub> groups have specific hydrogen bonding interactions with the RNA helix which is important for recognition. The 4-, 5-, and 6-OH groups are used as connectivity units and are responsible for the promiscuous nature of aminoglycosides. Due to this issue, the design we have proposed involves replacing the 4- and 6-OH groups with amide linkages, forming an unnatural amino acid structure (Figure 2.1). The 5-OH has been omitted to simplify the chemistry and also because the aminosugar subunits, when connected on the 5-OH position of 2-DOS, is projected out of the target RNA helix and does not participate in recognizing the RNA sequence.

Furthermore, the ability to target GU rich regions of RNA double helices is possible by connecting two or more of the monomeric building blocks through

amide bonds. This strategy could be beneficial in the process of designing RNA binding small molecules that consist of high sequence specificities and strong binding affinities.

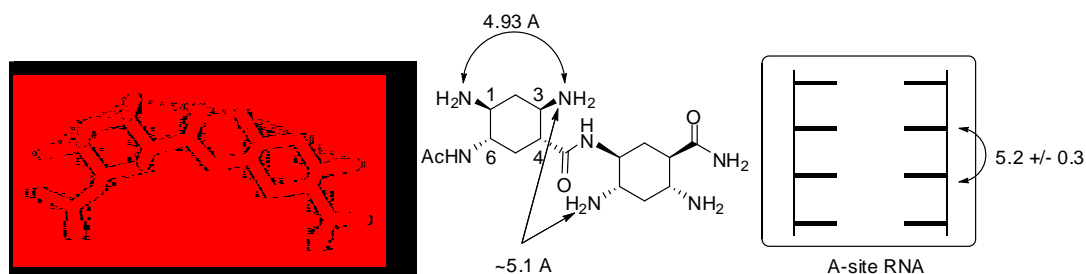
The addition of amide linkages to 2-DOS was first performed by Volourmis et al.<sup>5</sup> as discussed in the introduction. Their focus, however, was not on the binding specificity of small molecules to RNA. Yet, the introduction of amide linkages into the 2-DOS scaffold has several benefits that may help to promote specificity in binding. First of all, by replacing the glycosidic linkages with amide linkages the amount of free amino groups is decreased and limits the possibility of nonspecific electrostatic interactions. Also, amide linkages create rigidity in the backbone of the molecule, thus preventing the molecule to assume a variety of conformations.

Finally, the addition of amide linkages increases the ability of the small molecule to hydrogen bond. Hydrogen bonding is known to play a key role in specific ligand recognition and allows for the possibility to target certain RNA sequences that contain four or more consecutive nucleotides such as 5'-GUGU-3' for the first time.

Another essential component for a small molecule to have the ability to bind with specificity is to have the proper distance between recognition subunits. The approximate distance between RNA base steps of, specifically, the bacterial A-site is  $\sim 5.2 \pm 0.3$  angstroms. Introducing amide linkages to form a 2-DOS mimetic will give the small molecule the ability to perform hydrogen bonding between the amine recognition units. This will not only create a  $\sim 5.0$  angstrom

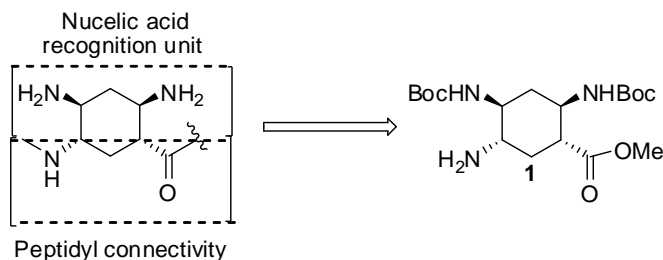


distance between the 1- and 3-NH<sub>2</sub> groups, but also between amino groups on neighboring monomers. The latter hydrogen bonding interaction causes the molecule to twist and may help to recognize RNA in a more specific manner (Figure 2.2).



**Figure 2.2** Hydrogen bonding interactions within the small molecule dimer causes a ~ 5.1 angstrom distance which is ideal for dsRNA recognition.

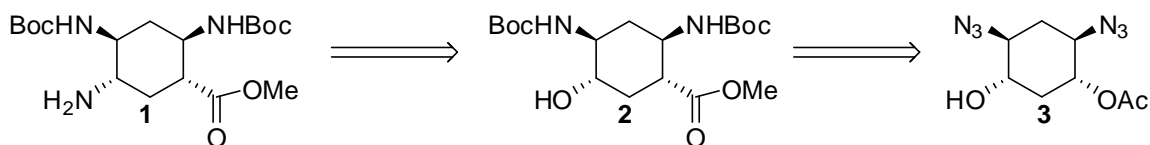
This project may lead to the first development of small molecules that recognize dsRNAs in a sequence-specific manner. Also, it has the potential to assist in the development of a new class of antibiotics that bacteria are not resistant to and have decreased toxicity characteristics to eukaryotes. Following is a discussion on the retrosynthesis and synthesis of the protected novel small molecule **1** as seen in Figure 2.3.



**Figure 2.3** The novel building block is formed through development of the protected small molecule **1**.

## 2.2 Synthesis of 2,4,5-Triaminocyclohexanecarboxylic acid as a 2-DOS mimic

As already discussed, a fully protected unnatural amino acid building block, **1**, is the target for the proposed research. The novel small molecule **1** can be developed from compound **3** which can be prepared from published procedures (Scheme 2.1).<sup>6, 7</sup>

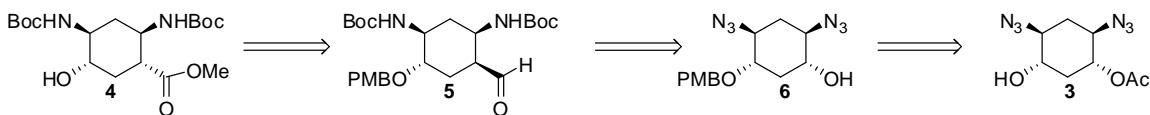


**Scheme 2.1** Retrosynthesis of the protected novel small molecule **1**.

Once **3** is formed, introduction of an ester followed by amino functional groups at the two hydroxyl positions are envisioned. Several different synthetic attempts were investigated before the most efficient method for making **1** was performed.

### 2.2.1 Introduction of Aldehyde Functionality

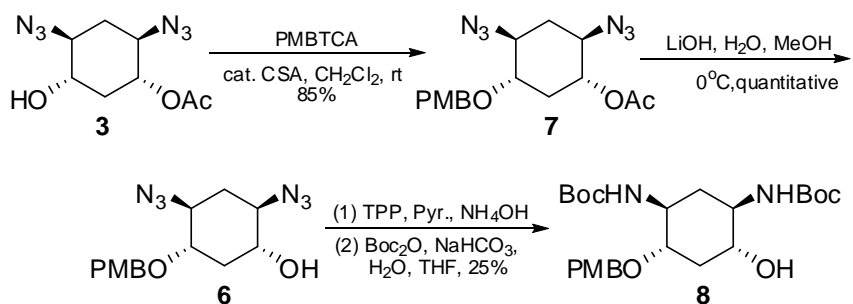
The initial approach involved using PMB as a protecting group and achieving **1** through an aldehyde moiety (Scheme 2.2).



**Scheme 2.2** Initial retrosynthetic analysis to synthesis compound **1**.

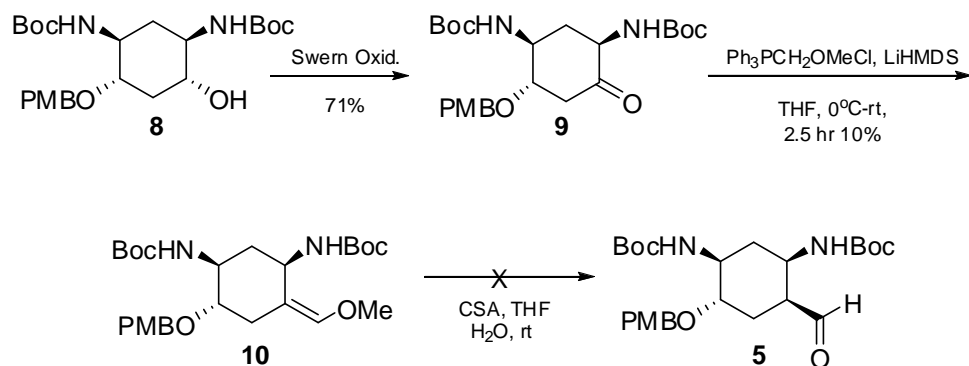
We proposed to begin with compound **3** which can be developed through two published procedures beginning with 1,4-cyclohexadiene and ending with a

stereospecific acetylation of a dihydroxy precursor using candida rugosa lipase.<sup>6,7</sup> Compound **3** was then protected using para-methoxybenzyl trichloroacetimidate (PMBTCA) and subsequently hydrolyzed to yield **7** and then **6** (Scheme 2.3).



**Scheme 2.3** Synthesis from compound **3** to **8**.

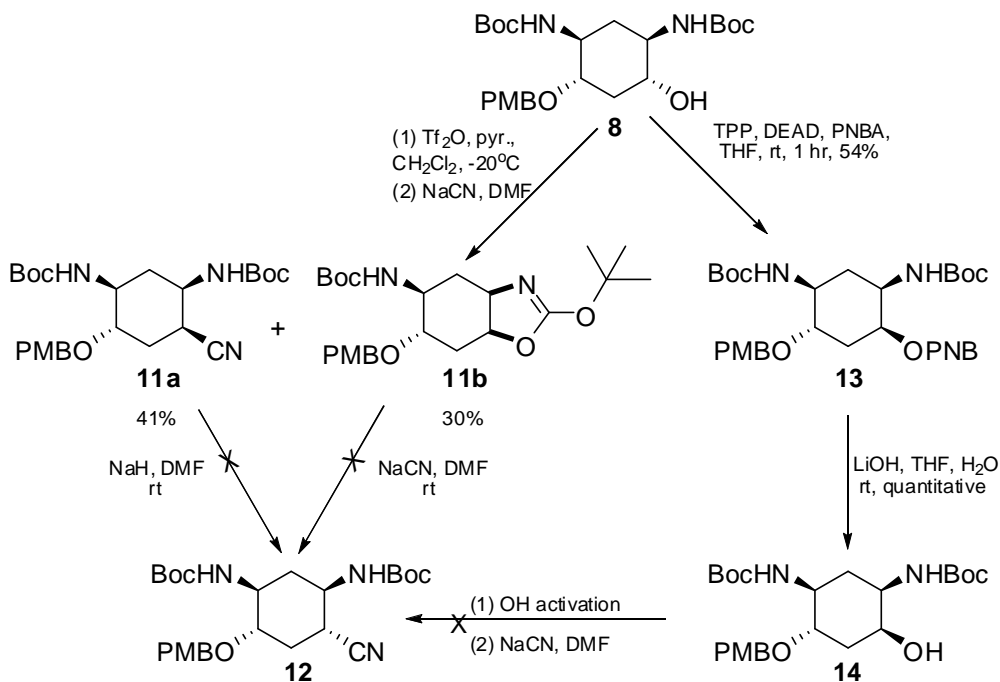
At this point the 1- and 3- position azide groups were reduced, and the corresponding amines were protected using di-tert-butyl dicarbonate (Boc<sub>2</sub>O) to form **8** (Scheme 2.3).



**Scheme 2.4** Synthesis from **8** to produce an aldehyde, **5**.

Initially we planned to convert the 6-OH of compound **8** to the corresponding carbonyl through the Swern oxidation reaction followed by a Wittig

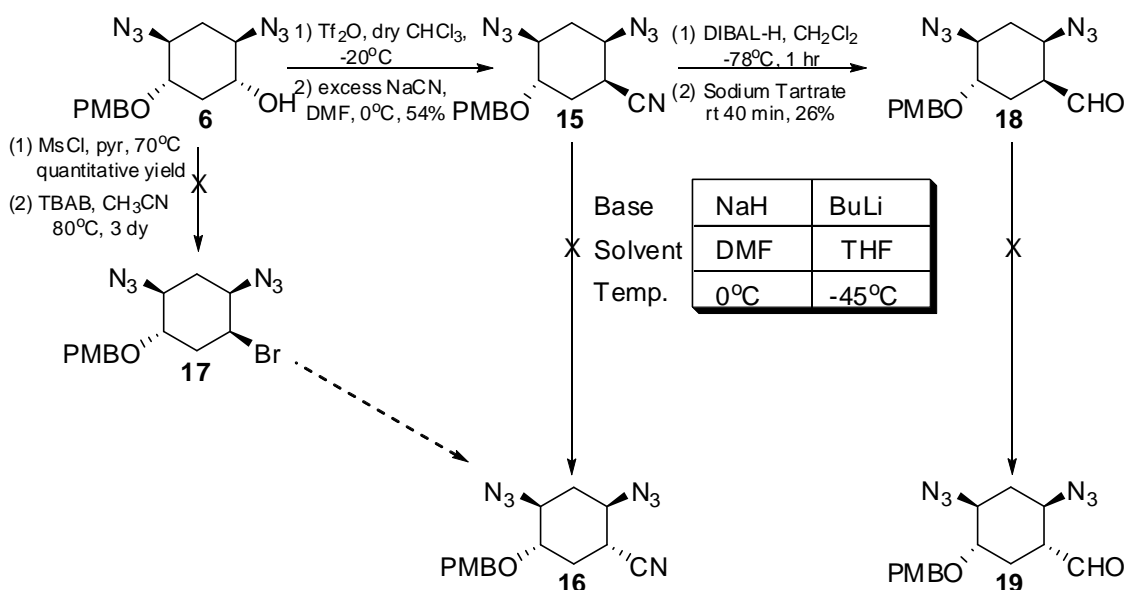
reaction, and then the isolated product after the Wittig reaction would then be transformed to an aldehyde.<sup>5</sup> Swern oxidation of **8** gave a 71% yield. However, the following Wittig reaction on **9** only gave **10** in a 10% yield and was not reproducible (Scheme 2.4).



**Scheme 2.5** Synthesis from **8** to produce the equatorial nitrile, compound **12**.

We then planned to convert the 6-OH group of **8** to the corresponding cyanide, but this product (**11a**) was obtained in low yield (Scheme 2.5). We also acquired product **11b**, which involved the 6-OH group, upon treatment with trifluoromethanesulfonic anhydride ( $\text{Tf}_2\text{O}$ ), being displaced by the neighboring carbamate oxygen in the Boc protected amine as depicted in Scheme 2.5. From there, we made an effort towards reopening the 5-membered ring with sodium cyanide ( $\text{NaCN}$ ), but the starting compound **11b** initially resulted in no reaction and upon heating at  $70^\circ\text{C}$  overnight became decomposed. With the small

amount of compound **11a** that was formed, we performed an epimerization on the axial nitrile to make compound **12**. However, no reaction was observed. We then performed a Mitsunobu on **8** using *p*-nitrobenzoic acid (PNBA), followed by hydrolysis. This resulted in the desired product, **14**; however, activation of the hydroxyl to do an S<sub>N</sub>2 displacement with NaCN resulted in a complex mixture of products (Scheme 2.5). At this stage, we determined that the Boc groups were interfering with the chemistry, so we returned to compound **6** to introduce the carbonyl functionality needed to make compound **1**.



**Scheme 2.6** Synthesis from compound **6** to introduce aldehyde.

From compound **6**, we set up to do a transformation on the 6-OH to either bromine or cyanide. Activating groups *p*-toluenesulfonyl chloride, methanesulfonyl chloride, 4-nitrobenzenesulfonyl chloride, and Tf<sub>2</sub>O were all studied. *p*-Toluenesulfonyl chloride and 4-nitrobenzenesulfonyl chloride did not react with **6**. It is believed that this result is due to steric hindrance with the PMB

protected 4-OH, thus making addition of the larger groups more challenging. On the other hand, when methanesulfonyl chloride was used, quantitative yields of the corresponding mesylated material was achieved. However, once the methanesulfonate activated compound was achieved, it was not able to be displaced by bromine or cyanide (Scheme 2.6).

The 6-OH of **6** was also able to be activated by reacting it with Tf<sub>2</sub>O in chloroform and then **15** could be formed with the use of excess NaCN. Once the cyanide product was achieved (54% yield), we then performed an epimerization reaction on the axial 6-CN using sodium hydride (NaH) or butyl lithium (*n*-butyl Li), but either no change was observed or a complex mixture of products was achieved (Scheme 2.6).

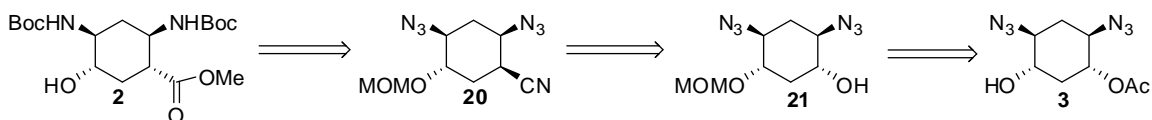
We next worked on transforming the cyanide product into an aldehyde using diisobutylaluminum hydride (DIBAL-H) but were only able to isolate the aldehyde product **18** with a 26% yield and mainly received a complex mixture of products.<sup>8</sup> We performed an epimerization reaction at this stage with the crude material. Several methods were studied as illustrated in table 2.1, but no change in the reaction was observed by TLC, MS or NMR (Scheme 2.5).

Base	Solvent	Temp.	Time
NaOH	THF/MeOH	rt	24 hr
K <sub>2</sub> CO <sub>3</sub>	DMF/MeOH	rt	24 hr
LDA	THF	-78°C	2-4 hr

**Table 2.1** Conditions for converting **18** to **19**.

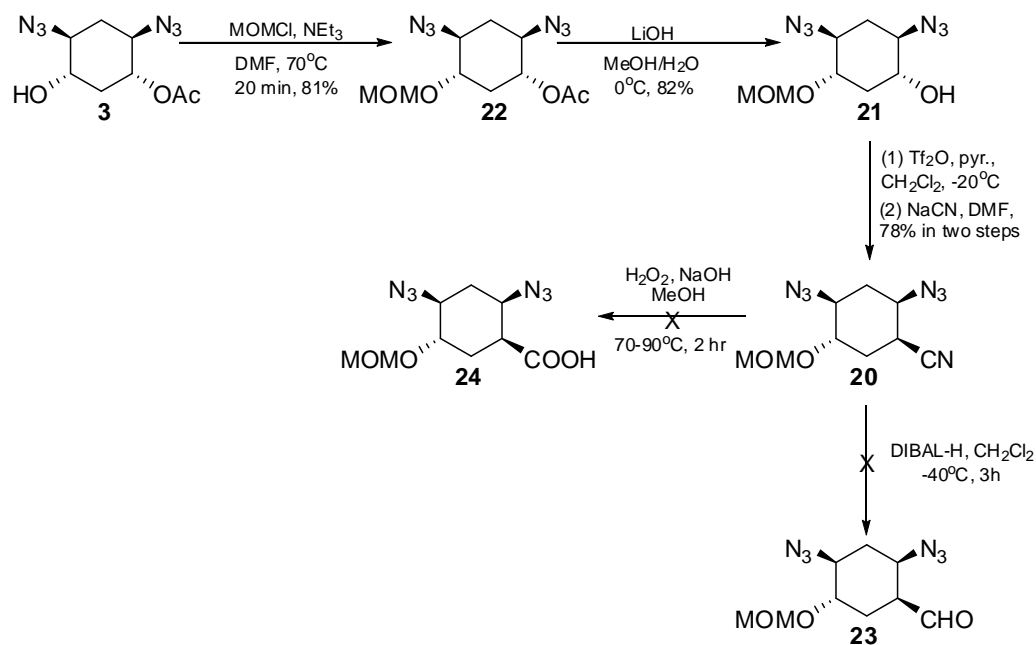
## 2.2.2 Introduction of Acid Functionality

After trials with tert-butyl-dimethylsilyl chloride (TBDMSCl), benzyl and trimethylsilyl chloride (TMSCl) protecting groups, we finally used methoxymethyl chloride (MOMCl) to protect the 4-OH group. Methoxymethyl (MOM) seemed to be a better candidate as it is a small protecting group that is not only easy to add but also easy to remove and doesn't leave byproducts that interfere with the reactions or the purity, unlike the PMB protecting group. Once the new protecting group was decided, we made a new retrosynthetic analysis that involved introducing the ester moiety through a nitrile functional group (**20**) (Scheme 2.7).



**Scheme 2.7** Retrosynthetic analysis to introduce acid functionality.

After redesigning the synthesis, we then set out to make compound **1**. We protected the 4-OH group of **3** with MOMCl to obtain **22**, and hydrolyzed the acetate group to form **21** in an isolated 82% yield (Scheme 2.8).



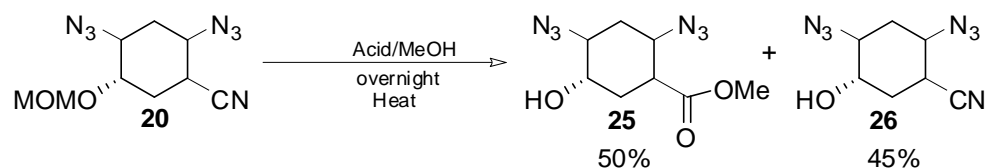
**Scheme 2.8** Synthesis from **3** to introduce either aldehyde or acid functionality.

Then the 6-OH group of **21** was converted to cyanide using  $\text{Tf}_2\text{O}$  and NaCN to give **20** over two steps in 78% yield (Scheme 2.8).

Our next attempts were to convert **20** to either an aldehyde, **23**, or an acid, **24**. The aldehyde conversion was performed once using DIBAL-H and a complex mixture of products was observed. (Scheme 2.8).<sup>8</sup>

From this point, an acid conversion method was completed. The acid conversion reaction was done using hydrogen peroxide and base in methanol (Scheme 2.8).<sup>9</sup> However, no reaction was observed.

Finally we performed an ester methanolysis on **20** (Scheme 2.9).



**Scheme 2.9** Reaction of **20** to form **25** and **26**.



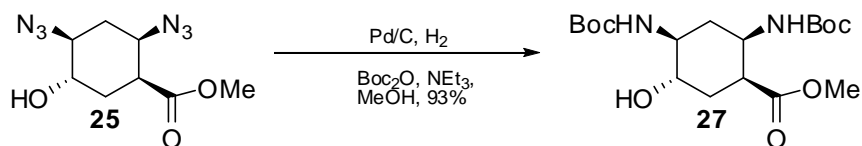
This method also gave the benefit of deprotecting MOM on the equatorial 4-OH group as well due to the convenient acid sensitive nature of the MOM substituent. This reaction required an extended reaction time in many cases and a wide range of yields were observed (Table 2.2).

Entry	Reagent	Solvent	Reaction vessel	Time	Temp °C watts	% yield
a	7.2 M HCl	dry MeOH	reflux	3 dy	70	50
b	H <sub>2</sub> SO <sub>4</sub> conc.	dry MeOH	reflux	8 dy	70	28
c	7.2 M HCl	dry MeOH	bomb flask	2 dy	90	50
d	H <sub>2</sub> SO <sub>4</sub> conc.	dry MeOH	bomb flask	2 dy	80-130	---
e	5.3 M HCl	dry MeOH	microwave	2 dy	70, 10	20
f	5.3 M HCl	dry MeOH	microwave	16 hr	100-110, 20	50
g	H <sub>2</sub> SO <sub>4</sub> conc.	dry MeOH	microwave	4 hr	100, 20	50
h	H <sub>2</sub> SO <sub>4</sub> conc.	dry MeOH	microwave	3 hr	140, 20	50

**Table 2.2** Esterification reaction studies going from compound **20** to **25**.

The method that we continued to use was anhydrous HCl in MeOH under reflux or bomb flask conditions overnight. This resulted in a 50% yield of product **25** as well as in a 45% yield isolation of **26**. It is important to note that heating the reaction higher than about 100°C would result in decomposition of the starting material, **20** (entry d, Table 2.2)

From this point, we reduced the azides of **25** and protected the corresponding amines with Boc to form **27** (Scheme 2.10).



**Scheme 2.10** Synthesis of **25** to **27**.

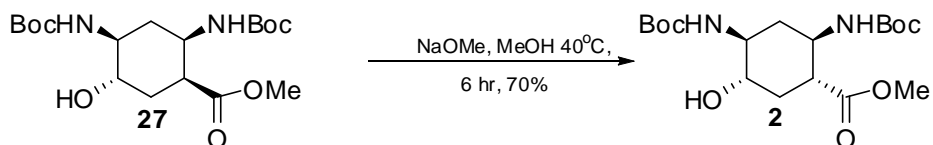
We then ran a series of epimerization reactions. Several different literature-reported conditions were employed for the epimerization that used bases such as LDA, LiHMDS, and KHMDS.<sup>10</sup>

	solvent	temp °C	% yield
LiHMDS	THF	-20, 0, rt	nr
KHMDS	THF	-20, 0	nr
NaH	THF	23, 40	nr
NaOMe	MeOH	23, 40, 55	30, 70, 15

formation of **2**

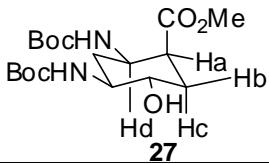
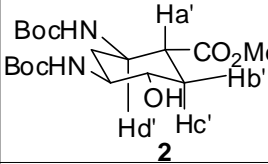
**Table 2.3** Epimerization reaction studies going from compound **27** to **2**.

None of these strong bases yielded product. NaH also resulted in no reaction at both room temperature and at 40°C. The best result was observed with sodium methoxide (NaOMe) in methanol (MeOH) at 40°C on the axial ester attachment **27** to transform the molecule to the more stable conformer, **2** (Scheme 2.11).



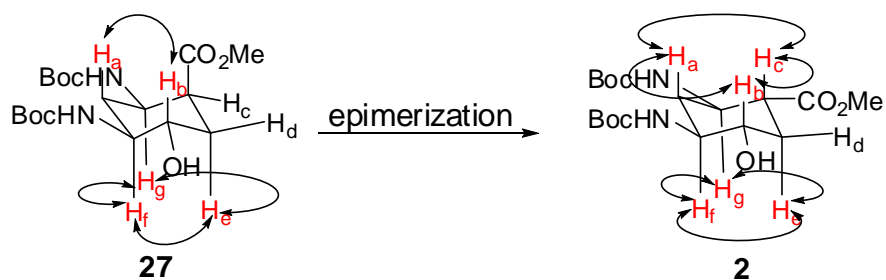
**Scheme 2.11** Epimerization of **27** to **2**.

The conformation of the compound **27** to **2** was confirmed by high-resolution NMR techniques (Table 2.4).

 <p style="text-align: center;"><b>27</b></p>	 <p style="text-align: center;"><b>2</b></p>
$J(\text{Ha}-\text{Hb}) = 4 \text{ Hz}$	$J(\text{Ha}'-\text{Hb}') = 4 \text{ Hz}$
$J(\text{Ha}-\text{Hc}) = 5 \text{ Hz}$	$J(\text{Ha}'-\text{Hc}') = 12 \text{ Hz}$
$J(\text{Ha}-\text{Hd}) = 8 \text{ Hz}$	$J(\text{Ha}'-\text{Hd}') = 12 \text{ Hz}$

**Table 2.4** Coupling constants between the neighboring Hydrogen's of the two epimers **27** and **2**.

The coupling constants between the neighboring hydrogen's provide clear evidence for the proper stereochemistry for both the starting compound **27** and the product **2**. In the case of **27**, the coupling constants were observed to be 4, 5, and 8 Hz, respectively for  $J(\text{H}_a-\text{H}_b)$ ,  $J(\text{H}_a-\text{H}_c)$  and  $J(\text{H}_a-\text{H}_d)$ , portraying an axial conformation for the ester subunit. Similarly, in the case of **2**, the NMR couplings  $J(\text{H}_{a'}-\text{H}_{b'})$ ,  $J(\text{H}_{a'}-\text{H}_{c'})$  and  $J(\text{H}_{a'}-\text{H}_{d'})$ , with values of 4, 12, and 12 Hz respectively, are consistent with the equatorial conformation of the ester. NOE studies further established the relative stereochemistry of both compounds (Figure 2.4).

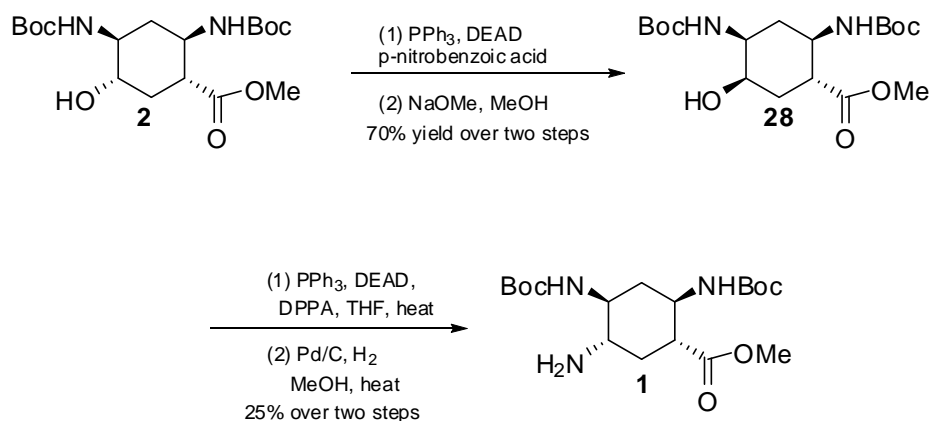


**Figure 2.4** NOE studies on transformation from **27** to **2**.

The NOE NMR studies showed only one NOE interaction between  $H_a$  and  $H_b$  on the top plane of molecule **27**. Three NOE interactions were observed between  $H_e$ ,  $H_f$ , and  $H_g$  indicating a 1,3-diaxial interaction for the hydrogens of compound **27** on the bottom plane. The NOE studies for compound **2** showed three interactions between  $H_a$ ,  $H_b$  and  $H_c$  as well as three interactions between  $H_e$ ,  $H_f$ ,  $H_g$  indicating 1,3-diaxial interactions between the hydrogens on both the upper and lower planes of compound **2**. These results further confirm the isolation of epimerized ester **2**.

### 2.2.3 Introduction of the Amine Functionality

After the successful addition of the ester onto the ring system, two consecutive Mitsunobu reactions were executed to introduce an equatorial amine in place of the 4-OH. The first Mitsunobu was performed on the 4-OH group of **2** using PNBA, switching the stereocenter of the equatorial 4-OH into the less stable axial position (Scheme 2.12).

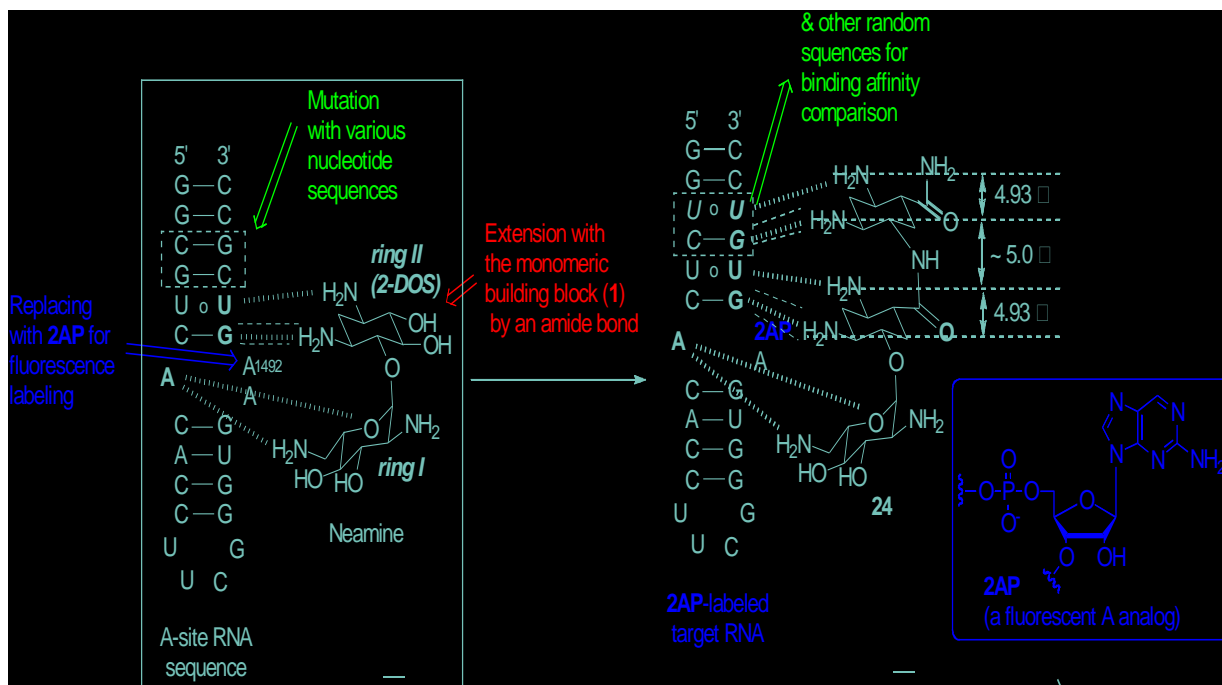


**Scheme 2.12** Formation of compound **1** from **2**.

This was followed by hydrolysis and another Mitsunobu reaction using DPPA which completed the introduction of an azide into the equatorial position (Scheme 2.12). The corresponding azide was transformed into an amine making compound **1** and completing the synthesis. The low yield is indicative of the Boc protecting groups inhibiting the formation of compound **1**. When the azide version of the Boc protected material was used instead, a much higher yield was obtained. Although only a 25% yield of **1** was isolated, the starting material was able to be recollected for further reactions. From here, **1** will be used to perform several fluorescence studies.

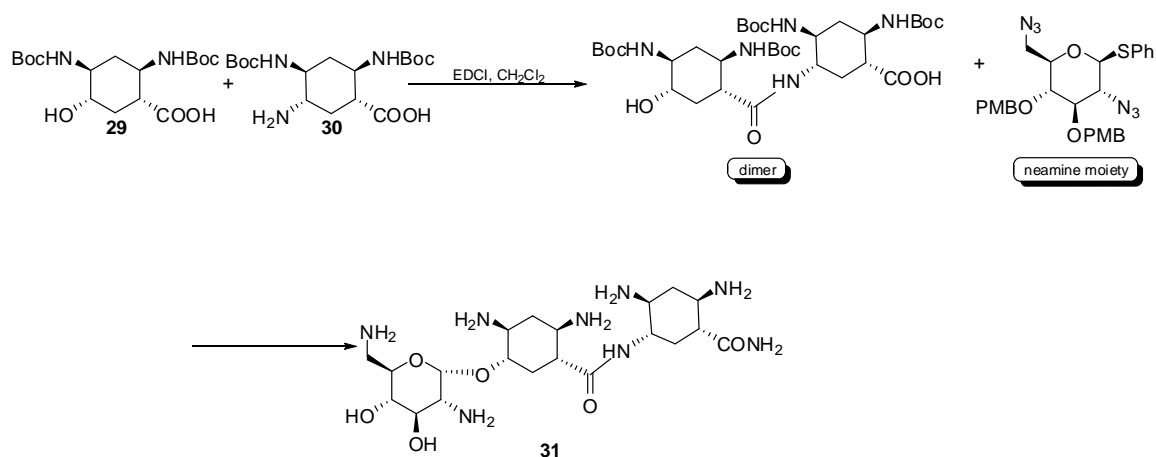
### 2.3 Conclusion and Future Works

Compound **1** was designed and synthesized as a novel 2-DOS mimetic, whose structure was developed through a rational design approach. In order to test whether the novel monomeric building block **1** has the ability to recognize the 5'-GU-3' RNA sequence, neamine will be used as a structural scaffold from which one or more units of the monomeric building block may be built upon (Figure 2.5).



**Figure 2.5** Sequence specific RNA binder and fluorescence assay. A hydrolyzed version of the novel monomeric building block **1** will be conjugated with a hydrolyzed version of **2** and a neamine moiety to recognize dsRNAs that contain the 5'GUGU-3' sequence step. The dotted line refers to interchangeable nucleotides for binding affinity and specificity studies. The A1492 residue will be replaced with a 2-aminopurine (2-AP), a fluorescent analog of adenosine. Upon the binding of the small molecule, the fluorescence of 2-AP will decrease.

The highly conserved binding interactions of rings I and II of neamine with a variety of aminoglycosides make it a valuable structural scaffold for this research. As a beginning experiment (**30**) or the hydrolyzed version of the novel monomeric building block **1**, will be coupled to a hydrolyzed version of compound **2** (**29**) to form a dimer. The dimer will then undergo a reaction with a neamine moiety<sup>11</sup> that can be prepared through a published procedure to form a novel dimer (**31**) (Scheme 2.13).



**Scheme 2.13** Proposed synthesis of initial molecular structure for RNA binding study.

The C-terminus of the novel peptidomimetic will be introduced with a carboxamide to avoid electrostatic repulsion between the carboxy end and the negatively charged RNA backbone. Meanwhile, the target RNA sequence will be replaced with 5'GU-3'/3'-CU-5' base pairs and other random sequences for the nucleotides indicated by the dotted rectangle in Figure 2.5. The proposed small molecule will be tested against each of the different sequences of RNA for the purpose of comparison between binding affinities which will be determined through a fluorescence assay. These studies will provide information on the binding specificity of the novel monomeric building block between the different sequences and whether it prefers the 5'-GU-3' base over the other sequences.

This research may lead to the first development of small molecules that not only recognize dsRNAs in a sequence-specific manner but also will lead to a better understanding of the underlying principles that govern RNA recognition by small molecules and ultimately allow us to be able to develop small molecular codes or sequences for sequence- and or site-specific RNA recognition. We

could then have the opportunity to be able to study or to control important cellular functions. These molecular codes, once developed, may also be utilized in the process of designing novel antibiotics, antiviral and anticancer pharmaceuticals or agents as well as assist in the understanding of gene regulation mechanisms such as riboswitches and microRNAs. Further studies with our novel small molecule involve utilizing the unnatural  $\gamma$ -amino acid utility to build synthetic foldamers that mimic the structures and/or functions of natural proteins.



## 2.4 References

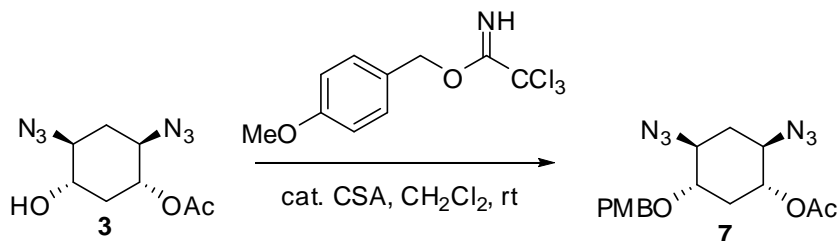
- (1) Hobbie, S. N.; Pfister, P.; Brull, C.; Westhof, E.; Bottger, E. C. *Antimicrob. Agents Chemother.* **2005**, *49*, 5112-5118.
- (2) Mei, H. Y.; Galan, A. A.; Halim, N. S.; Mack, D. P.; Moreland, D. W.; Sanders, K. B.; Truong, H. N.; Czarnik, A. W. *Bioorg. Med. Chem. Lett.* **1995**, *5*, 2755.
- (3) Francois, B.; Russell, R. J. M.; Murray, J. B.; Aboula-ela, F.; Masquida, B.; Vicens, Q.; Westhof, E. *Nucleic Acids Res.* **2005**, *33*, 5677-5690.
- (4) Yoshizawa, S.; Fourmy, D.; Eason, R. G.; Puglisi, J. D. *Biochemistry* **2002**, *41*, 6263-6270.
- (5) Vourloumis, D.; Takahashi, M.; Winters, G. C.; Simonsen, K. B.; Ayida, B. K.; Barluenga, S.; Qamar, S.; Shandrick, S.; Zhao, Q.; Hermann, T. *Bioorg. Med. Chem. Lett.* **2002**, *12*, 3367-3372.
- (6) Magnet, S.; Blanchard, J. *Chem. Rev.* **2002**, *105*, 477-497.
- (7) Chenevert, R.; Jacques, F. *Tetrahedron-Assymetr.* **2006**, *17*, 1017-1021.
- (8) Papahatjis, D. P.; Nahmias, V. R.; Nikas, S. P.; Andreou, T.; Alapafuja, S. O.; Tsotinis, A.; Guo, J.; Fan, P.; Makriyannis, A. *J. Med. Chem.* **2007**, *50*, 4048-4060.
- (9) Sekiyama, Y.; Palaniappan, N.; Reynolds, K. A.; Osada, H. *Tetrahedron* **2003**, *7465*, 7471.
- (10) Klotz, P.; Mann, A. *Tetrahed. Lett.* **2003**, *44*, 1927-1930.
- (11) Vourloumis, D.; Winters, G.; Takahashi, M.; Simonsen, K.; Ayida, B.; Shandrick, S.; Zhao, Q.; Hermann, T. *ChemBioChem* **2003**, *4*, 879-885.

## CHAPTER 3. EXPERIMENTAL AND SPECTROSCOPIC DATA

### 3.1 General Methods

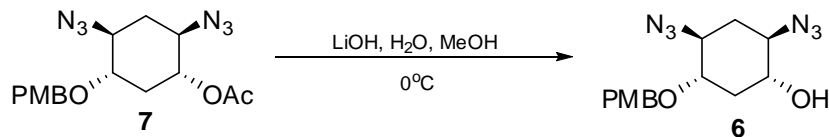
Tetrahydrofuran, N,N-dimethylformamide, triethylamine, methylene chloride, methanol, pyridine, acetonitrile, and dimethyl sulfoxide were dried by a glass contour solvent drying system containing cylinders activated alumina. Flash chromatography was done using 60 to 230 mesh silica gel. <sup>1</sup>H NMR spectra were obtained on Varian 500 MHz spectrometer, with chloroform (7.27 ppm), dimethylsulfoxide (2.50 ppm) or tetramethylsilane (0.00 ppm) as an internal reference. Signals are reported as follows: s (singlet), d (doublet), t (triplet), q (quartet), dd (doublet of doublets), ddd (doublet of doublet of doublets), dt (doublet of triplets), br s (broad singlet), br d (broad doublet), br q (broad quartet), br dt (broad doublet of triplet), m (multiplet). Coupling constants are reported in hertz (Hz). <sup>13</sup>C NMR spectra were obtained on a Varian spectrometer operating at 125 MHz, with chloroform (77.23 ppm) or dimethylsulfoxide (40.45 ppm) as internal reference. Optical rotations were obtained using a Perkin-Elmer 241 Polarimeter. Mass spectral data were obtained using ESI techniques from the Brigham Young University mass spectrometry facility. Melting point data were obtained using a Meltemp electrothermal apparatus. Microwave reactions were run on a CEM Discover System. Reactions for compounds from **25**, **27**, **2**, **28**, and **1** were primarily run by Dr. Maruthi Chittapragada, a postdoctoral candidate in our laboratory. Studies for those reactions were also carried out by Dr. Chittapragada

### 3.2 Experimental Data



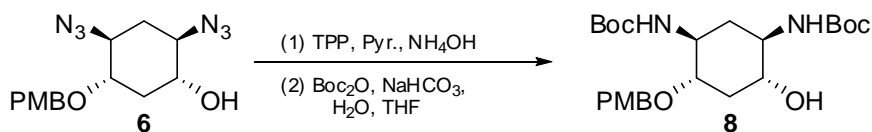
#### **(1R,2R,4S,5S)-2,4-diazido-5-(4-methoxybenzyloxy)cyclohexyl acetate (7).**

380 mg of compound **3** (1.6 mmol) was added to a flask of dry dichloromethane (3 mL). Camphorsulfonic acid was added into the mixture (0.32 mmol, 74 mg). Para-methoxybenzyl trichloroacetimidate (15.9 mmol, 3.3 mL) was added and the reaction mixture was stirred at room temperature for two days. The reaction was then transferred to a separatory funnel with dichloromethane and the organic mixture was washed with 1.0 N HCl followed by saturated  $\text{NaHCO}_3$  and brine. The organic layers were collected and dried with anhydrous  $\text{MgSO}_4$  and then filtered. After concentrating down, the crude material was purified by flash chromatography on silica gel. 1.5 g of material was obtained. TLC  $R_f = 0.52$ ;  $^1\text{H}$  NMR (500 MHz,  $\text{CDCl}_3$ )  $\delta$  7.30 (d, 2H,  $J = 8.79$  Hz), 6.90 (d, 2H,  $J = 8.79$  Hz), 4.68 (m, 1H), 4.57 (q, 1H,  $J = 10.74$  Hz), 3.81 (s, 3H), 3.5-3.38 (m, 4H), 2.55 (m, 1H), 2.3 (m, 1H), 2.11 (s, 3H), 1.45 (q, 1H,  $J = 11.72$  Hz), 1.3 (q, 1H,  $J = 12.69$  Hz);  $^{13}\text{C}$  NMR (125 MHz,  $\text{CDCl}_3$ )  $\delta$  170, 160, 130, 114, 78, 73, 72, 62, 61, 55, 34, 33, 21; HRMS (ESI) found 378.1884  $[\text{M} + \text{NH}_4]^+$ , calcd 360.1500 for  $[\text{C}_{16}\text{H}_{20}\text{N}_6\text{O}_4]^+$ .



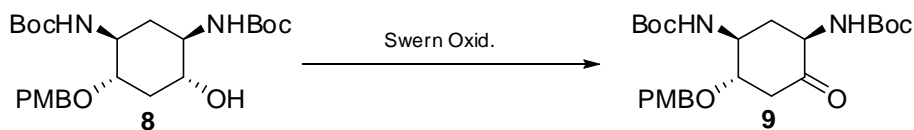
**(1R,2R,4S,5S)-2,4-diazido-5-(4-methoxybenzyloxy)cyclohexanol(6).**

Intermediate to **6** (1.5 g, 4.0 mmol) was then placed in an ice bath at 0°C. Methanol and water were added in a 1:1 ratio (10 mL) and 1.0 N NaOH (4.8 mmol, 4.8 mL) was added. The reaction was stirred for 4 hours from 0°C to room temperature. After checking TLC, the reaction was quenched by concentrating down and extracting with dichloromethane and water. The organic layer was dried over anhydrous MgSO<sub>4</sub>, filtered and concentrated down again. The crude material was purified by flash chromatography on silica gel. This procedure afforded 290 mg (58% yield over two steps). TLC  $R_f$  = 0.20; <sup>1</sup>H NMR (500 MHz, CDCl<sub>3</sub>) δ 7.30 (d, 2H,  $J$  = 8.31 Hz), 6.90 (d, 2H,  $J$  = 8.30 Hz), 4.58 (q, 2H,  $J$  = 11.23 Hz), 3.81 (s, 3H), 3.50-3.29 (m, 4H), 2.41(dt, 1H,  $J$  = 13.19, 4.39 Hz), 2.29 (br d, 1H,  $J$  = 3.42 Hz), 2.22 (dt, 1H,  $J$  = 13.18, 4.88 Hz), 1.45 (q, 1H,  $J$  = 11.47 Hz), 1.30 (q, 1H,  $J$  = 11.47 Hz); <sup>13</sup>C NMR (125 MHz, CDCl<sub>3</sub>) δ 160, 130, 114, 78, 72, 71, 64, 62, 56, 36, 32; HRMS (ESI) found 341.1333 [M + Na]<sup>+</sup>, calcd 318.1400 for [C<sub>14</sub>H<sub>18</sub>N<sub>6</sub>O<sub>3</sub>]<sup>+</sup>.



**tert-butyl (1S,3R,4R,6S)-4-hydroxy-6-(4-methoxybenzyloxy)cyclohexane-1,3-diylidicarbamate (8).** Compound **6** (150 mg, 0.46 mmol) was stirred with a mixture of pyridine and ammonium hydroxide (7:1 ratio). Triphenylphosphine (420 mg, 1.6 mmol) was added, and the reaction was stirred for 4 hours at room temperature. The reaction was checked by TLC and then concentrated down until a white solid was achieved. After which, the corresponding amine compound was placed in an ice bath 0°C. Dioxane, water, and sodium bicarbonate were added in a 1:1: 0.7 ratio. While the solution was stirring, Boc anhydride (350 mg, 1.6 mmol) was added. The reaction was allowed to stir for 4 hours from 0°C to room temperature. The reaction mixture turned white and cloudy. After 4 hours, the reaction was checked by TLC and concentrated down. Compound **8** was then dissolved in dichloromethane and washed with 1.0 N HCl, followed by saturated NaHCO<sub>3</sub> and then brine. The organic layer was dried with anhydrous MgSO<sub>4</sub>, filtered and concentrated in vacuo. The resulting crude compound was purified by flash chromatography on silica gel and resulted in a white powder for pure **8**, with 54 mg (25% yield). TLC  $R_f = 0.80$ ; <sup>1</sup>H NMR (500 MHz, DMSO)  $\delta$  7.20 (d, 2H,  $J = 8.79$  Hz), 6.80 (d, 2H,  $J = 8.79$  Hz), 6.79 (br d, 1H,  $J = 8.30$  Hz), 6.60 (br d, 1H,  $J = 7.33$  Hz), 4.61 (br d, 1H,  $J = 5.37$  Hz), 4.45 (d, 1H,  $J = 11.23$  Hz), 4.38 (d, 1H,  $J = 11.23$  Hz), 3.70 (s, 3H), 3.30-3.0 (bm, 4H), 2.19 (dt, 1H,  $J = 12.7$ . 3.90 Hz), 1.70-1.80 (br d, 1H,  $J = 12.2$  Hz), 1.39 (s, 18H), 1.26-1.04 (m, 2H); <sup>13</sup>C NMR (125 MHz, DMSO)  $\delta$  160, 156, 132, 129, 114, 79 (two peaks), 71, 69, 56,

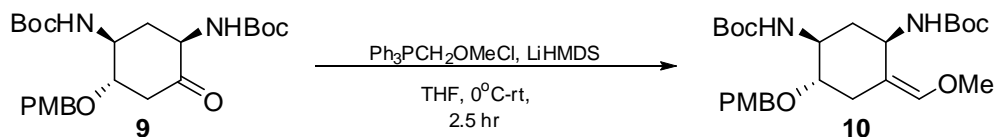
55, 53, 38, 36, 29; HRMS (ESI) found 467.2752  $[M + H]^+$ , calcd 466.2752 for  $[C_{24}H_{38}N_2O_7]^+$ ; MP = 179.1-182.6°C;  $[\alpha]_D^{24} = -0.198^\circ$  (c 1.01, MeOH).



**tert-butyl(1R,3S,4S)-4-(4-methoxybenzyloxy)-6-oxocyclohexane-1,3-**

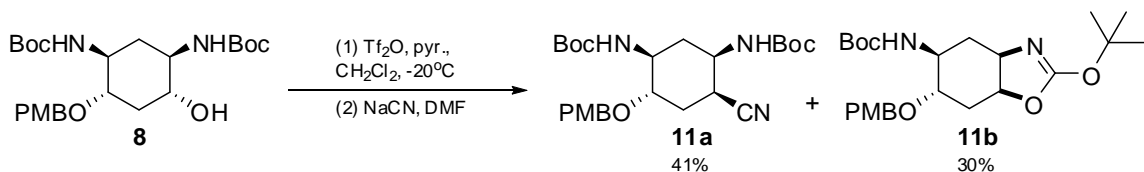
**diydicarbamate (9).** In a -60°C dry ice bath, oxalyl chloride (88  $\mu$ l, 1.0 mmol) and dry dimethylsulfoxide (140  $\mu$ l, 2.0 mmol) were added to a dry round bottom flask under argon. The two chemicals were allowed to stir together for 10 minutes, after which compound **8** (94 mg, 0.2 mmol) in dichloromethane was added to the solution. At this point, the reaction mixture was allowed to stir for 1 hour. After which, dry triethylamine (700  $\mu$ l, 5.0 mmol) was added and the reaction was warmed to -20°C, and allowed to stir at that temperature for 15 minutes. After which the reaction was allowed to stir at room temperature for 30 minutes. The reaction was extracted with dichloromethane and washed with 1.0 N HCl followed by saturated  $NaHCO_3$  and dried on anhydrous  $MgSO_4$  and filtered. The reaction mixture was then concentrated down in vacuo and was purified using flash chromatography on silica gel. A white solid was isolated in a yield of 76 mg or 81%. TLC  $R_f = 0.60$ ;  $^1H$  NMR (500 MHz,  $CDCl_3$ )  $\delta$  7.30 (d, 2H,  $J = 8.79$  Hz), 6.90 (d, 2H,  $J = 8.30$  Hz), 5.22 (br s, 1H), 4.60 (d, 1H,  $J = 11.72$  Hz), 4.40 (d, 1H,  $J = 11.72$  Hz), 4.35 (br s, 1H), 3.90 (m, 1H), 3.80 (s, 3H), 3.50 (m, 1H), 2.98 (dd, 1H,  $J = 13.67, 4.88$  Hz), 2.80 (m, 1H), 2.55 (t, 1H,  $J = 12.2$  Hz);  $^{13}C$  NMR (125 MHz,  $CDCl_3$ )  $\delta$  204, 160, 155, 130, 114, 80, 71, 70, 57, 56, 54, 52, 44, 35, 29;

HRMS (ESI) found 465.2595  $[M + H]^+$ , calcd 464.2500 for  $[C_{24}H_{38}N_2O_7]^+$ ;  $[\alpha]_D^{24} = +3.99^\circ$  (c 0.025,  $CHCl_3$ ).



**tert-butyl(1R,3S,4S,Z)-4-(4-methoxybenzyloxy)-6-(methoxymethylene)cyclohexane-1,3-diyl dicarbamate(10).** Triphenylphosphinemethoxymethyl

chloride (270 mg, 0.78 mmol) and LiHMDS (150  $\mu$ l, 0.77 mmol) were added to dry THF at 0°C and allowed to stir together. After 10 minutes **9** was added and the reaction was stirred for 2.5 hours and monitored by TLC.{{134 Vourloumis, D. 2002}} The reaction was then dissolved in dichloromethane and washed with 1.0 N HCl and saturated  $NaHCO_3$ . The organic layer was then dried over anhydrous  $MgSO_4$ , filtered and concentrated down. The reaction mixture was then purified by flash chromatography and yielded a white solid, **10** (5.6 mg, 10% yield). TLC  $R_f = 0.80$ ;  $^1H$  NMR (500 MHz, Solvent)  $\delta$  7.20 (d, 2H,  $J = 8.79$  Hz), 6.85 (d, 2H,  $J = 8.79$  Hz), 5.95 (d, 1H,  $J = 8.79$  Hz Hz), 4.60 (d, 1H,  $J = 11.72$  Hz), 4.50 (m, 1H), 4.40 (d, 1H,  $J = 11.23$  Hz), 4.30 (br s, 1H), 3.90 (br s, 1H), 3.80 (s, 3H), 3.75 (s, 3H), 3.70 (d, 1H,  $J = 9.72$ ), 2.95 (m, 1H), 2.70 (m, 1H), 2.55 (t, 1H,  $J = 12.21$ ), 2.0 (br s, 2H);  $^{13}C$  NMR (125 MHz, Solvent)  $\delta$  132, 131, 129, 117, 114, 71, 71, 62, 60, 58, 55, 54, 34, 30, 28, 18, 15; HRMS (ESI) found 493.2403  $[M + H]^+$ , calcd 492.2800 for  $[C_{26}H_{40}N_2O_7]^+$ .

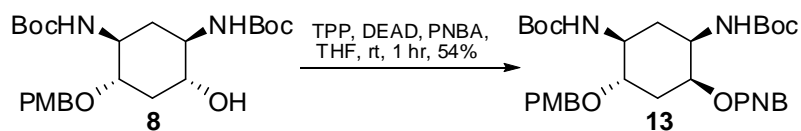


**tert-butyl (1S,3R,4S,6S)-4-cyano-6-(4-methoxybenzyloxy)cyclohexane-1,3-diyl**dicarbamate (**11a**) and **byproduct (11b)**. Compound **8** (42 mg, 0.091 mmol)

was dissolved in excess dry dichloromethane and cooled to  $-20^{\circ}\text{C}$ . The vial was purged with argon gas after which pyridine (15  $\mu\text{l}$ , 0.18 mmol) and then trifluoromethanesulfonic anhydride (30  $\mu\text{l}$ , 0.18 mmol) were added. Reaction was monitored by TLC. After the starting material was gone, the reaction was washed with cold 1.0 N HCl and dried on anhydrous  $\text{MgSO}_4$ . The organic layer was then concentrated down with no heat and placed in an ice bath. Minimal amounts of dimethylformamide were added, followed by excess sodium cyanide. The reaction was allowed to stir for 30 minutes. The TLC was checked and the reaction was concentrated down under high vacuum. The resulting reaction mixture was then dissolved in dichloromethane and washed with 1.0 N HCl, and saturated  $\text{NaHCO}_3$  until all the dimethylformamide was removed. The dichloromethane layer was collected and dried over anhydrous  $\text{MgSO}_4$  followed by filtration. The liquid was then concentrated down to result in a yellow oil **11a/11b** (**11a** 18 mg, 41%; **11b** 12 mg, 30%). **11a**: TLC  $R_f = 0.80$ ;  $^1\text{H}$  NMR (500 MHz,  $\text{CDCl}_3$ )  $\delta$  7.30 (d, 2H,  $J = 7.34$  Hz), 6.90 (d, 2H,  $J = 8.56$  Hz), 4.80 (br s, 1H), 4.60 (d, 1H,  $J = 11.49$  Hz), 4.50 (br s, 1H), 4.40 (d, 1H,  $J = 11.49$  Hz), 3.80 (s, 3H), 3.78 (br s, 1H), 3.50 (m, 1H), 3.30 (m, 1H), 2.55 (m, 2H), 2.30 (m, 2H) 1.60 (m, 1H), 1.40 (d, 18H,  $J = 17.12$  Hz);  $^{13}\text{C}$  NMR (125 MHz,  $\text{CDCl}_3$ )  $\delta$  161,

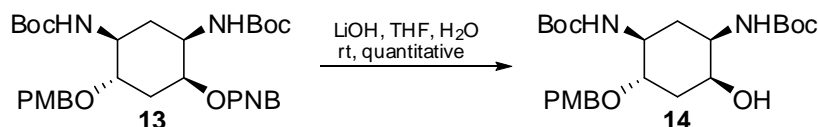


160, 156, 155, 130 (2 peaks), 114, 76, 72, 71.5, 71, 64, 56, 54, 34, 28. **11b**: TLC  $R_f = 0.30$ ;  $^1\text{H NMR}$  (500 MHz,  $\text{CDCl}_3$ )  $\delta$  7.30 (d, 2H  $J = 8.80$  Hz), 6.90 (d, 2H,  $J = 8.56$  Hz), 4.60 (d, 1H,  $J = 11.49$  Hz), 4.58-4.45 (m, 2H), 4.38 (d, 1H,  $J = 11.49$  Hz), 3.80 (s, 3H), 3.50-3.30 (m, 3H), 3.30-3.10 (m, 2H), 2.50 (m, 1H), 2.30 (m, 1H), 1.40 (s, 18H); HRMS (ESI) found 449.2646  $[\text{M} + \text{H}]^+$ , calcd 448.2600 for  $[\text{C}_{24}\text{H}_{36}\text{N}_2\text{O}_6]^+$ .

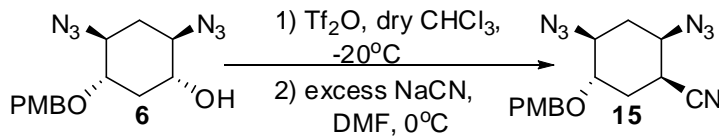


**(1S,2R,4S,5S)-2,4-bis(tert-butoxycarbonylamino)-5-(4-methoxybenzyloxy)**

**cyclohexyl 4-nitrobenzoate (13)**. Triphenyl Phosphine (66.1 mg, 0.25 mmol), DEAD (46  $\mu\text{l}$ , 0.25 mmol), and PNBA (42 mg, 0.25 mmol) were mixed together in dry THF for 10 minutes at room temperature, after which **8** was added (78 mg, 0.17 mmol). Reaction was stirred for 3 hours and monitored by TLC. Reaction was concentrated down and purified by flash chromatography. A white solid, **13**, was achieved (56 mg, 54%). TLC  $R_f = 0.75$ ;  $^1\text{H NMR}$  (500 MHz,  $\text{CDCl}_3$ )  $\delta$  8.30 (m, 2H), 8.10 (m, 2H), 7.20 (d, 2H,  $J = 8.30$  Hz), 6.70 (d, 2H,  $J = 7.81$  Hz), 5.45 (s, 1H), 4.70 (br s, 1H), 4.50 (d, 1H,  $J = 11.72$  Hz), 4.35 (d, 1H,  $J = 11.72$  Hz), 3.90 (br s, 1H), 3.70 (s, 3H), 3.60 (br s, 1H), 2.50 (br d, 1H,  $J = 14.16$  Hz), 2.30 (br d, 1H,  $J = 11.72$  Hz), 1.80 (br s, 1H), 1.60 (t, 1H,  $J = 12.21$  Hz).

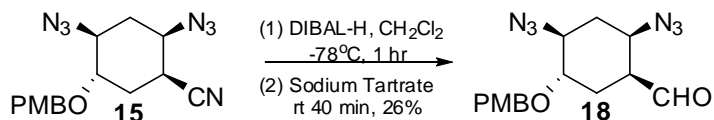


**tert-butyl (1S,3R,4S,6S)-4-hydroxy-6-(4-methoxybenzyloxy)cyclohexane-1,3-diyl dicarbamate (14).** Compound **13** (56 mg, 0.091 mmol) was dissolved in a 1:1 mixture of THF and water. After which, LiOH was added (110  $\mu$ l, 0.11 mmol). Reaction was stirred at room temperature for 2 hours and monitored by TLC. The reaction was quenched with 1.0 N HCl and extracted with dichloromethane. The organic layer was then washed with saturated NaHCO<sub>3</sub>, dried on anhydrous MgSO<sub>4</sub> and filtered. The organic layer was concentrated down and resulted in a white solid, **14**. TLC  $R_f$  = 0.50 ; <sup>1</sup>H NMR (500 MHz, Solvent)  $\delta$  7.25 (d, 2H,  $J$  = 8.81 Hz), 6.85 (d, 2H,  $J$  = 8.32 Hz), 4.80 (br s, 1H), 4.60 (d, 1H,  $J$  = 11 Hz), 4.40 (d, 1H,  $J$  = 11.49 Hz), 4.20 (m, 1H), 4.10 (br s, 1H), 3.65 (br s, 1H), 3.50 (br s, 1H), 2.30 (br d, 1H,  $J$  = 11.82 Hz), 2.10 (br s, 1H), 1.60 (br s, 1H), 1.25 (m, 1H).



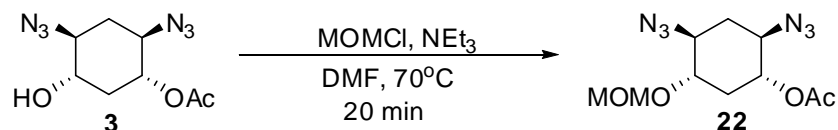
**(1S,2R,4S,5S)-2,4-diazido-5-(4-methoxybenzyloxy)cyclohexanecarbonitrile (15).** Compound **6** (15 mg, 0.047 mmol) was dissolved in excess dry chloroform and cooled to -20°C. The vial was purged with argon gas after which pyridine (26  $\mu$ l, 0.33 mmol) and then trifluoromethanesulfonic anhydride (55  $\mu$ l, 0.33 mmol) were added 1.0 equivalent at a time with 5 minutes between each addition. The reaction was monitored by TLC. After the starting material was gone, the reaction was washed with cold 1.0 N HCl and dried on anhydrous MgSO<sub>4</sub>. The organic layer was then concentrated down with no heat and placed in an ice bath.

Minimal amounts of dimethylformamide were added, followed by excess sodium cyanide. The reaction was allowed to stir for 30 minutes. The TLC was checked and the reaction was concentrated down under high vacuum. The resulting reaction mixture was then dissolved in dichloromethane and washed with 1.0 N HCl, and saturated NaHCO<sub>3</sub> until all the dimethylformamide was removed. The dichloromethane layer was collected and dried over anhydrous MgSO<sub>4</sub> followed by filtration. The liquid was then concentrated down to result in yellow oil **15** (8.1 mg, 54%). TLC  $R_f = 0.30$ ; <sup>1</sup>H NMR (500 MHz, CDCl<sub>3</sub>) δ 7.30 (d, 2H,  $J = 8.3$  Hz), 6.90 (d, 2H,  $J = 8.30$  Hz), 4.60 (q, 2H,  $J = 17.0, 10.74$  Hz), 3.80 (s, 3H), 3.79 (s, 1H), 3.65 (br s, 1H), 3.50 (br s, 1H), 3.15 (br s, 1H), 2.30 (m, 2H), 1.85 (q, 1H,  $J = 11.97$ ), 1.60 (m, 1H); <sup>13</sup>C NMR (125 MHz, CDCl<sub>3</sub>) δ 141, 130, 128, 115, 110, 76, 75, 74, 73, 68, 66, 30, 29, 23, 16.

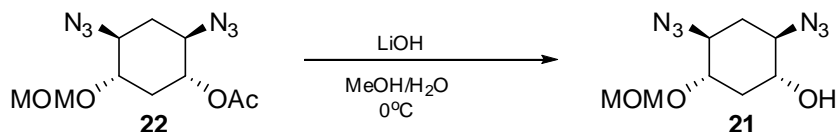


**(1S,2R,4S,5S)-2,4-diazo-5-(4-ethoxybenzyloxy)cyclohexanecarbaldehyde**

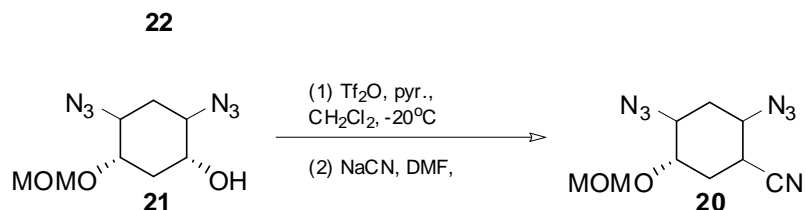
**(18).** **15** (19 mg, 0.058 mmol) was dissolved in dichloromethane and cooled to -78°C, after which DIBAL-H (150 μl, 0.15 mmol) was added. The reaction was stirred for 2 hours. Sodium tartrate was added and the reaction was allowed to warm to room temperature for 40 minutes. The reaction was concentrated down and purified by flash chromatography. Compound **18** was isolated as yellow oil (5.0 mg, 26%). TLC  $R_f = 0.60$ ; <sup>1</sup>H NMR (500 MHz, CDCl<sub>3</sub>) δ 9.40 (s, 1H), 7.30 (d, 2H,  $J = 8.30$ ), 6.90 (d, 2H,  $J = 8.30$ ), 6.70 (m, 1H), 4.60-4.40 (m, 3H), 3.80 (s, 3H), 3.60 (m, 1H), 2.80-2.20 (m, 6H).



**(1R,2R,4S,5S)-2,4-diazido-5-(methoxymethoxy)cyclohexyl acetate (22).** In a dry round bottom flask, **3** (4.4 g, 18.0 mmol) was added with dry dimethylformamide and dry triethylamine (13 ml, 9.2 mmol). The reaction was stirred at room temperature for 5 minutes. Afterwards, methoxymethylchloride (14 ml, 180.0 mmol) was added under argon gas and the reaction stirred at reflux for 20 minutes. The reaction was cooled down and the TLC was checked. The mixture was concentrated down under high vacuum and was then dissolved in dichloromethane. The crude material was then washed with water and brine and dried over anhydrous  $\text{MgSO}_4$ . The material was concentrated down in vacuo and the resulting light yellow oil, **22**, was achieved (4.1 g, 81% yield). TLC  $R_f = 0.44$ ;  $^1\text{H}$  NMR (500 MHz,  $\text{CDCl}_3$ )  $\delta$  4.70 (m, 3H), 3.50 (m, 2H), 3.40-3.30 (m, 1H), 3.30 (s, 3H), 2.40 (dt, 1H,  $J = 12.7, 4.89$  Hz), 2.20 (dt, 1H,  $J = 12.7, 4.89$  Hz), 2.10 (s, 3H), 1.40 (q, 1H,  $J = 12.21$  Hz), 1.25 (q, 1H,  $J = 12.21$  Hz);  $^{13}\text{C}$  NMR (125 MHz,  $\text{CDCl}_3$ )  $\delta$  170, 96, 76, 72, 62, 60, 56, 35, 32, 21; HRMS (ESI) found 307.1571 [ $\text{M} + \text{Na}$ ] $^+$ , calcd 284.1200 for  $[\text{C}_{10}\text{H}_{16}\text{N}_6\text{O}_4]^+$ ;  $[\alpha]_D^{24} = -13.20^\circ$  (c 2.042,  $\text{CHCl}_3$ ).

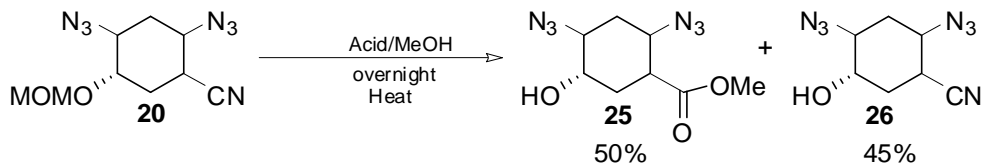


**(1R,2R,4S,5S)-2,4-diazido-5-(methoxymethoxy)cyclohexanol (21).** Compound **22** (4.1 g, 15.0 mmol) was dissolved in THF, after which was added water and methanol (1:1). The reaction was cooled to 0°C and 1.0 N LiOH was added (22 ml, 22.0 mmol). The reaction was run for 4 hours, after which it was concentrated down and dissolved in dichloromethane. The reaction mixture was then washed with water and dried with anhydrous MgSO<sub>4</sub> and filtered. This was then concentrated down to result in the yellow oil **21** (2.9 g, 82% yield). TLC  $R_f$  = 0.30; <sup>1</sup>H NMR (500 MHz, CDCl<sub>3</sub>) δ 4.78 (m, 2H), 3.50-3.40 (m, 3H), 3.40 (s, 3H), 3.30 (m, 1H) 2.60 (br s, 1H), 2.40 (dt, 1H,  $J$  = 13.18, 3.91 Hz), 2.20 (dt, 1H,  $J$  = 13.18, 3.91 Hz), 1.50 (q, 1H,  $J$  = 11.48 Hz), 1.35 (q, 1H,  $J$  = 11.48 Hz); <sup>13</sup>C NMR (125 MHz, CDCl<sub>3</sub>) δ 96, 76, 71, 64, 62, 56, 36, 32; HRMS (ESI) found 243.1200 [M + H]<sup>+</sup>, calcd 242.1100 for [C<sub>8</sub>H<sub>14</sub>N<sub>6</sub>O<sub>3</sub>]<sup>+</sup>; [α]<sub>D</sub><sup>24</sup> = -31.09° (c 1.22, CHCl<sub>3</sub>).



**(1S,2R,4S,5S)-2,4-diazido-5-(methoxymethoxy)cyclohexanecarbonitrile (20).** Compound **21** (250 mg, 1.0 mmol) was dissolved in excess dry dichloromethane and cooled to -20°C. The vial was purged with argon gas after which pyridine (330 μl, 4.1 mmol) and then trifluoromethanesulfonic anhydride (690 μl, 4.1 mmol) were added, 1.0 equivalent at a time with 5 minutes between each addition.

Reaction was monitored by TLC. After the addition of four equivalents, the reaction was washed with ice water and dried on anhydrous  $\text{MgSO}_4$ . The organic layer was then concentrated down with no heat and placed in an ice bath. Minimal amounts of dimethylformamide was added, followed by excess sodium cyanide until the reaction mixture changed colors from bright yellow to orange-yellow and back to bright yellow. The reaction was allowed to stir for 30 minutes. The TLC was checked and the reaction was concentrated down under high vacuum. The resulting reaction mixture was then dissolved in dichloromethane and washed with water and brine until all the dimethylformamide was removed. The dichloromethane layer was collected and dried over anhydrous  $\text{MgSO}_4$  followed by filtration. The liquid was then concentrated down to result in yellow-orange oil **21** (200 mg, 78% yield). TLC  $R_f = 0.41$ ;  $^1\text{H}$  NMR (500 MHz,  $\text{CDCl}_3$ )  $\delta$  4.70 (dd, 2H,  $J = 10.73, 6.38$  Hz), 3.75-3.65 (m, 2H), 3.45 (m, 1H), 3.40 (s, 3H), 3.20-3.10 (br q, 1H,  $J = 3.72$  Hz), 2.40 (dt, 1H,  $J = 14.16, 5.77$  Hz), 2.25 (dt, 1H,  $J = 13.67, 3.15$  Hz), 1.85 (m, 1H), 1.65 (dt, 1H,  $J = 12.38, 3.9$  Hz);  $^{13}\text{C}$  NMR (125 MHz,  $\text{CDCl}_3$ )  $\delta$  118, 96, 75, 61, 56, 55, 32,31,30; HRMS (ESI) found 252.1204 [ $\text{M} + \text{H}$ ] $^+$ , calcd 251.1100 for  $[\text{C}_9\text{H}_{13}\text{N}_7\text{O}_2]^+$ ;  $[\alpha]_D^{24} = -10.2^\circ$  (c 0.570,  $\text{CHCl}_3$ ).

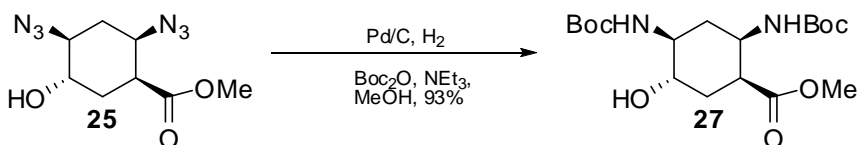


**(1S,2R,4S,5S)-methyl 2,4-diazido-5-hydroxycyclohexanecarboxylate (25) and (1S,2R,4S,5S)-2,4-diazido-5-hydroxycyclohexanecarbonitrile (26).**

Compound **20** (46 mg, 0.18 mmol) was placed under reflux conditions with 4 ml of 5.3 M HCl in MeOH and allowed to run overnight (15 hours) at 70°C. There

was a 50% conversion observed by TLC. This crude mixture was concentrated down with a few drops of saturated NaHCO<sub>3</sub>, after which the crude mixture was washed with dichloromethane and water, dried with anhydrous MgSO<sub>4</sub> and filtered. The crude material was purified by flash chromatography which resulted in a yellow oil, **25** and brown solid crystals, **26**. **25**: TLC  $R_f = 0.34$ ; <sup>1</sup>H NMR (500 MHz, CDCl<sub>3</sub>) δ 3.78-3.63 (m, 2H), 3.5 (m, 1H), 3.4 (s, 3H), 3.19 (br d, 1H,  $J = 3.42$  Hz), 2.45-2.40 (dt, 1H,  $J = 13.94$  Hz, 4.16 Hz), 2.38-2.30 (br dt, 1H,  $J = 13.94$ , 2.93 Hz), 1.95 (q, 1H,  $J = 11.25$  Hz), 1.65 (m, 1H), 1.25 (bs, 1H); <sup>13</sup>C NMR (125 MHz, CDCl<sub>3</sub>) δ 172, 69, 62, 58, 52, 42, 30, 29; HRMS (ESI) found 263.0863 [M + Na]<sup>+</sup>, calcd 240.0979 for [C<sub>8</sub>H<sub>12</sub>N<sub>6</sub>O<sub>3</sub>]<sup>+</sup>; [α]<sub>D</sub><sup>24</sup> = +34.02° (c 0.088, CHCl<sub>3</sub>).

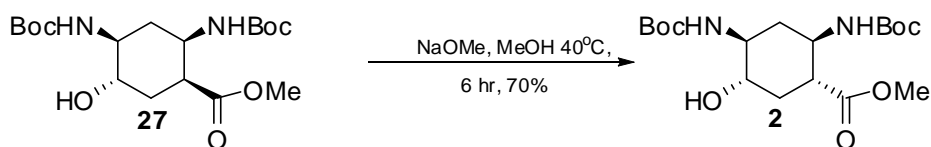
**26**: TLC  $R_f = 0.20$ ; <sup>1</sup>H (500 MHz, CDCl<sub>3</sub>) δ 3.82 (br m 1H), 3.60 (dt, 1H,  $J = 11.71$ , 4.4 Hz), 3.36 (m, 1H), 3.2 (br d, 1H,  $J = 3.91$  Hz), 2.60 (br s, 1H), 2.4-2.3 (m, 2H), 1.74 (q, 1H,  $J = 13.18$  Hz), 1.66 (m, 1H); <sup>13</sup>C (125 MHz, CDCl<sub>3</sub>) δ 118, 69, 63, 56, 32.2, 32, 32.4; ESI HRMS found 230.0761 [M + Na]<sup>+</sup>, calcd 207.0900 for [C<sub>7</sub>H<sub>9</sub>N<sub>7</sub>O]<sup>+</sup>; [α]<sub>D</sub><sup>23</sup> = +37.43° (c 0.16, CHCl<sub>3</sub>); MP = 116.9°C-119.1°C.



**(1S,2R,4S,5S)-methyl-2,4-bis(tert-butoxycarbonylamino)-5-**

**hydroxycyclohexanecarboxylate (27).** To a solution of azide (**25**) (88 mg, 0.36 mmol) in methanol (10 ml) was added triethylamine (0.15 ml, 1.1 mmol), Boc<sub>2</sub>O (240 mg, 1.1 mmol) followed by 10% Pd/C catalyst (0.025 g). The mixture was agitated for 12 hr at 25°C, under a hydrogen atmosphere of 6 bar before the catalyst was removed by gravity filtration. Evaporation of the solvent, followed by

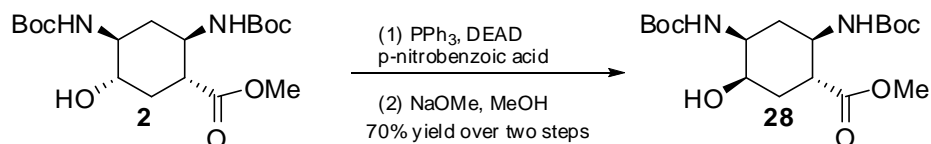
column purification yielded **27** as a white solid (130 mg, 0.33 mmol, 92% yield).  $^1\text{H}$  NMR (500 MHz,  $\text{CDCl}_3$ )  $\delta$  5.43 (br s, 1H), 4.71 (br s, 1H), 3.83-3.76 (ddd,  $J = 3, 8, 13$  Hz, 2H), 3.70 (s, 3H), 3.45 (ddd,  $J = 3, 11, 13$  Hz, 1H), 3.35 (ddd,  $J = 2, 10, 11$  Hz, 1H), 2.93 (ddd,  $J = 4, 5, 8$  Hz, 1H), 2.40-2.37 (ddd,  $J = 2, 4, 14$  Hz, 1H), 2.03-2.00 (ddd,  $J = 3, 3, 13$  Hz, 1H), 1.78-1.71 (ddd,  $J = 13, 13, 13$  Hz, 1H), 1.65-1.59 (ddd,  $J = 5, 10, 14$  Hz, 1H), 1.42 (s, 9H), 1.41 (s, 9H);  $^{13}\text{C}$  NMR (125 MHz,  $\text{CDCl}_3$ )  $\delta$  174.1, 157.4, 155.3, 80.6, 79.8, 71.9, 55.1, 52.1, 48.3, 43.2, 34.4, 33.9, 28.6, 28.5; HRMS (ESI) Found 388.2232 for  $[\text{M}]^+$ ; calcd. 388.2209 for  $[\text{C}_{18}\text{H}_{32}\text{N}_2\text{O}_7\text{H}]^+$ .



**(1R,2R,4S,5S)-methyl-2,4-bis(tert-butoxycarbonylamino)-5-**

**hydroxycyclohexanecarboxylate (2).** To a solution of **27** (80 mg, 0.20 mmol) in methanol (5 ml) at  $0^\circ\text{C}$  was added a solution of sodium methoxide (0.42 M, 15 ml, 6.2 mmol) in methanol and heated at  $40^\circ\text{C}$  for about 6 h. The reaction mixture was made acidic using Amberlite resin and then filtered. The filtrate was concentrated and the compound was purified by column chromatography to obtain the epimer **2** (58 mg, 0.15 mmol, 72%).  $^1\text{H}$  NMR (500 MHz,  $\text{CDCl}_3$ )  $\delta$  4.65 (br s, 1H), 4.61 (br s, 1H), 3.69 (s, 3H), 3.64-3.58 (m, 1H), 3.51-3.36 (m, 2H), 2.49-2.45 (m, 1H), 2.30-2.25 (m, 1H), 2.22-2.17 (m, 1H), 1.74-1.65 (m, 1H), 1.44 (s, 10H), 1.41 (s, 9H);  $^{13}\text{C}$  NMR (125 MHz,  $\text{CDCl}_3$ )  $\delta$  173.2, 157.9, 155.1, 80.7, 79.9, 73.8, 54.8, 52.3, 50.5, 47.4, 37.0, 35.1, 29.9, 28.5; HRMS (ESI) Found 388.2222  $[\text{M}]^+$ ; calcd. 388.2209 for  $[\text{C}_{18}\text{H}_{32}\text{N}_2\text{O}_7\text{H}]^+$ .





**(1R,2R,4S,5R)-methyl-2,4-bis(tert-butoxycarbonylamino)-5-**

**hydroxycyclohexanecarboxylate (28).** To a solution of **2** (20 mg, 0.05 mmol),

PPh<sub>3</sub> (80 mg, 0.3 mmol), and 4-nitrobenzoic acid (52 mg, 0.3 mmol) in dry THF

(50 ml) and under Nitrogen was added in one portion diethylazodicarboxylate (56

μl, 0.30 mmol) with stirring at 0-5 °C. The resulting solution was refluxed

overnight after which the solvent was removed in vacuo. The residue was

trituated in EtOAc and most of the triphenylphosphine oxide and

diethylhydrazinedicarboxylate was removed by filtration. The filtrate was

evaporated and the residue was dissolved in methanol to which sodium

methoxide (0.42 M, 5 ml, 1.5 mmol) in methanol was added. The reaction mixture

was made acidic using Amberlite resin after 1 hr and filtered. The filtrate was

chromatographed on silica gel to yield **2** (14 mg, 0.036 mmol, 70 %). <sup>1</sup>H NMR

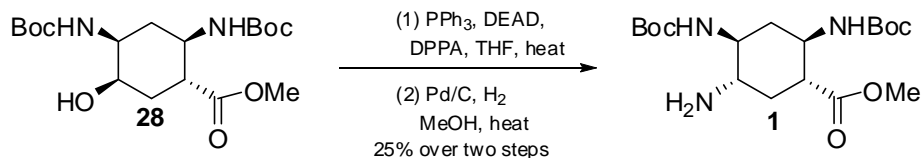
(500 MHz, CDCl<sub>3</sub>) δ 4.79 (br s, 1H), 4.53 (br s, 1H), 4.06 (s, 2H), 3.74-3.69 (m,

2H), 3.67 (s, 3H), 3.66-3.62 (m, 1H), 2.70-2.66 (m, 1H), 2.06-1.95 (m, 2H), 1.84-

1.79 (m, 1H), 1.63-1.56 (m, 1H), 1.44 (s, 9H), 1.42 (s, 9H); <sup>13</sup>C NMR (125 MHz,

CDCl<sub>3</sub>) δ 174.3, 155.3, 154.9, 79.7, 79.5, 53.2, 52.0, 51.0, 50.1, 42.9, 34.6, 29.6,

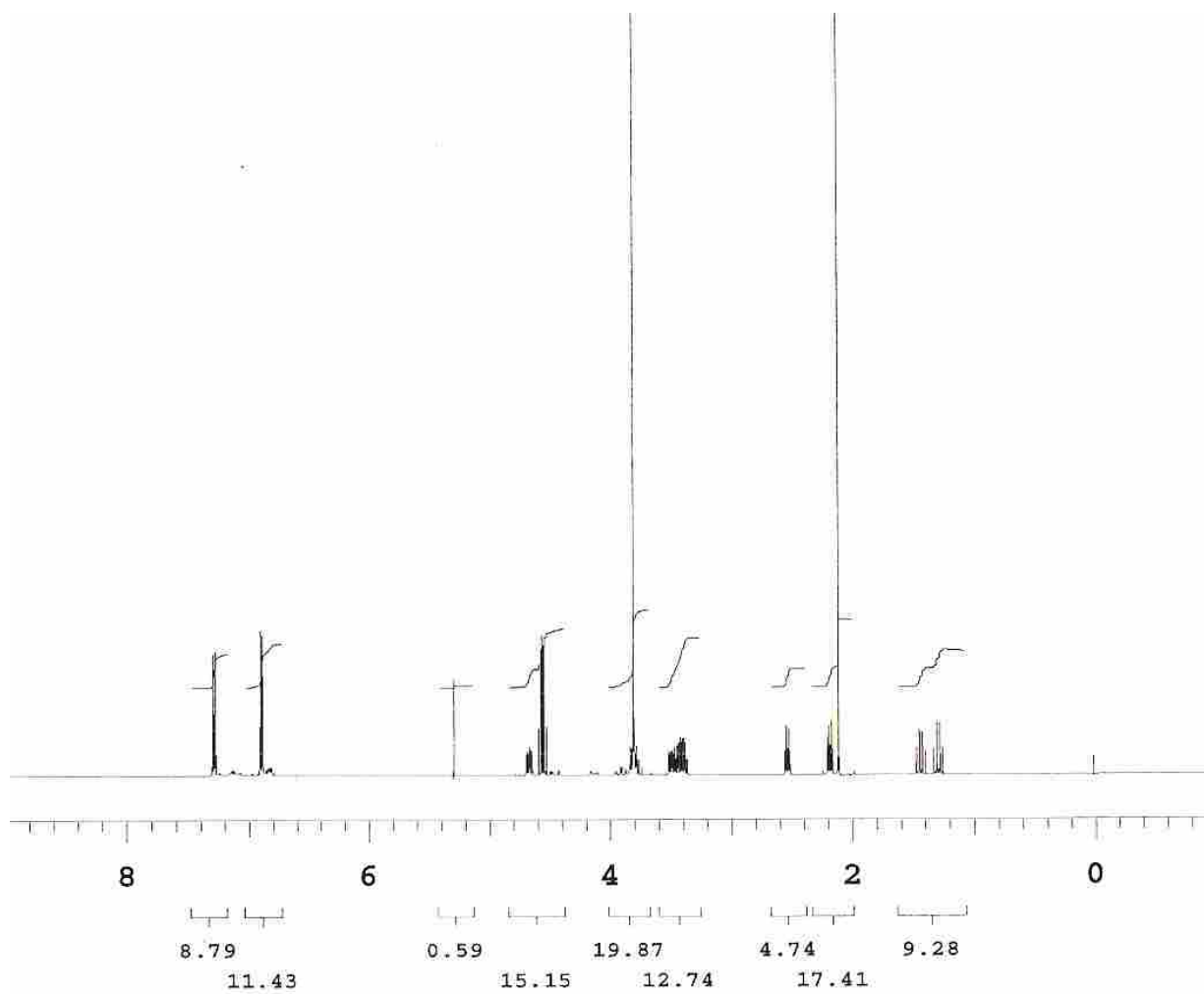
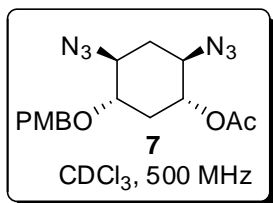
28.5; HRMS (ESI) Found 388.2259 [M]<sup>+</sup>; calcd. 388.2209 for [C<sub>18</sub>H<sub>32</sub>N<sub>2</sub>O<sub>7</sub>H]<sup>+</sup>.

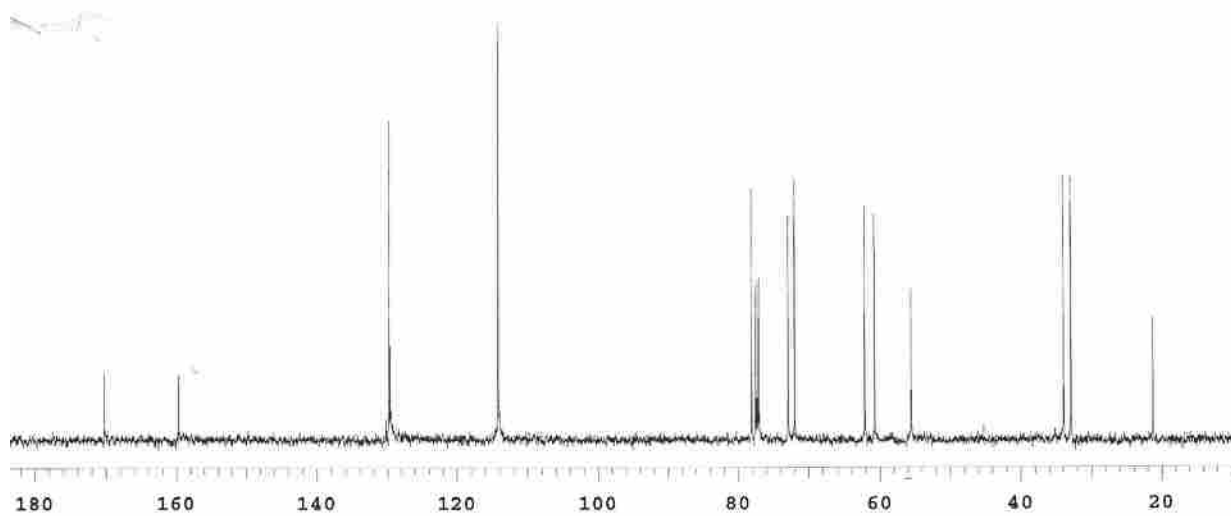
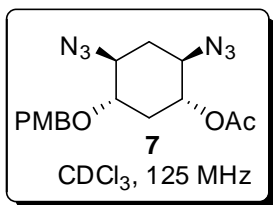


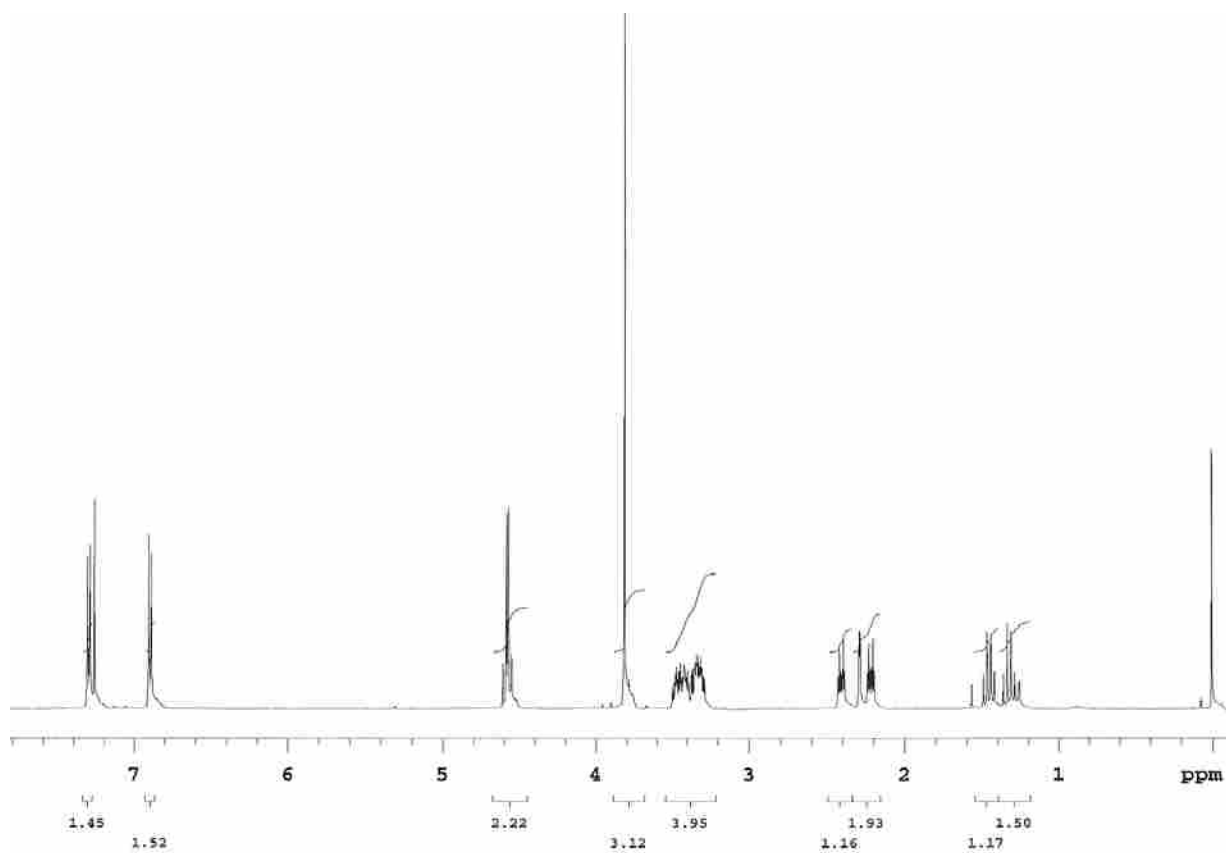
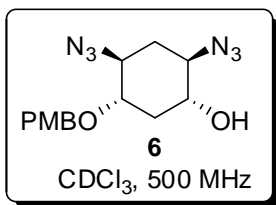
**(1*R*,2*R*,4*S*,5*S*)-methyl 5-amino-2,4-bis( *tert*-butoxycarbonylamino)**

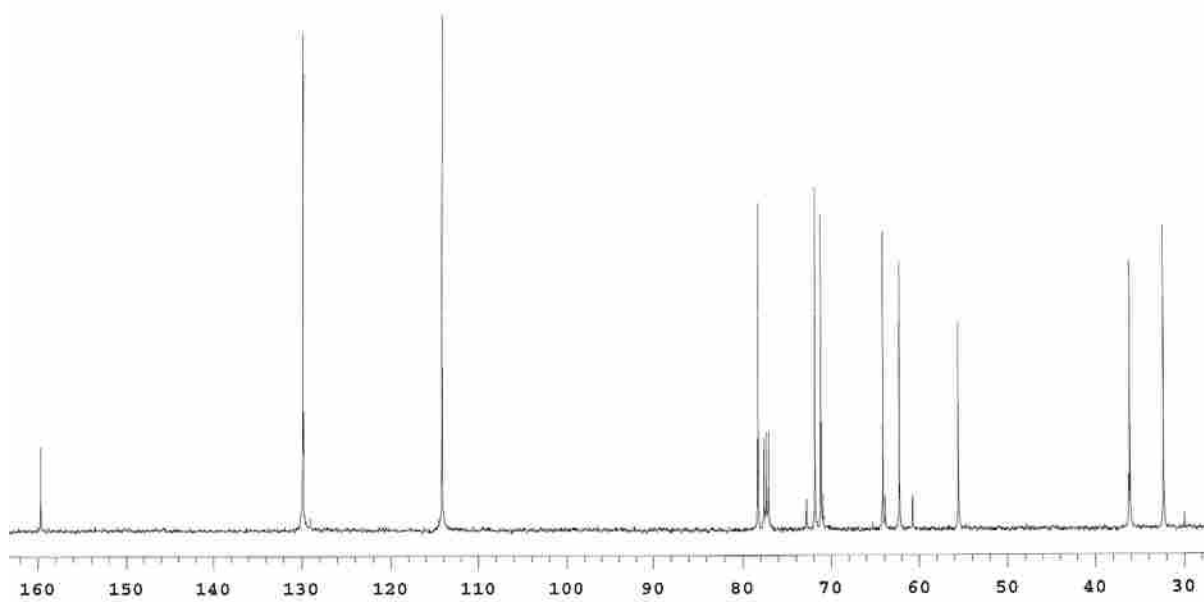
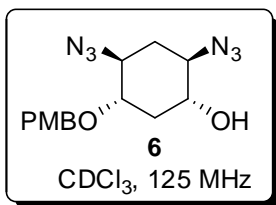
**cyclohexanecarboxylate (1).** To a cooled (0°C) diethylazodicarboxylate (67  $\mu$ l, 0.15 mmol) in THF (2 ml) were added **28** (12 mg, 0.03 mmol) in THF (3 ml) and Ph<sub>3</sub>P (16 mg, 0.06 mmol). After 15 min, diphenyl phosphorazide (DPPA; 17  $\mu$ l, 0.08 mmol) was added and the reaction mixture allowed to warm to room temperature. After stirring overnight, the solvent was removed in vacuo to give a yellow oil. The crude material was purified by flash column chromatography to give azide (5 mg, 0.012 mmol) which in turn was dissolved in methanol (10 ml). 10% Pd/C catalyst (1.0 mg) was then added to the reaction mixture and was agitated for 3-4 hr at 25°C, under a hydrogen atmosphere of 6 bar before the catalyst was removed by gravity filtration. Evaporation of the solvent, followed by column purification yielded **1** as a yellow liquid (4 mg, 0.010 mmol, 85% yield). <sup>1</sup>H NMR (500 MHz, CDCl<sub>3</sub>)  $\delta$  4.78 (br s, 1H), 4.53 (br s, 1H), 4.10-4.06 (m, 1H), 3.76-3.60 (m, 2H), 3.68 (s, 3H), 2.73-2.65 (m, 1H), 2.08-1.98 (m, 3H), 1.90-1.79 (m, 1H), 1.44 (s, 9H), 1.42 (s, 9H); <sup>13</sup>C NMR (125 MHz, CDCl<sub>3</sub>)  $\delta$  174.3, 155.4, 155.0, 66.7, 52.3, 43.2, 33.7, 29.9, 28.5, 14.6; HRMS (ESI) Found 387.2466 [M]; calcd. 387.2374 for [C<sub>18</sub>H<sub>33</sub>N<sub>2</sub>O<sub>6</sub>].

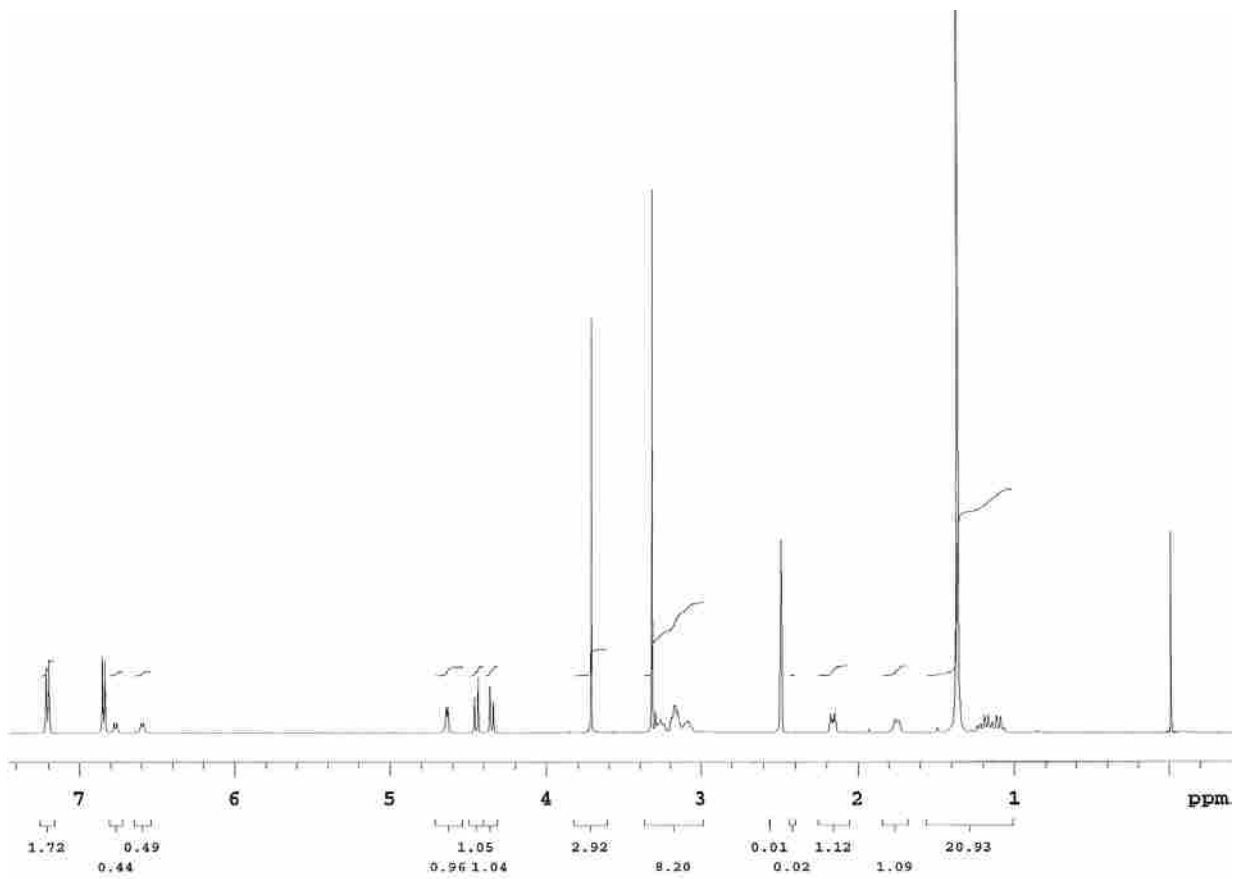
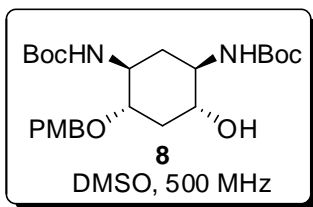
### 3.3 Selected NMR Spectra

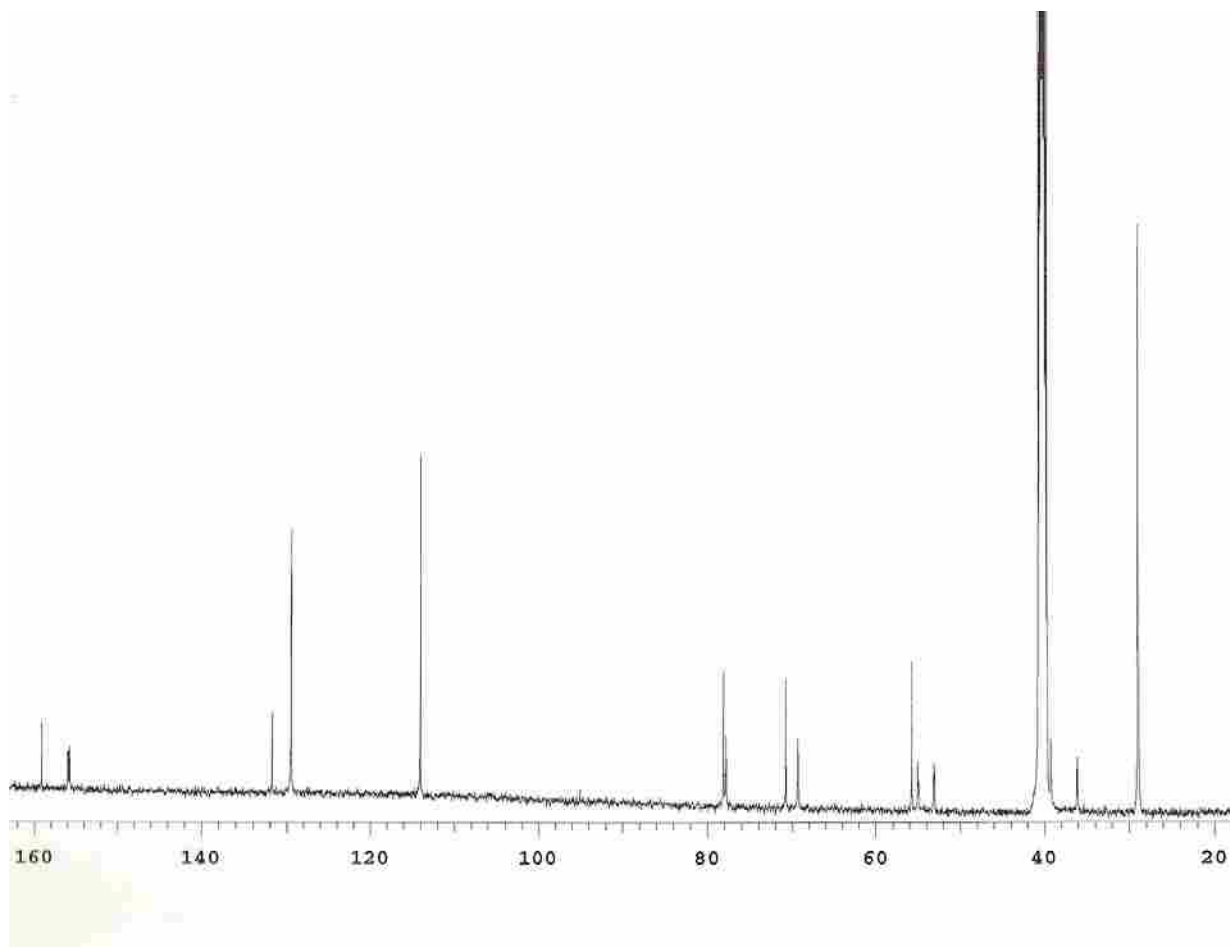
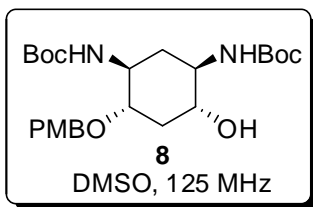




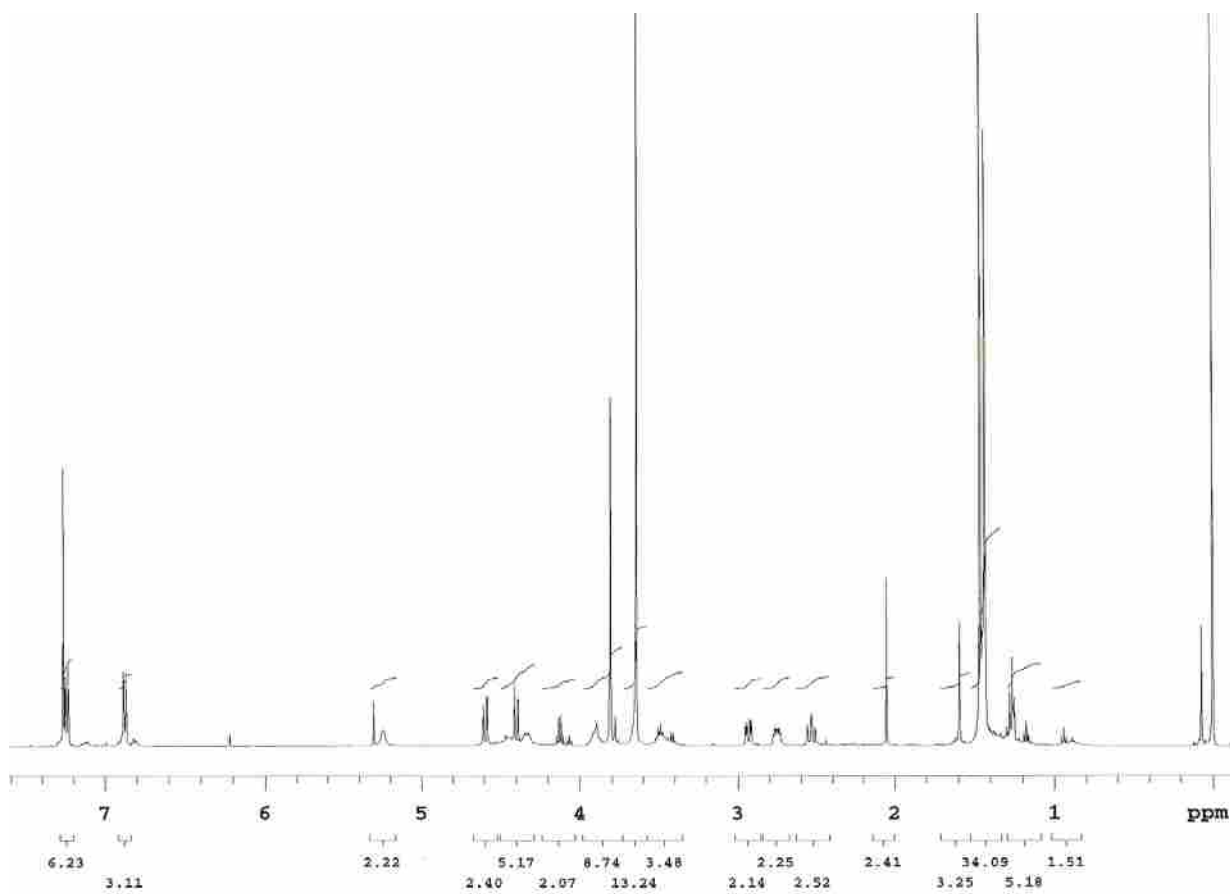
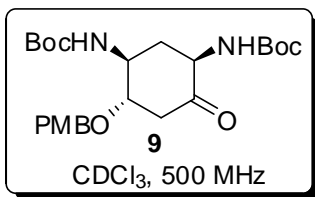


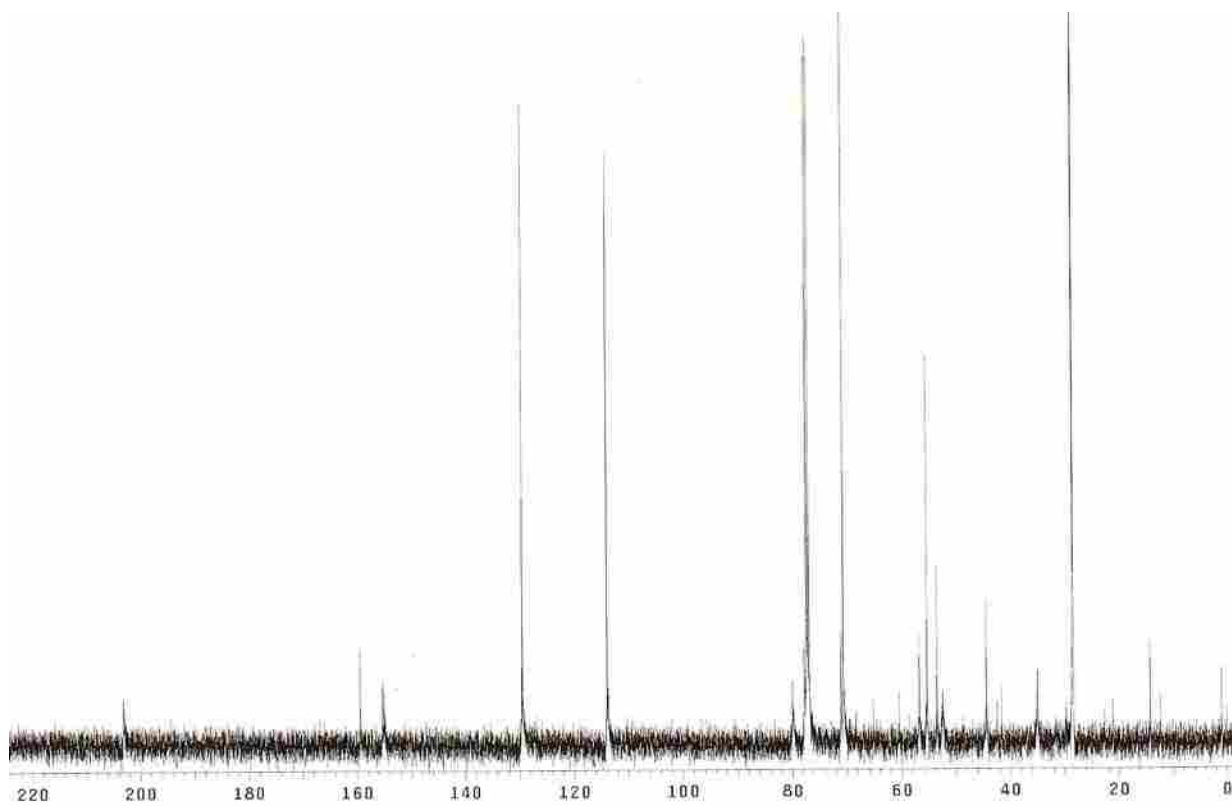
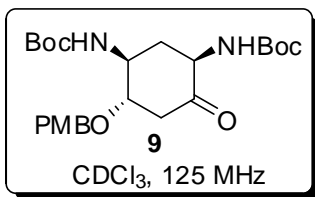


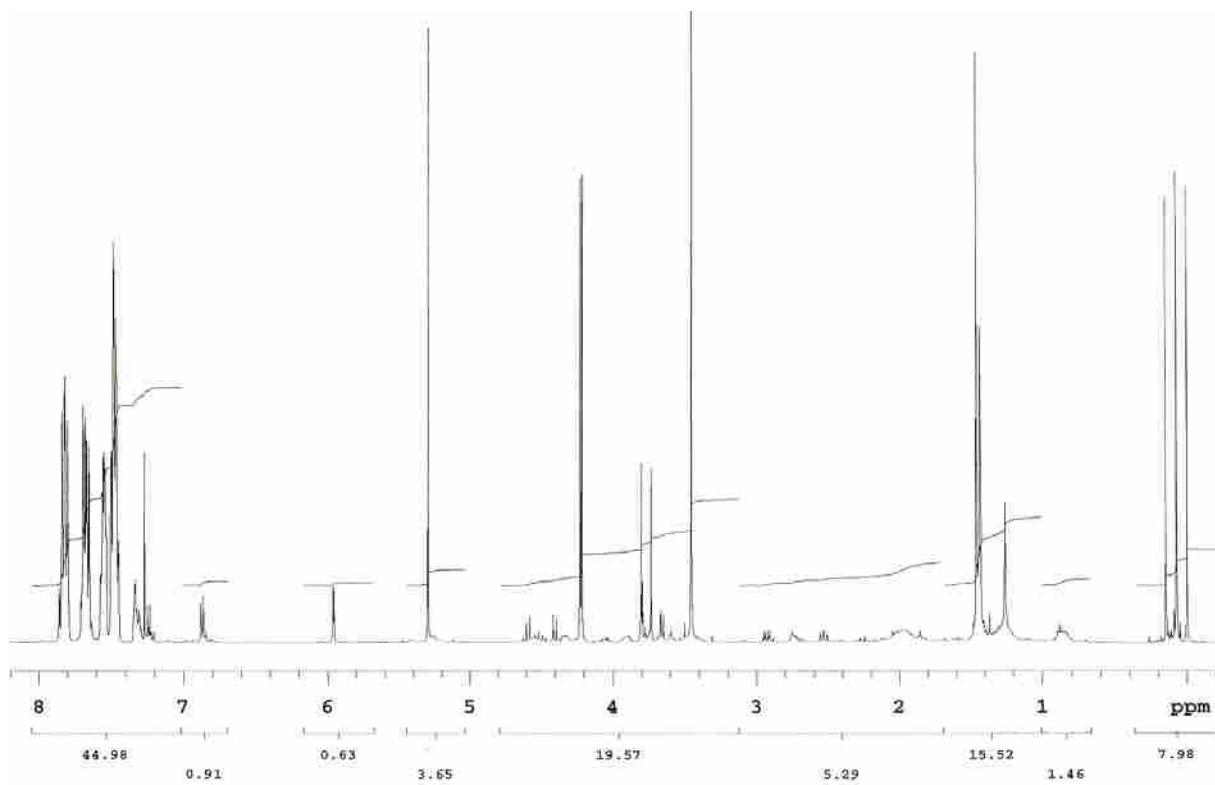
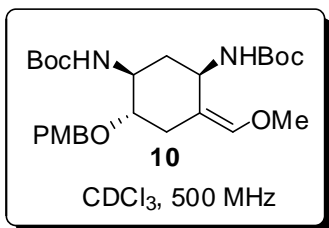


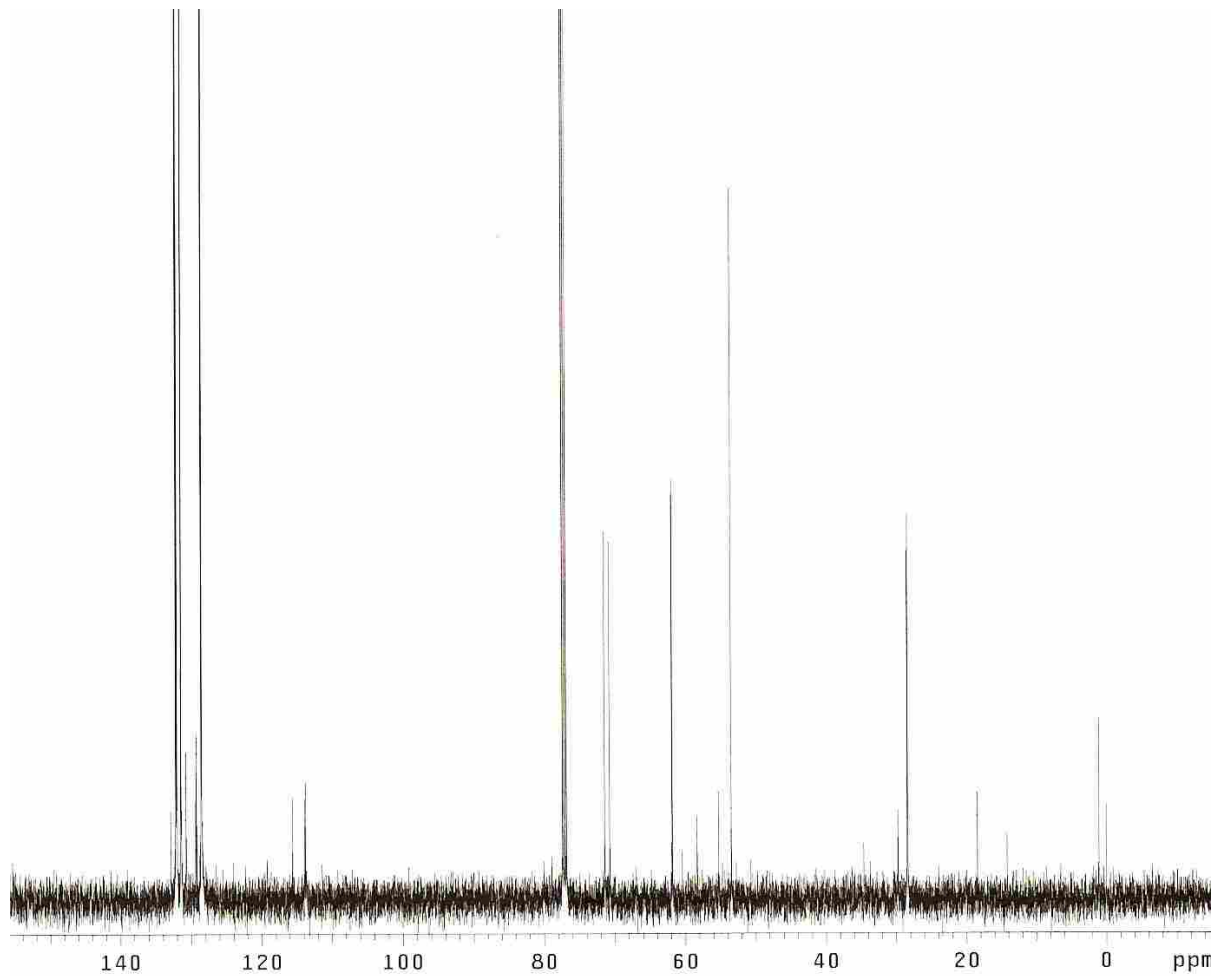
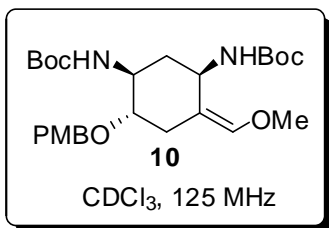


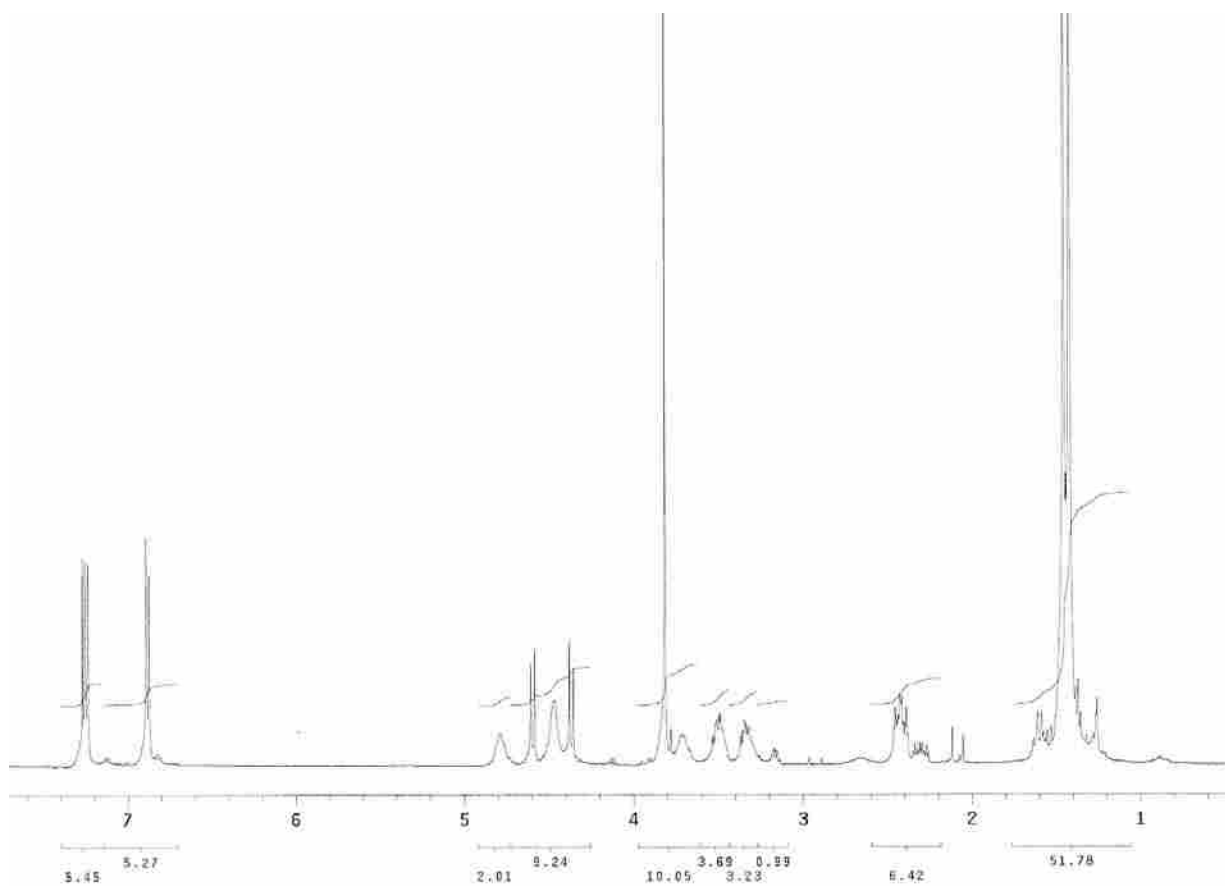
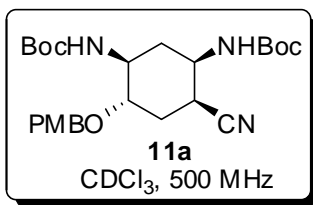


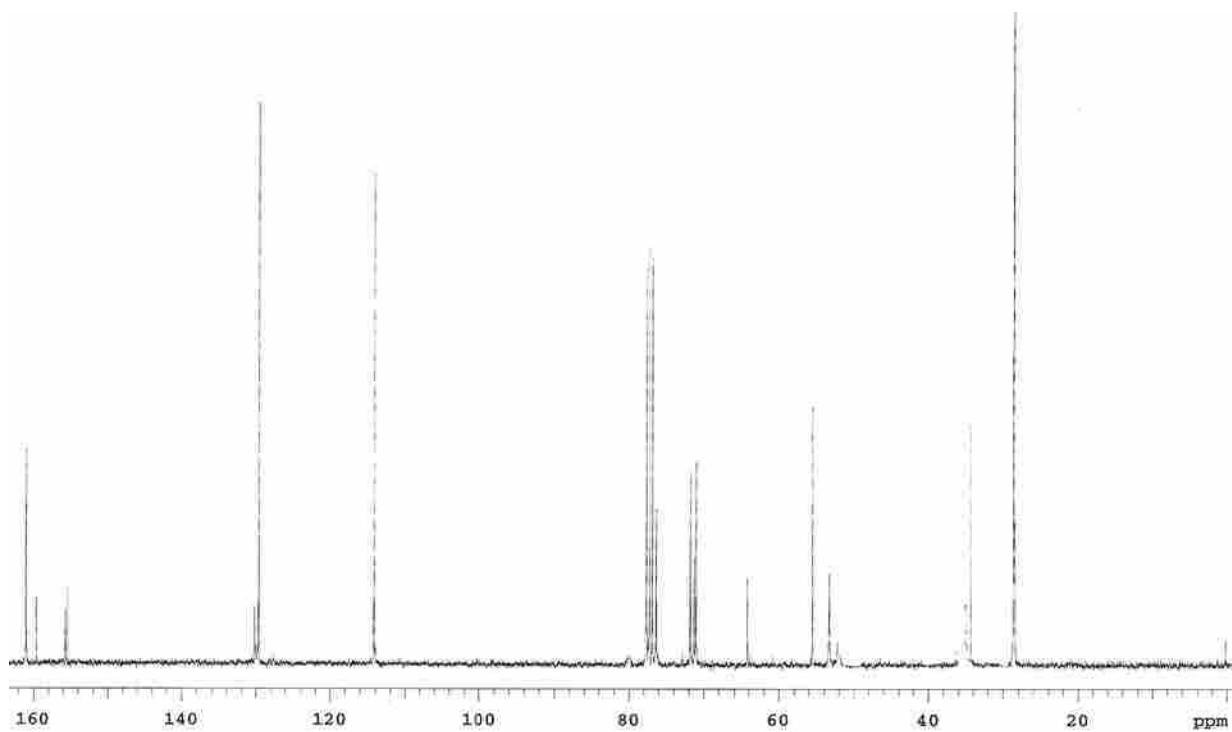
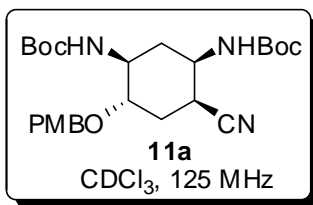


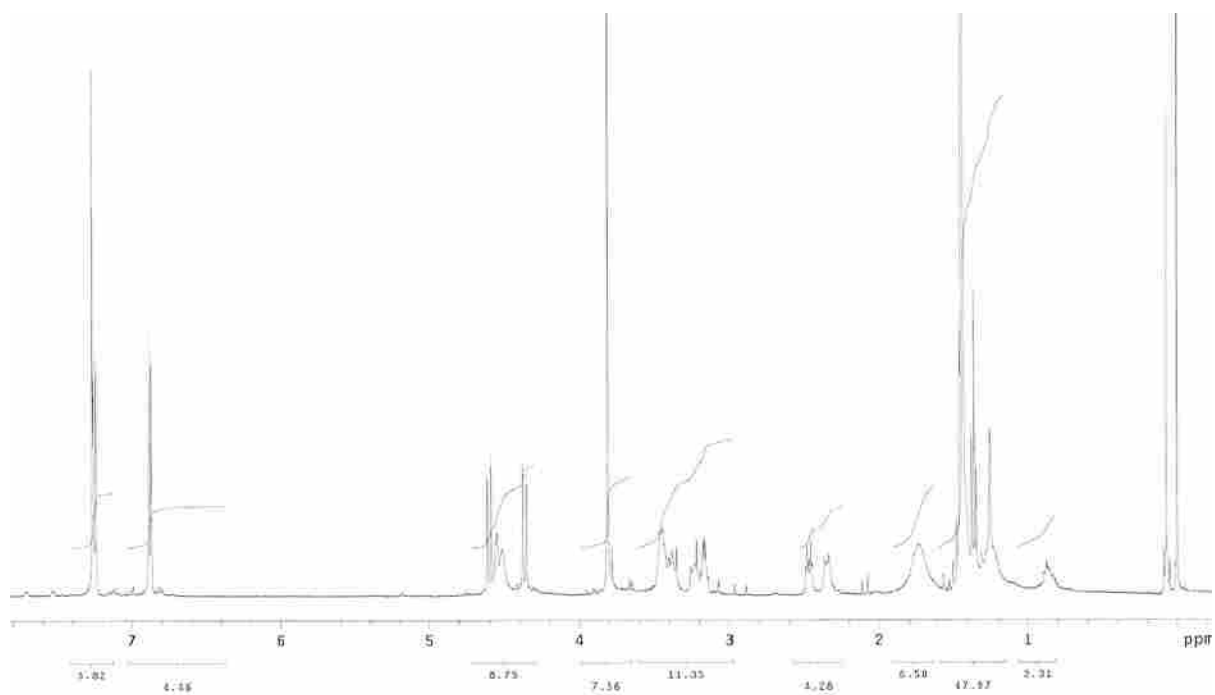
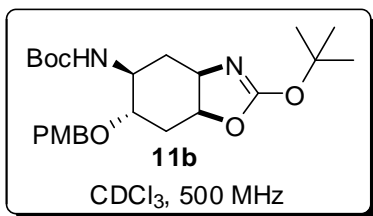


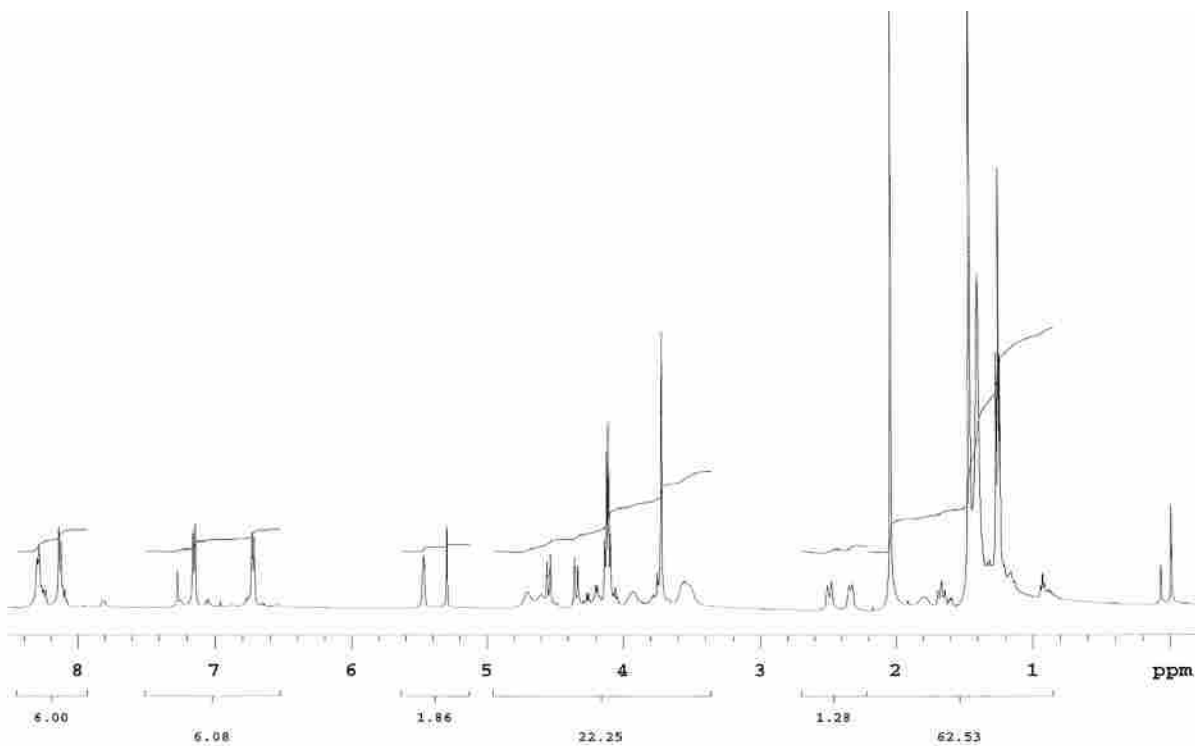
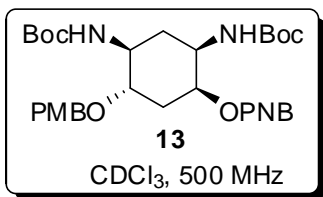




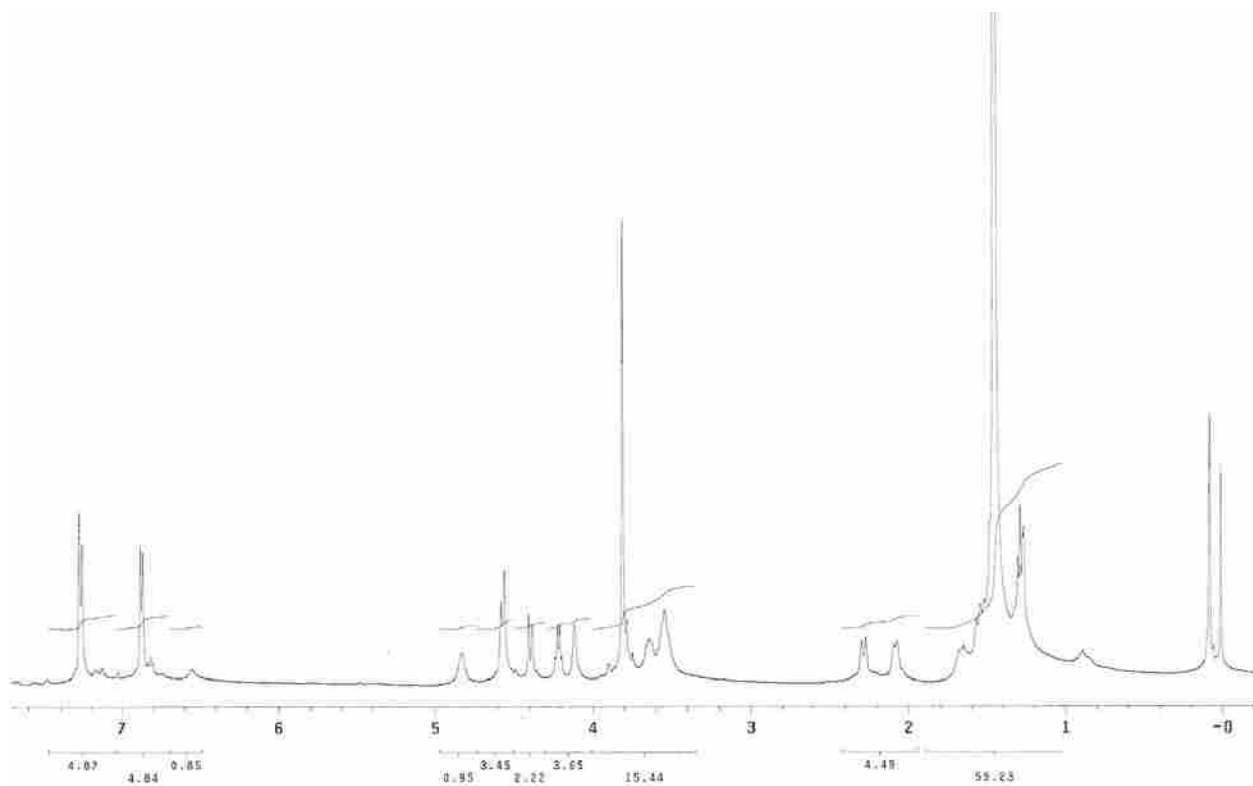
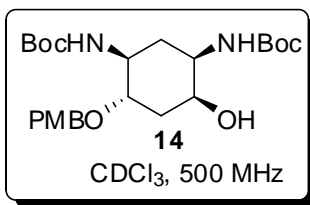


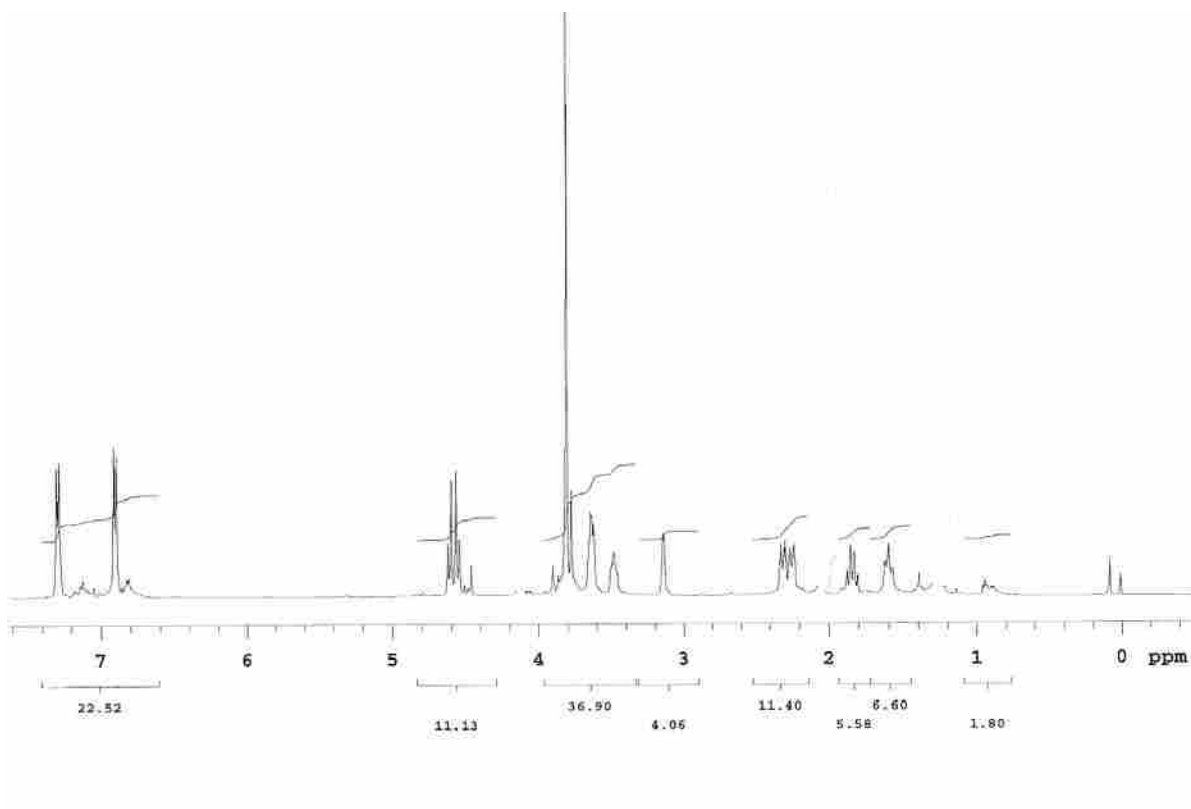
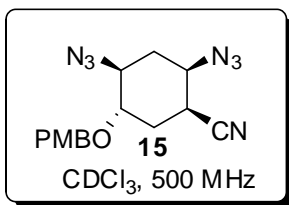


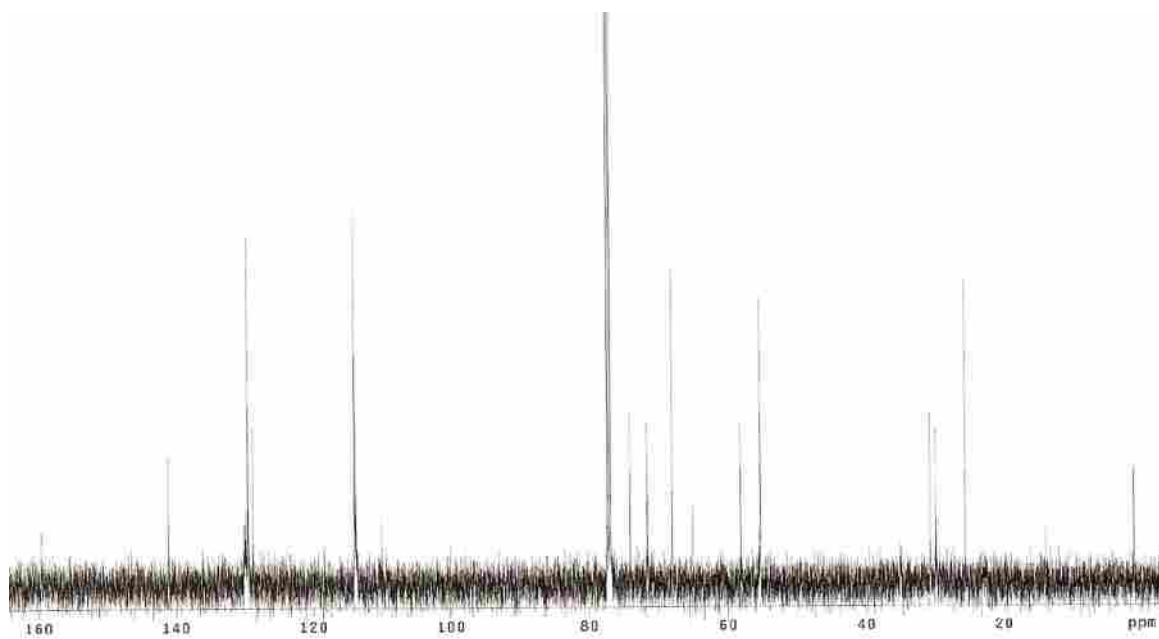
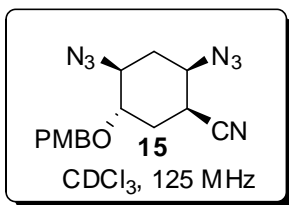


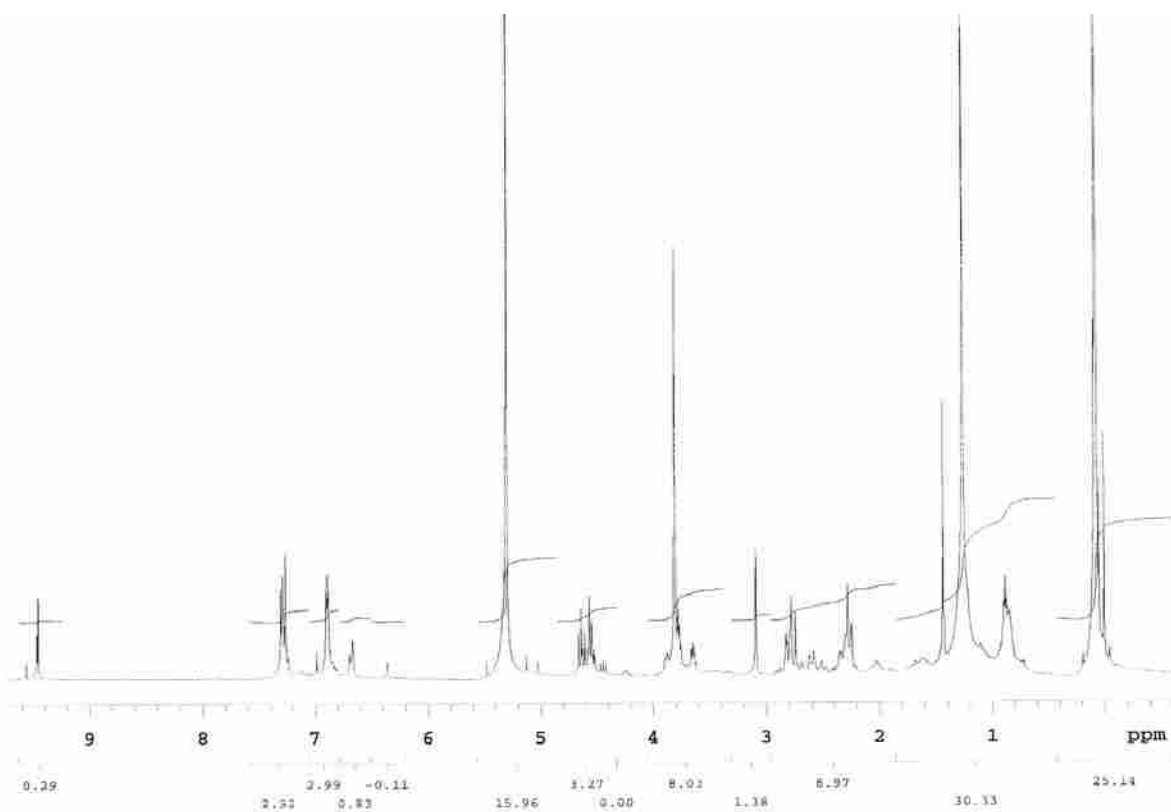
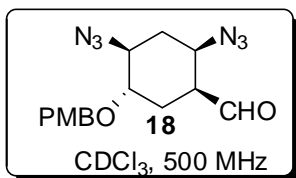


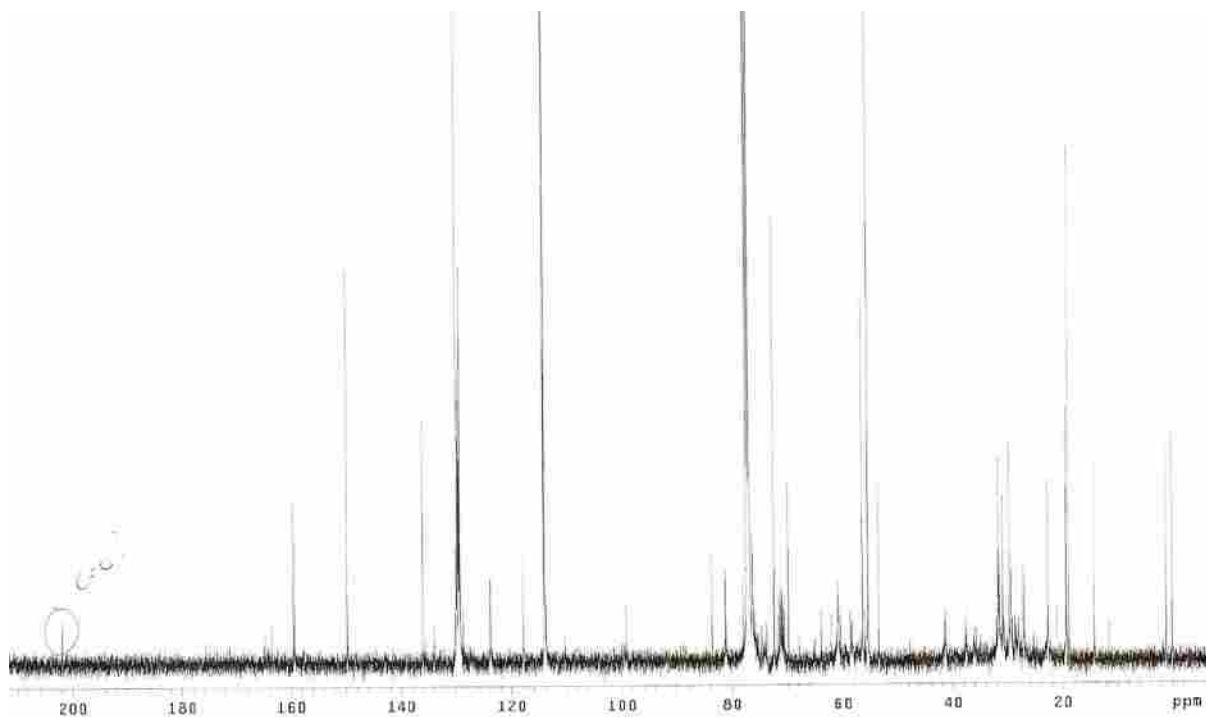
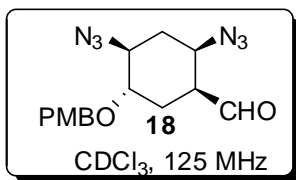


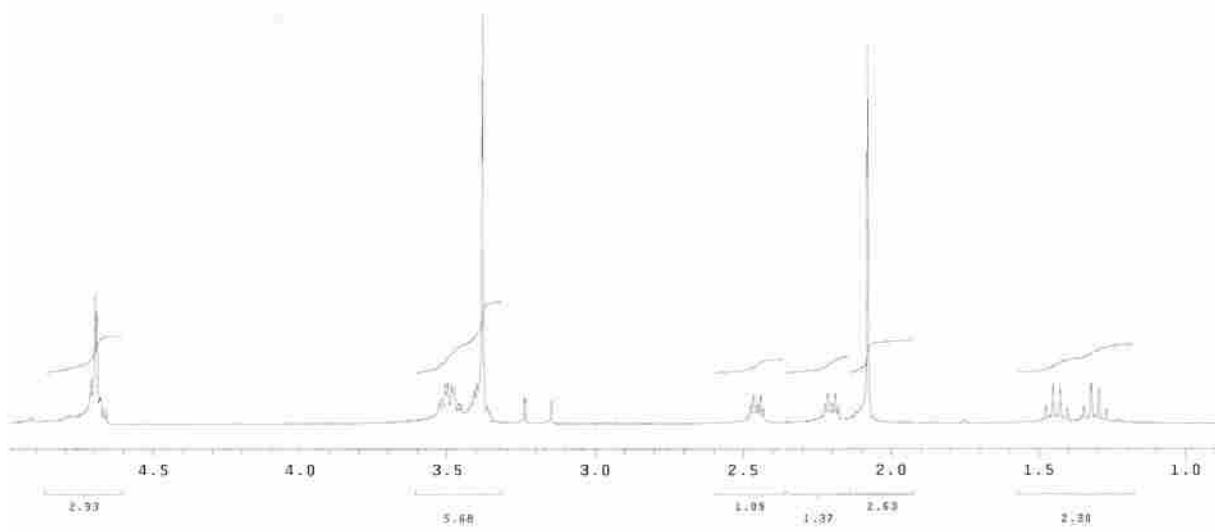
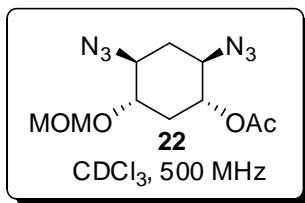


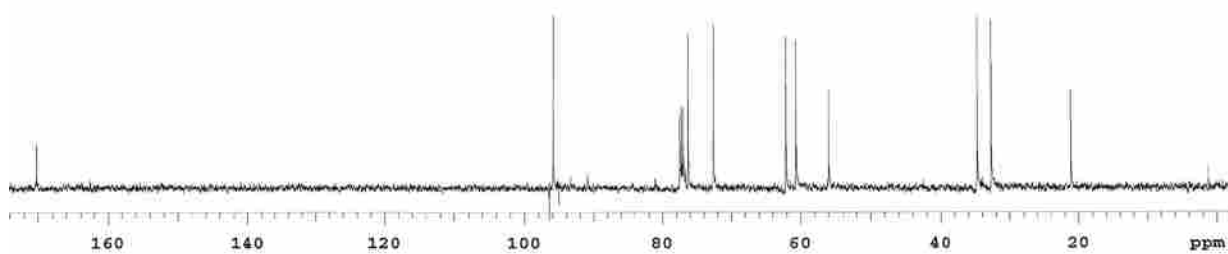
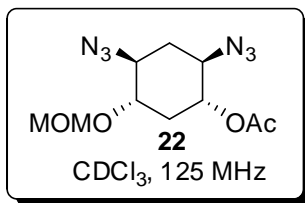


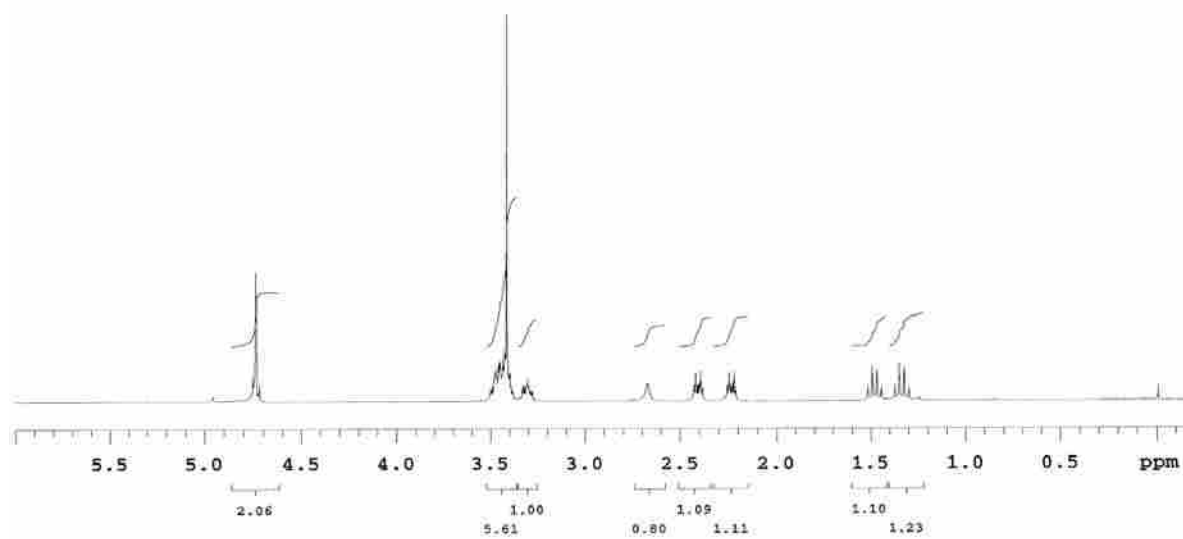
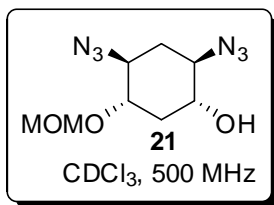




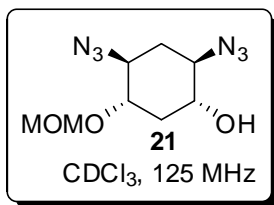


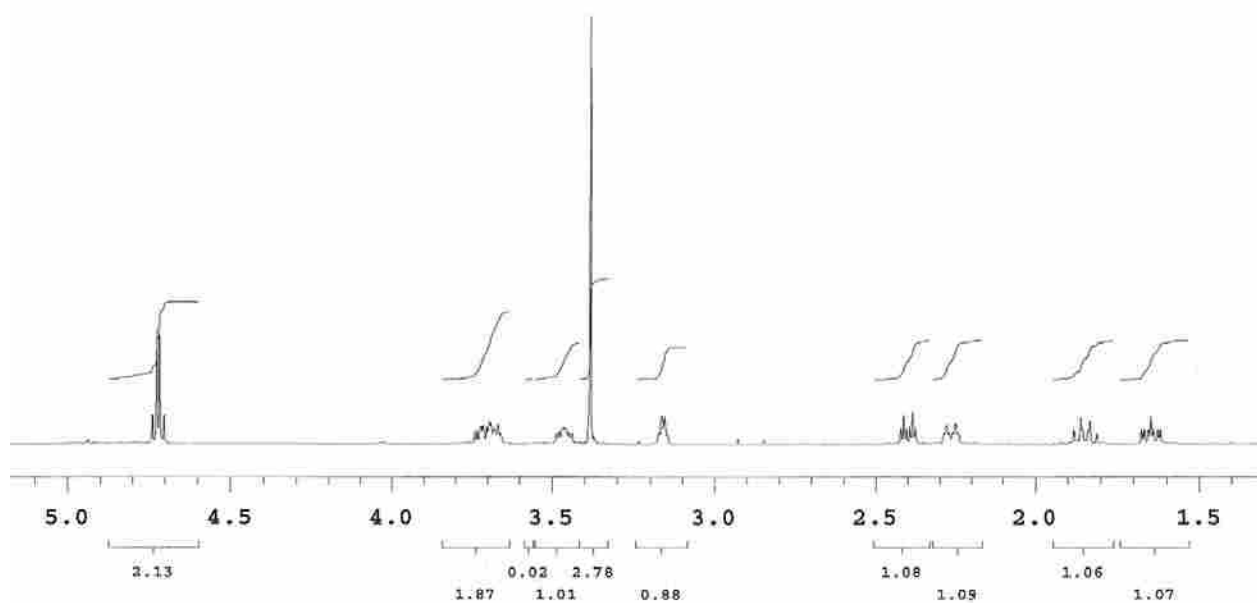
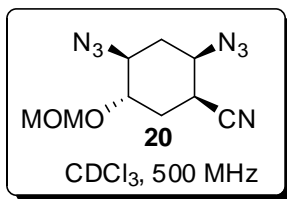


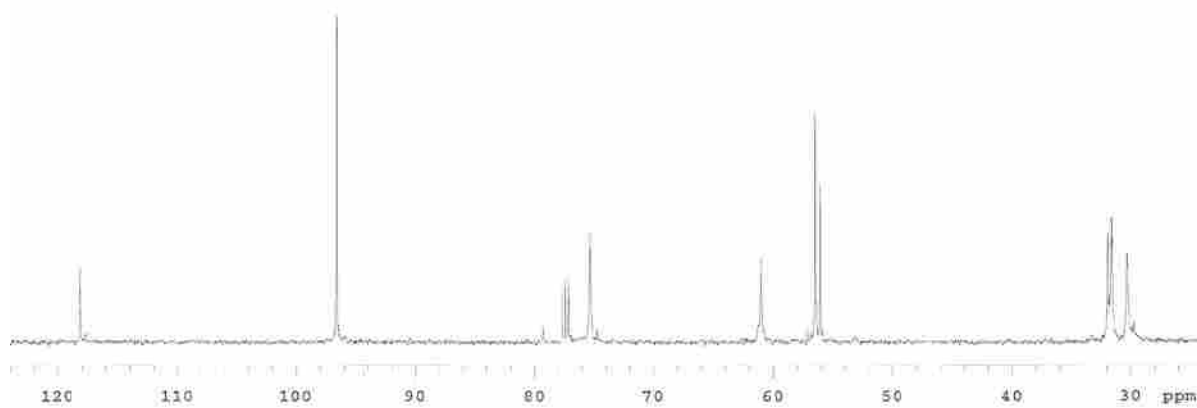
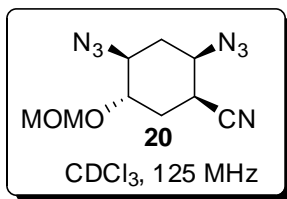


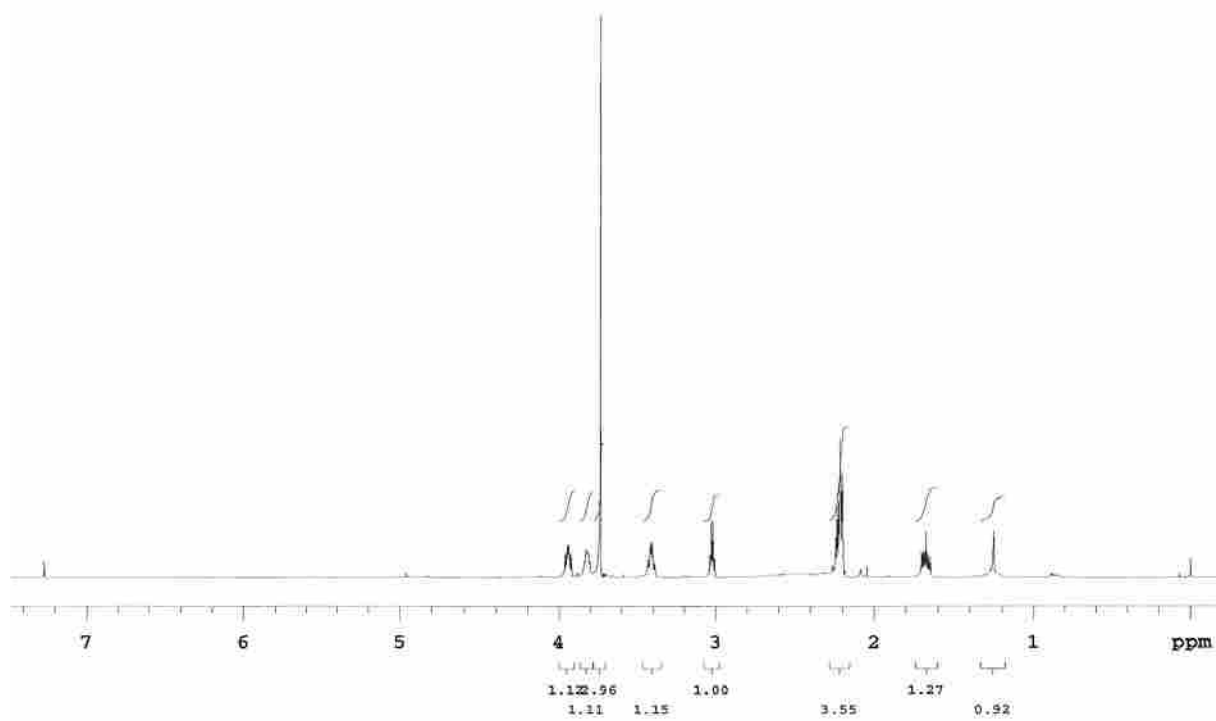
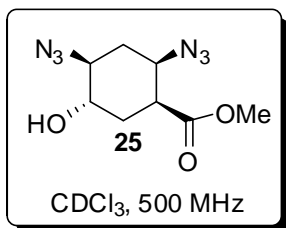


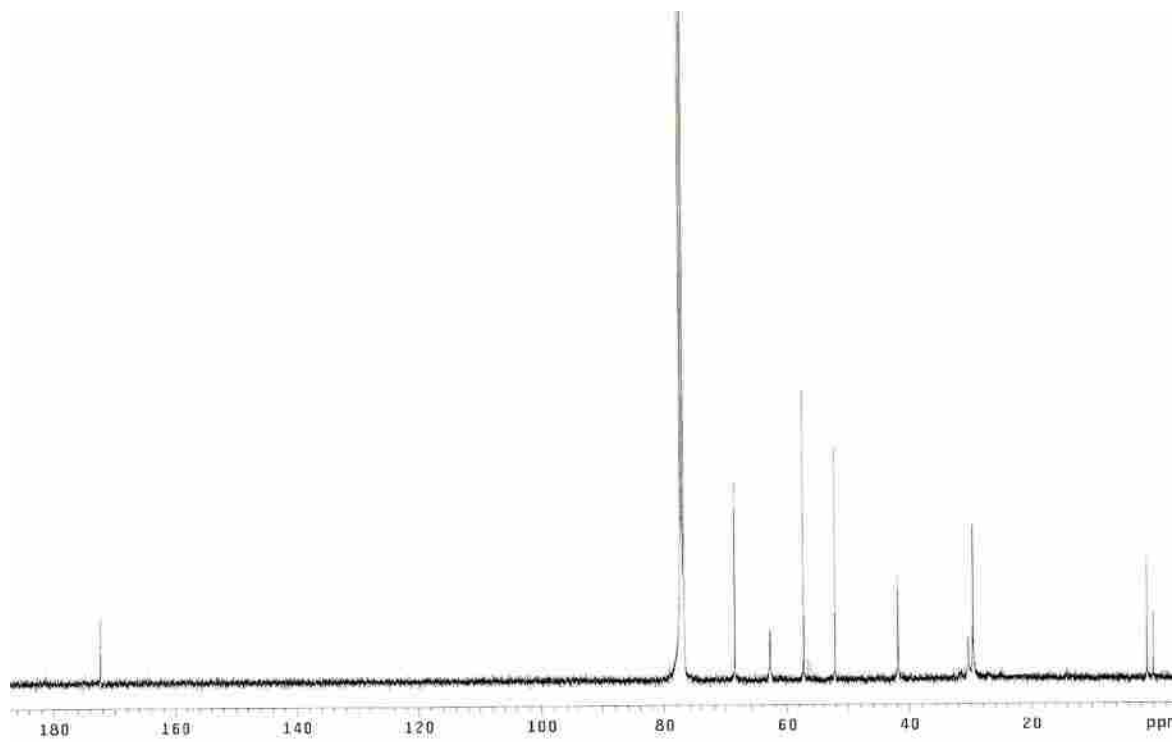
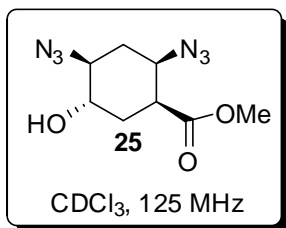


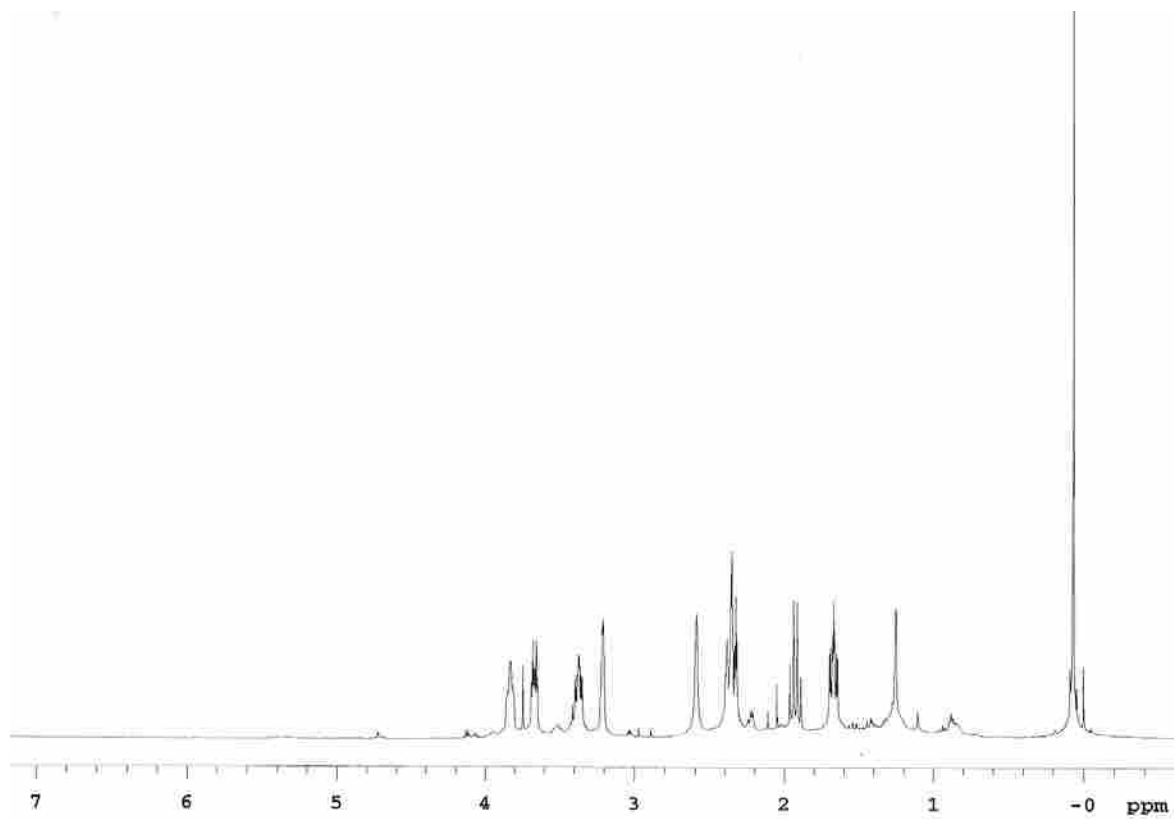
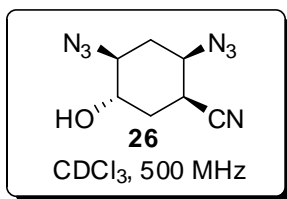


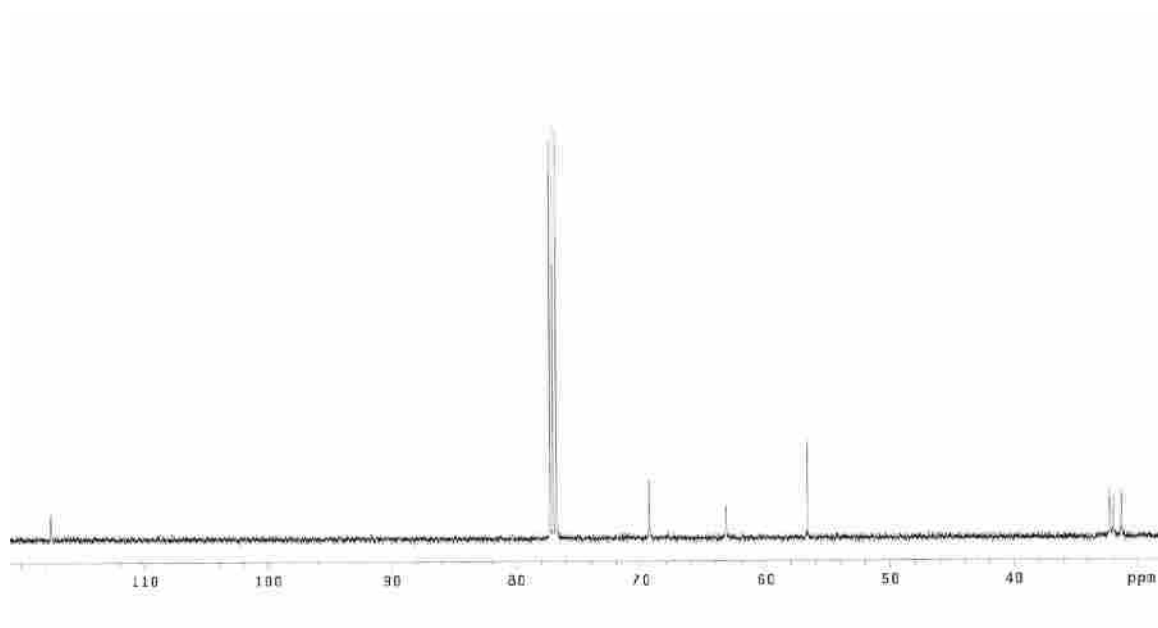
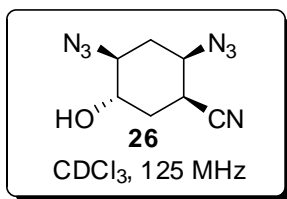


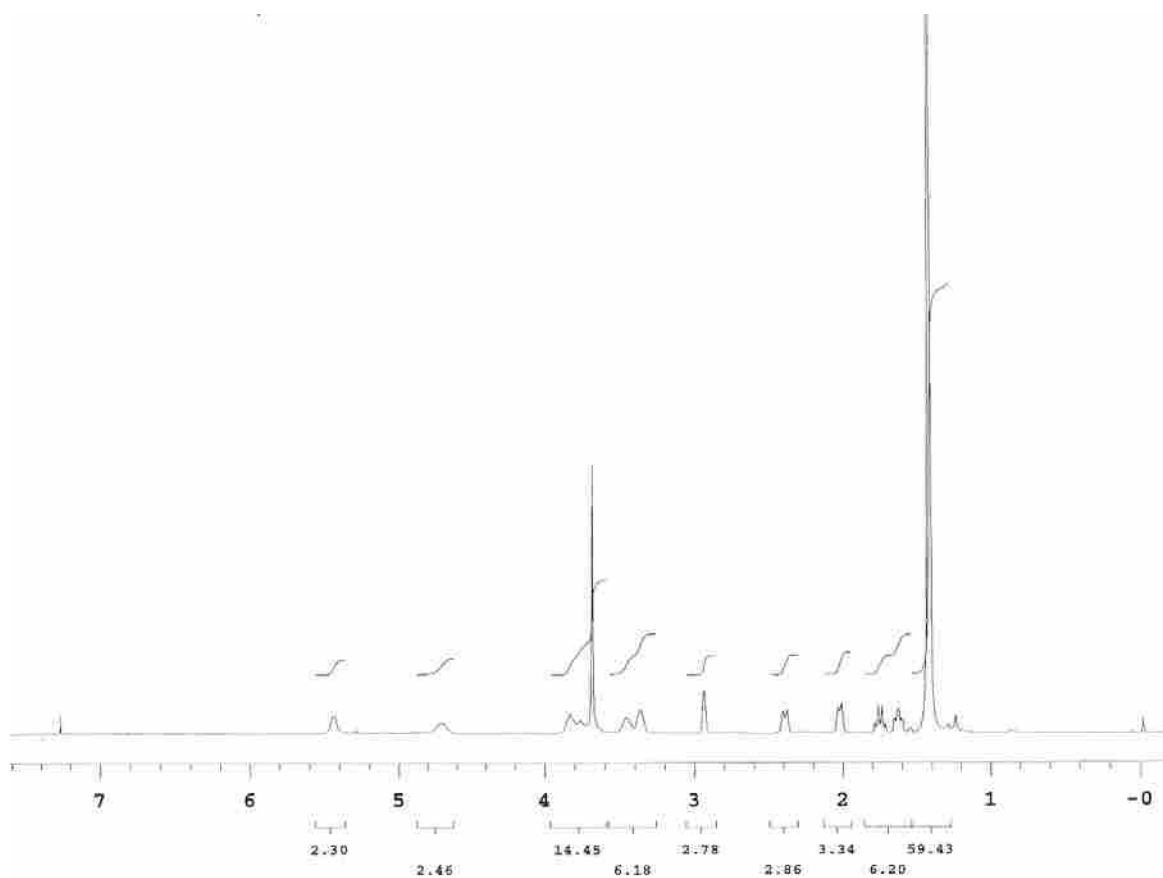
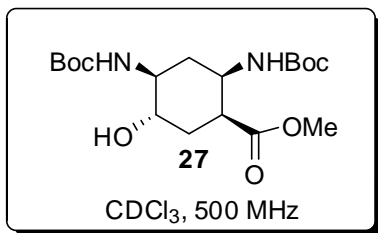




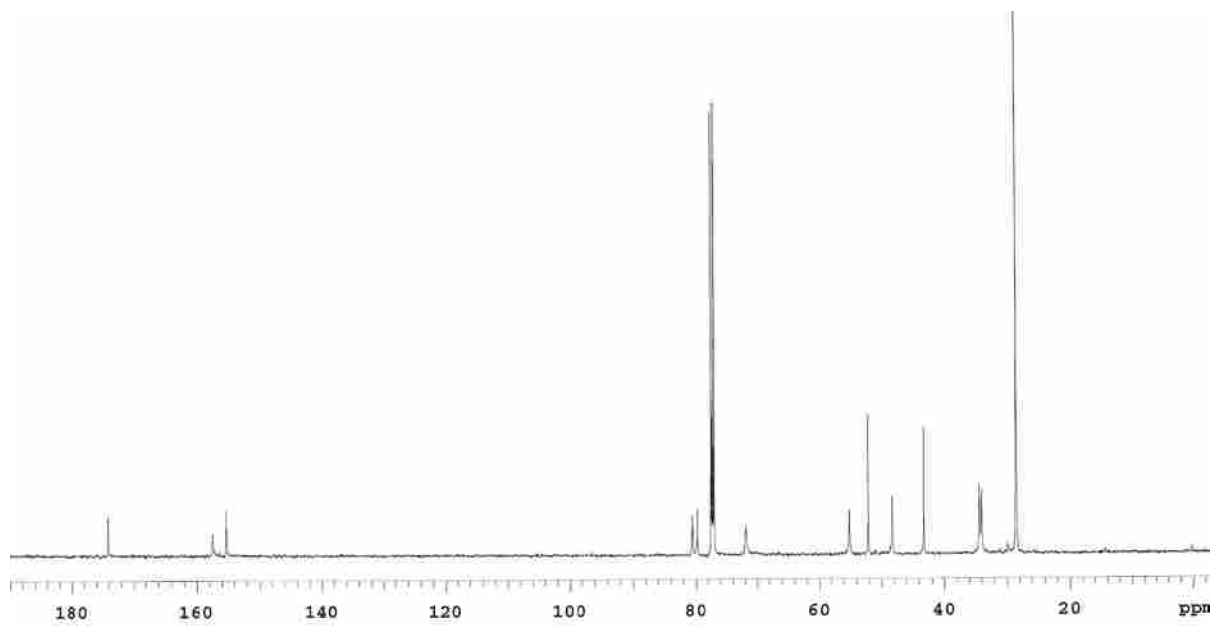
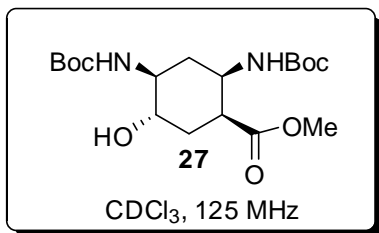


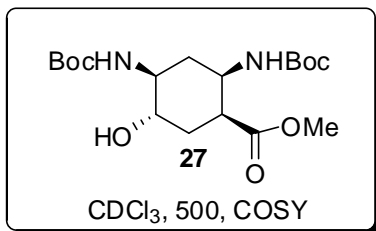










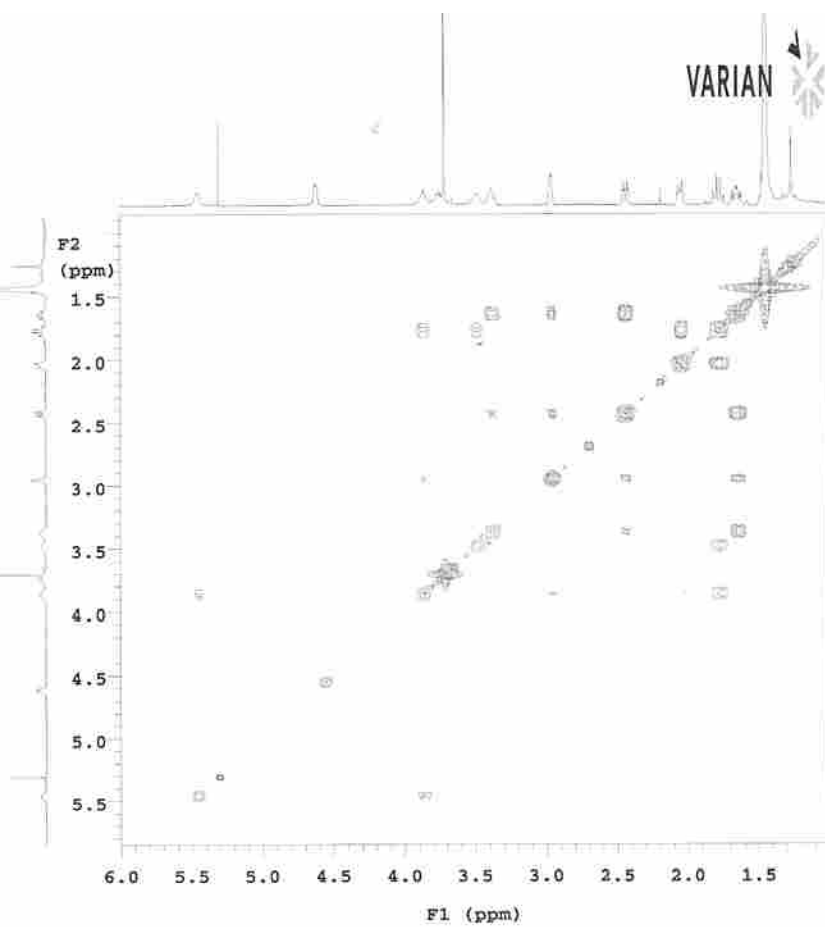


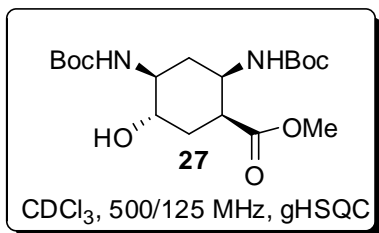
STANDARD PROTON PARAMETERS

Sample Name:  
 Archive directory:  
 Sample directory:  
 FidFile: mpcl-125cosy  
 Pulse Sequence: relayh  
 Solvent: CDCl<sub>3</sub>  
 Data collected on: Dec 8 2008

Operator: schittap  
 VNMRS-500 "nmr"

Relax. delay 0.100 sec  
 COSY 90-80  
 Acq. time 0.128 sec  
 Width 8000.0 Hz  
 2D Width 8000.0 Hz  
 4 repetitions  
 512 increments  
 OBSERVE H1, 499.9133738 MHz  
 DATA PROCESSING  
 Sine bell 0.064 sec  
 F1 DATA PROCESSING  
 Sine bell 0.032 sec  
 FT size 2048 x 2048  
 Total time 0 min 24 sec





STANDARD PROTON PARAMETERS

Sample Name:

Archive directory:

Sample directory:

Fidfile: mpcl\_125\_HMBC

Pulse Sequence: gHSQC

Solvent: CDCl3

Data collected on: Jan 6 2009

Operator: schittap

VDSS-500 "nmr"

Relax. delay 1.000 sec

Acq. time 0.128 sec

Width 8000.0 Hz

3D Width 21367.5 Hz

4 repetitions

2 x 128 increments

OBSERVE H1, 499.913373F MHz

DECOUPLE C13, 125.712715F MHz

Power 35 dB

on during acquisition

off during delay

W40\_swbw modulated

DATA PROCESSING

Resol. enhancement 4.0 Hz

Gauss apodization 0.038 sec

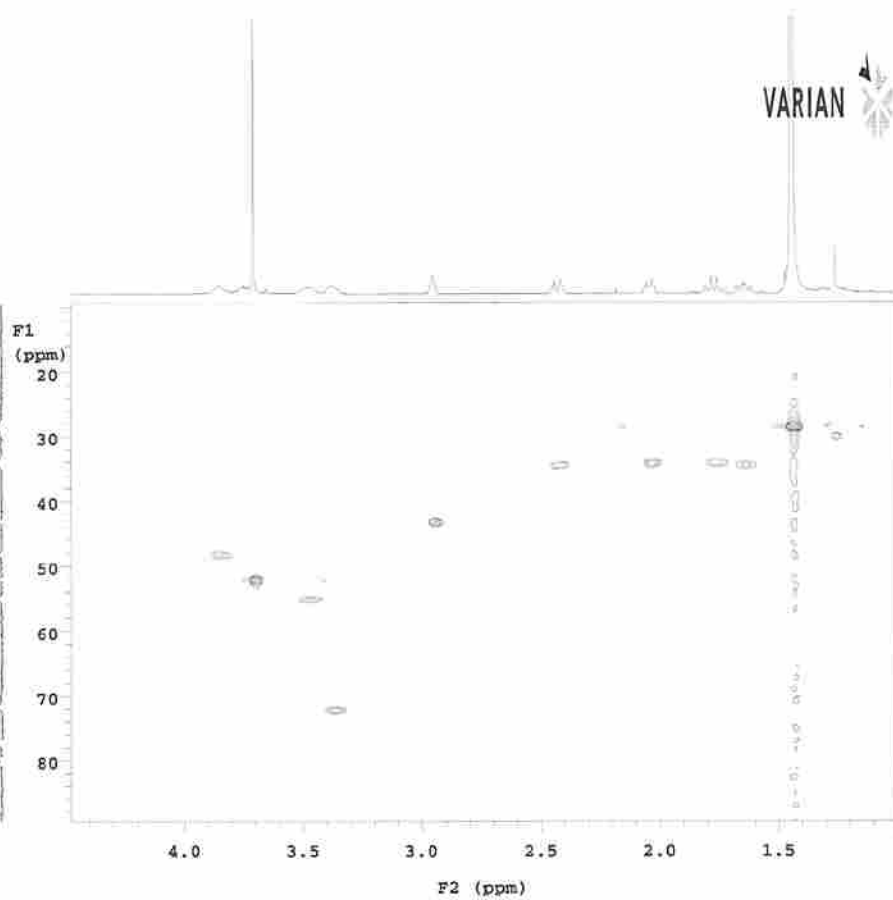
F1 DATA PROCESSING

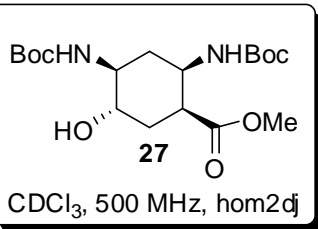
Resol. enhancement 0.0 Hz

Gauss apodization 0.007 sec

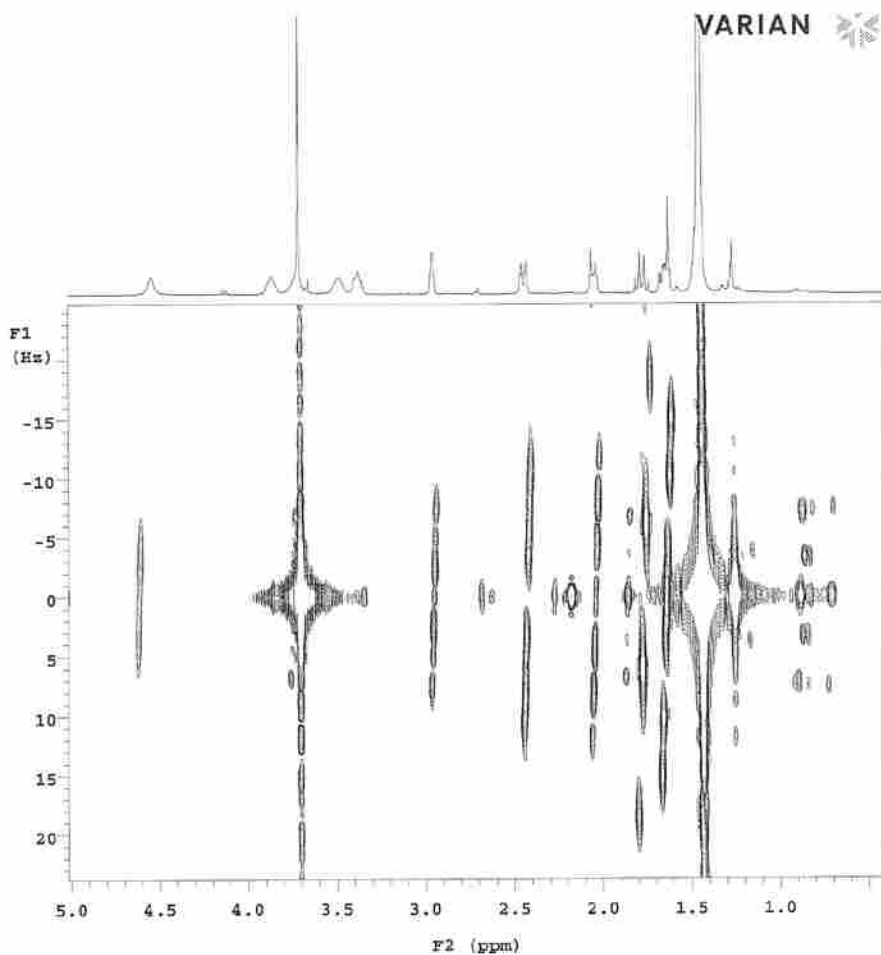
FT size 4096 X 4096

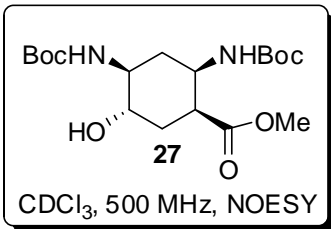
Total time 0 min 24 sec





STANDARD PROTON PARAMETERS  
 Sample Name:  
 Data Collected on:  
 num-vnmr500  
 Archive directory:  
 Sample directory:  
 Fidfile: spcl\_125\_2dj  
 Pulse Sequence: hom2dj  
 Solvent: CDCl3  
 Data collected on: Jan 7 2009  
 Operator: schittap  
 Relax. delay 2.000 sec  
 Acq. time 0.128 sec  
 Width 8000.0 Hz  
 2D Width 50.0 Hz  
 4 repetitions  
 128 increments  
 OBSERVE HL, 499.9133738 MHz  
 DATA PROCESSING  
 Sine bell 0.064 sec  
 F1 DATA PROCESSING  
 Sine bell 0.640 sec  
 FT size 8192 x 256  
 Total time 8 min 40 sec





starting material - NOESY  
 S' NOE-E,G,F -Jcoup-H,C,D  
 A' NOE-D,NH,DI Jcoup-A  
 A NOE-NH,NH Jcoup-A',E,G  
 S NOE-F Jcoup-B',C,D  
 C NOE- Jcoup-B',E,G  
 D NOE-A',F,NH Jcoup-B,E,B'  
 E NOE-B',F,G Jcoup-A,A'  
 F NOE-G,B',D,E Jcoup-  
 C NOE-B',E,NH Jcoup-A,C,A'  
 NH NOE-A',A,D  
 NH NOE-A',G,X

Sample Name:

Archive directory:

Sample directory:

File: mpcl\_125\_noesy

Pulse Sequence: NOESY

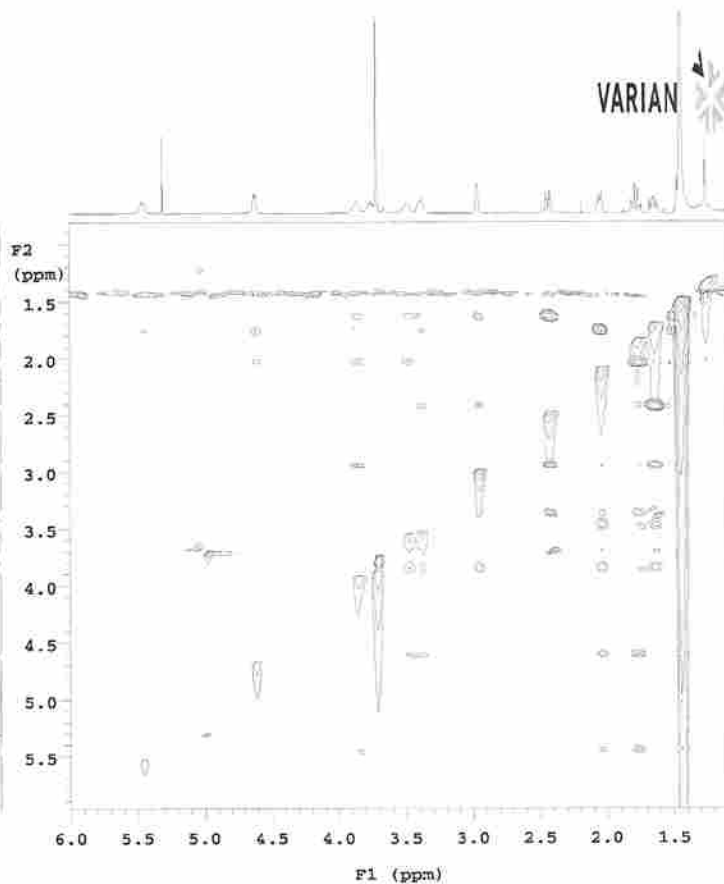
Solvent: CDCl<sub>3</sub>

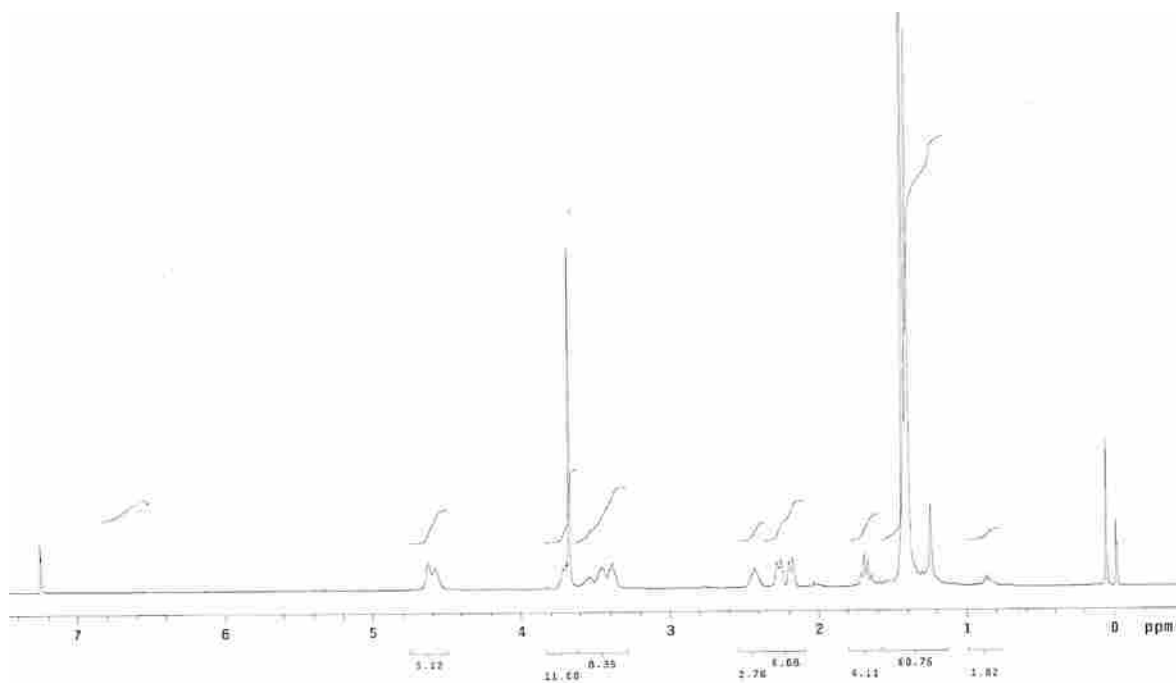
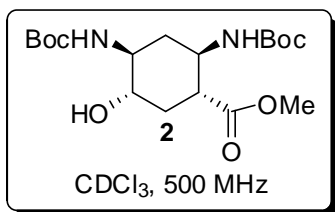
Data collected on: Jan 6 2009

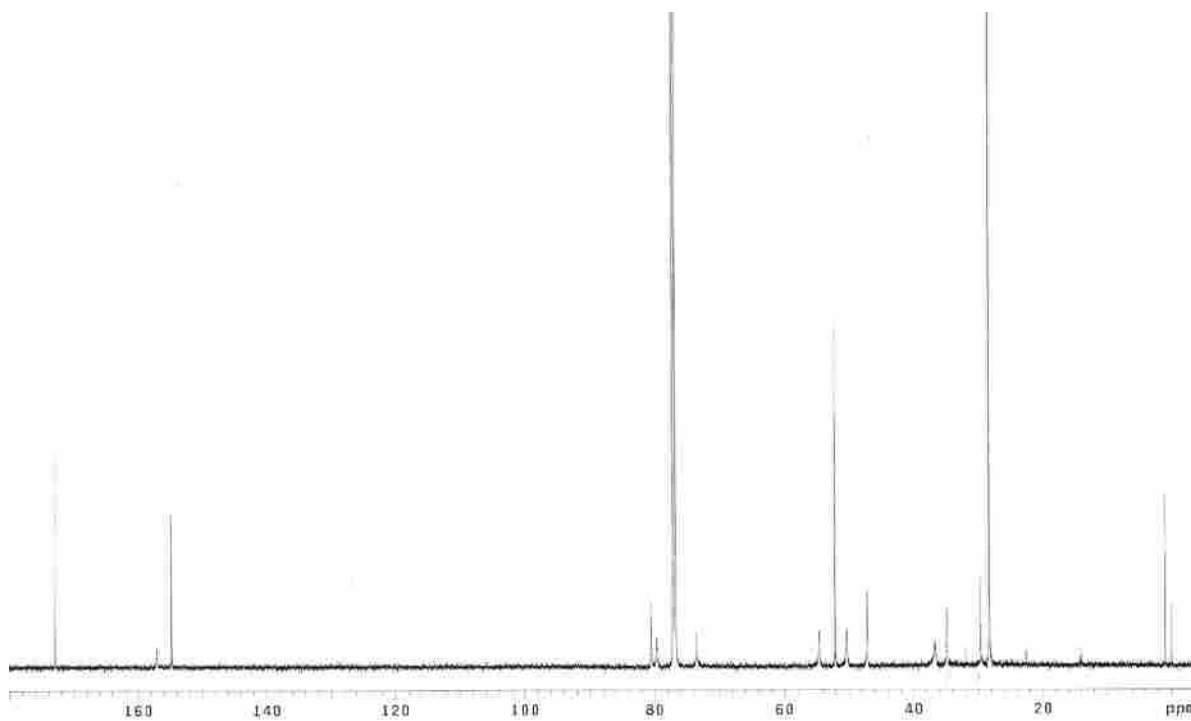
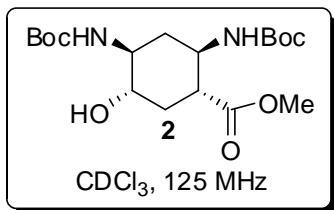
Operator: schittap

WVHM-500 "nmr"

Relax. delay 0.500 sec  
 Mixing 0.200 sec  
 Acq. time 0.128 sec  
 Width 8000.0 Hz  
 2d Width 8000.0 Hz  
 8 repetitions  
 2 x 200 increments  
 OBSERVE HI. 499.9133738 MHz  
 DATA PROCESSING  
 Resol. enhancement 4.0 Hz  
 Gauss apodization 0.038 sec  
 F1 DATA PROCESSING  
 Gauss apodization 0.033 sec  
 FT size 2048 x 2048  
 Total time 0 min 24 sec

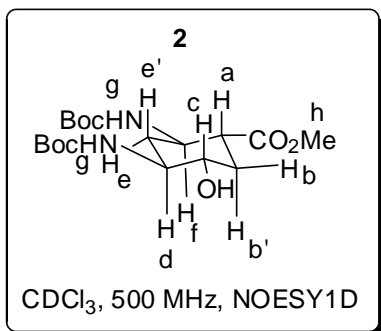












```

mpc1_epimer_1H
invert F - NOE to B', D
j coupling to E',E,A, EDC NH
!signal on C, is it from NOE to D then JDC?
2009 Feb 27
  Selective Band center: 3.72 (ppm); width: 35.8 (Hz)

-Sample Name:

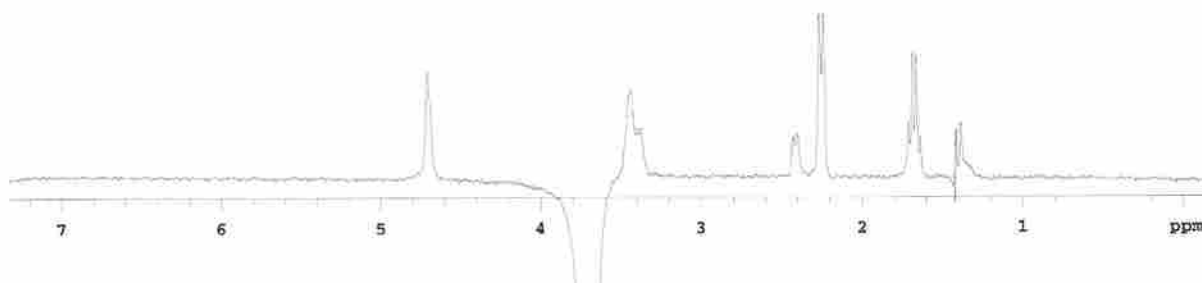
-Archive directory:

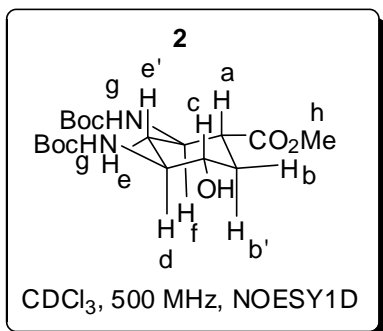
-Sample directory:

-File: NOESY1D

Pulse Sequence: NOESY1D
Solvent: cdcl3
Data collected on: Feb 27 2009

```





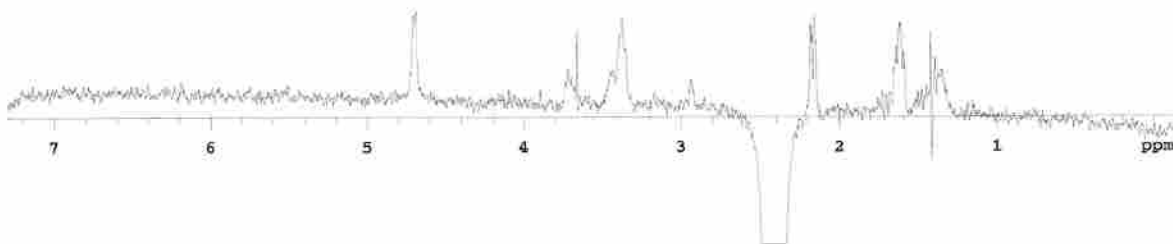
```

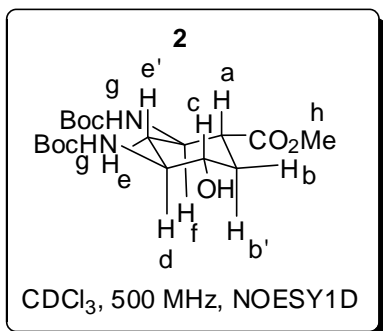
sp1_epimer_1H
invert A - NOE E',C,BOC HN
| coupling artifact to E',B,F
|009 Feb 27
Selective band center: 2.42 (ppm); width: 44.6 (Hz)

Sample Name:
Archive directory:
Sample directory:
Fidfile: NOESY1D

Pulse sequence: NOESY1D
Solvent: cdcl3
Data collected on: Feb 27 2009

```





```

spci_epimer_1H
invert B' - NOE to D,F and ester methyl
| coupling artifact to B and C
1009 feb 27
Selective band center: 1.68 (ppm), width: 47.4 (Hz)

Sample Name:

Archive directory:

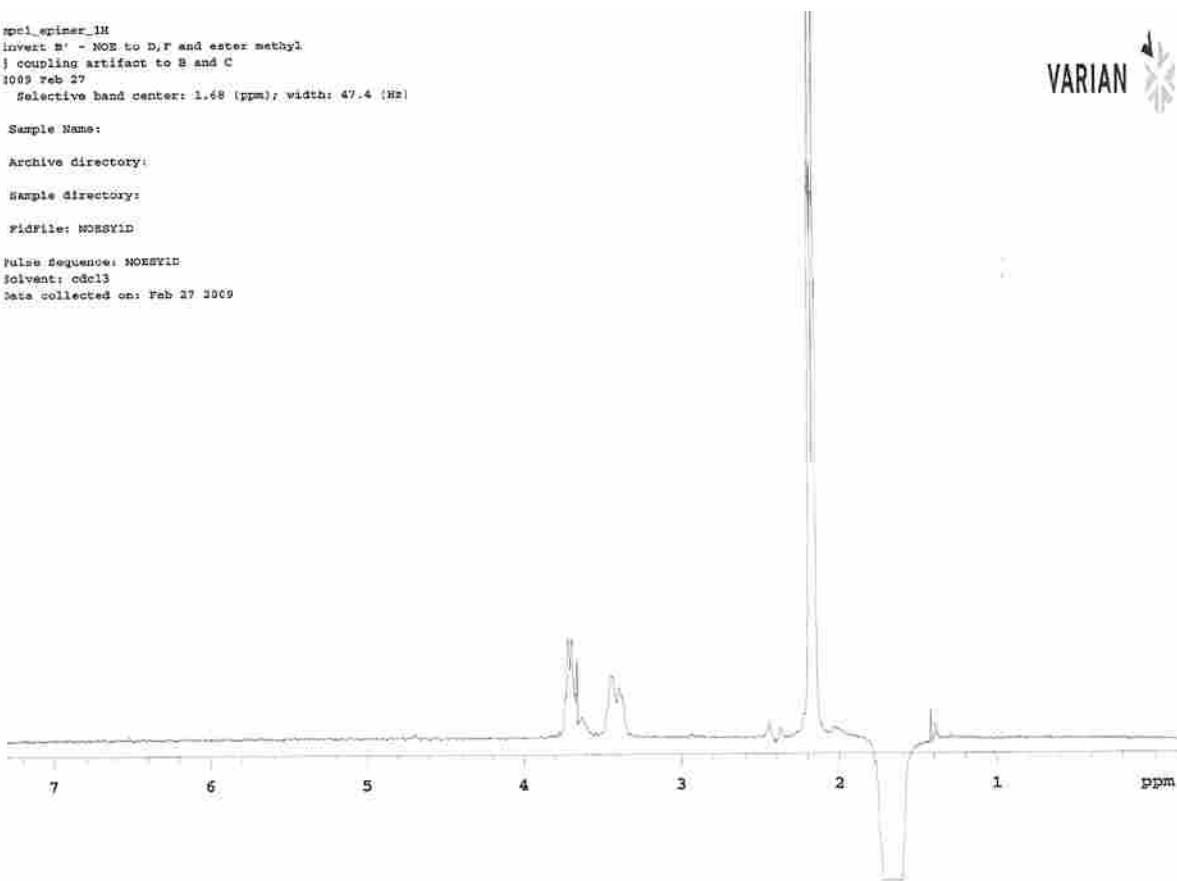
Sample directory:

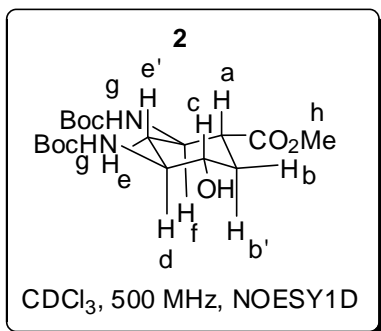
Fidfile: NOESY1D

Pulse Sequence: NOESY1D
Solvent: cdcl3
Data collected on: Feb 27 2009

```

VARIAN 





mpc1\_spiner\_1H  
 invert C - NOE E', A, BOC NH  
 (partial inversion of D, so some NOE to F)  
 J coupling artifact - B, B'  
 2009 Feb 27  
 Selective band center: 3.37 (ppm); width: 29.7 (Hz)

Sample Name:  
 Archive directory:  
 Sample directory:  
 Fidfile: NOESY1D

Pulse Sequence: NOESY1D  
 Solvent: cdcl3  
 Data collected on: Feb 27 2009

